10 CFR 50, Appendix H

CP&L
A Progress Energy Company

Serial: RNP-RA/02-0033

APR 2 5 2002

United States Nuclear Regulatory Commission
Attn: Document Control Desk
Washington, DC 20555

H. B. ROBINSON STEAM ELECTRIC PLANT, UNIT NO. 2
DOCKET NO. 50-261/LICENSE NO. DPR-23

REPORT OF THE ANALYSIS OF SURVEILLANCE CAPSULE X
FOR THE REACTOR VESSEL RADIATION SURVEILLANCE PROGRAM

Ladies and Gentlemen:

In accordance with the provisions of the Code of Federal Regulations, Title 10, Part 50, Appendix H (10 CFR 50, Appendix H), Carolina Power and Light (CP&L) Company is submitting the enclosed report pertaining to the results of the analysis of Surveillance Capsule X for H. B. Robinson Steam Electric Plant (HBRSEP), Unit No. 2. This capsule was removed from the HBRSEP, Unit No. 2, reactor vessel on April 29, 2001, during Refueling Outage 20. This submittal satisfies the 10 CFR 50, Appendix H, requirement to report the results of capsule testing within one year of the date of capsule withdrawal. The enclosed report is titled: WCAP-15805, "Analysis of Capsule X from the Carolina Power and Light Company H. B. Robinson Unit 2 Reactor Vessel Radiation Surveillance Program."

If you have any questions concerning this matter, please contact Mr. C. T. Baucom.

Sincerely,

Gary L. Howell for

B. L. Fletcher III
Manager - Regulatory Affairs

Robinson Nuclear Plant
3581 West Entrance Road
Hartsville, SC 29550

A008

CAC/cac

Enclosure

c: Mr. L. A. Reyes, NRC, Region II
Mr. R. Subbaratnam, NRC, NRR
NRC Resident Inspector, HBRSEP

H. B. ROBINSON STEAM ELECTRIC PLANT, UNIT NO. 2

ANALYSIS OF CAPSULE X FROM THE CAROLINA POWER AND LIGHT COMPANY H. B. ROBINSON UNIT 2 REACTOR VESSEL RADIATION SURVEILLANCE PROGRAM

Westinghouse Non-Proprietary Class 3

WCAP-15805

ANALYSIS OF CAPSULE X FROM THE CAROLINA POWER AND LIGHT COMPANY H.B. ROBINSON UNIT 2 REACTOR VESSEL RADIATION SURVEILLANCE PROGRAM

Westinghouse Electric Company LLC

WCAP-15805

Analysis of Capsule X from the Carolina Power & Light Company H.B. Robinson Unit 2 Reactor Vessel Radiation Surveillance Program

T. J. Laubham
E. P. Lippincott
J. Conermann

MARCH 2002

Prepared by the Westinghouse Electric Company
for the Carolina Power & Light Company

Approved: C. H. Boyd
C. H . Boyd, Manager
Equipment & Materials Technology

Westinghouse Electric Company LLC
Nuclear Services Division
P.O. Box 355
Pittsburgh, Pennsylvania 15230-0355

© 2002 Westinghouse Electric Company LLC
All Rights Reserved

TABLE OF CONTENTS

LIST OF TABLES ii

LIST OF FIGURES v

PREFACE vii

EXECUTIVE SUMMARY (OR) ABSTRACT viii

1 SUMMARY OF RESULTS 1-1

2 INTRODUCTION 2-1

3 BACKGROUND 3-1

4 DESCRIPTION OF PROGRAM 4-1

5 TESTING OF SPECIMENS FROM CAPSULE X 5-1
- 5.1 OVERVIEW 5-1
- 5.2 CHARPY V-NOTCH IMPACT TEST RESULTS 5-3
- 5.3 TENSILE TEST RESULTS 5-5

6 RADIATION ANALYSIS AND NEUTRON DOSIMETRY 6-1
- 6.1 INTRODUCTION 6-1
- 6.2 DISCRETE ORDINATES ANALYSIS 6-2
- 6.3 NEUTRON DOSIMETRY 6-5
- 6.4 PROJECTIONS OF REACTOR VESSEL EXPOSURE 6-13

7 SURVEILLANCE CAPSULE REMOVAL SCHEDULE 7-1

8 REFERENCES 8-1

APPENDIX A LOAD-TIME RECORDS FOR CHARPY SPECIMEN TESTS

APPENDIX B CHARPY V-NOTCH PLOTS FOR EACH CAPSULE USING HYPERBOLIC TAGENT CURVE-FITTING METHOD

APPENDIX C CHARPY V-NOTCH SHIFT RESULTS FOR EACH CAPSULE HAND-FIT VS. HYPERBOLIC TANGENT CURVE-FITTING METHOD (CVGRAPH, VERSION 4.1)

APPENDIX D H.B. ROBINSON UNIT 2 SURVEILLANCE PROGRAM CREDIBILITY ANALYSIS

LIST OF TABLES

Table 4-1 Chemical Composition (wt %) and Heat Treatment of Material for the H.B. Robinson Unit 2 Reactor Vessel Surveillance Material 4-4

Table 5-1 Charpy V-Notch Data for the H.B. Robinson Unit 2 Intermediate Shell Plate W10201-4 Irradiated to a Fluence of 4.49 x 10^{19} n/cm^2 (E > 1.0 MeV) (Longitudinal Orientation) 5-6

Table 5-2 Charpy V-notch Data for the H.B. Robinson Unit 2 Surveillance Weld Metal Irradiated to a Fluence of 4.49 x 10^{19} n/cm^2 (E > 1.0 MeV) 5-7

Table 5-3 Charpy V-notch Data for the H.B. Robinson Unit 2 Heat Affected Zone (HAZ) Material Irradiated to a Fluence of 4.49 x 10^{19} n/cm^2 (E > 1.0 MeV) 5-8

Table 5-4 Charpy V-notch Data for the H.B. Robinson Unit 2 Correlation Monitor Material Irradiated to a Fluence of 4.49 x 10^{19} n/cm^2 (E > 1.0 MeV) 5-9

Table 5-5 Instrumented Charpy Impact Test Results for the H.B. Robinson Unit 2 Intermediate Shell Plate W10201-4 Irradiated to a Fluence of 4.49 x 10^{19} n/cm^2 (E > 1.0 MeV) (Longitudinal Orientation) 5-10

Table 5-6 Instrumented Charpy Impact Test Results for the H.B. Robinson Unit 2 Surveillance Weld Metal Irradiated to a Fluence of 4.49 x 10^{19} n/cm^2 (E > 1.0 MeV) 5-11

Table 5-7 Instrumented Charpy Impact Test Results for the H.B. Robinson Unit 2 Heat Affected Zone (HAZ) Material Irradiated to a Fluence of 4.49 x 10^{19} n/cm^2 (E > 1.0 MeV) 5-12

Table 5-8 Instrumented Charpy Impact Test Results for the H.B. Robinson Unit 2 Correlation Monitor Material Irradiated to a Fluence of 4.49 x 10^{19} n/cm^2 (E > 1.0 MeV) 5-13

Table 5-9 Effect of Irradiation to 4.49 x 10^{19} n/cm^2 (E > 1.0 MeV) on the Notch Toughness Properties of the H.B. Robinson Unit 2 Reactor Vessel Surveillance Materials 5-14

Table 5-10 Comparison of the H.B. Robinson Unit 2 Surveillance Material 30 ft-lb Transition Temperature Shifts and Upper Shelf Energy Decreases with Regulatory Guide 1.99, Revision 2, Predictions 5-15

Table 5-11 Tensile Specimens From Intermediate Shell Course Plate W10201-4 and Weld Material 5-16

Table 6-1 Calculated Neutron Exposure Rates and Integrated Exposures at the Surveillance Capsule Center 6-15

Table 6-2 Calculated Azimuthal Variation of Maximum Exposure Rates and Integrated Exposures at the Reactor Vessel Clad/Base Metal Interface 6-19

Table 6-3 Relative Radial Distribution of Neutron Fluence (E > 1.0 MeV) Within the Reactor Vessel Wall 6-23

LIST OF TABLES (CONTINUED)

Table 6-4 Relative Radial Distribution of Iron Atom Displacement (dpa) Within the Reactor Vessel Wall 6-23

Table 6-5 Nuclear Parameters Used in the Evaluation of Neutron Sensors 6-24

Table 6-6 Monthly Thermal Generation During The First 20 Fuel Cycles of the H.B. Robinson Unit 2 Reactor (Reactor Power of 2300 MWt) 6-25

Table 6-7 Calculated $\phi(E > 1.0$ MeV) and C_j Factors at the Surveillance Capsule Center Core Midplane Elevation 6-29

Table 6-8 Measured Sensor Activities And Reaction Rates 6-30
- Surveillance Capsule S 6-30
- Surveillance Capsule V 6-31
- Surveillance Capsule T 6-32
- Surveillance Capsule X 6-33

Table 6-9 Comparison of Measured, Calculated, and Best Estimate Reaction Rates at the Surveillance Capsule Center 6-34

Table 6-10 Comparison of Calculated and Best Estimate Exposure Rates at the Surveillance Capsule Center 6-36

Table 6-11 Comparison of Calculated/Measured (C/M) Sensor Reaction Rate Ratios for Fast Neutron Threshold Reactions 6-37

Table 6-12 Comparison of Calculated/Best Estimate (C/BE) Exposure Rate Ratios 6-37

Table 6-13 Calculated Fast Neutron Exposure of Surveillance Capsules Withdrawn from H.B. Robinson Unit 2 6-38

Table 6-14 Calculated Maximum Fast Neutron Exposure of the H. B. Robinson Unit 2 Reactor Pressure Vessel at the Clad/Base Metal Interface at Selected Azimuthal Angles 6-39

Table 6-15 Calculated Maximum Fast Neutron Exposure of the H. B. Robinson Unit 2 Upper Circumferential Vessel Weld at the Clad/Base Metal Interface at Selected Azimuthal Angles 6-40

Table 6-16 Calculated Maximum Fast Neutron Exposure of the H. B. Robinson Unit 2 Lower Circumferential Vessel Weld at the Clad/Base Metal Interface at Selected Azimuthal Angles 6-41

LIST OF TABLES (CONTINUED)

Table 6-17 Calculated Surveillance Capsule Lead Factors 6-42

Table 6-18 Calculated Fast Neutron Exposure of the H. B. Robinson Unit 2 Nozzle Components 6-42

Table 7-1 H.B. Robinson Unit 2 Reactor Vessel Surveillance Capsule Withdrawal Schedule 7-1

LIST OF FIGURES

Figure 4-1 Arrangement of Surveillance Capsules in the H.B. Robinson Unit 2 Reactor Vessel 4-2

Figure 4-2 Typical H.B. Robinson Unit 2 Surveillance Capsule Assembly 4-3

Figure 5-1 Charpy V-Notch Impact Energy vs. Temperature for H.B. Robinson Unit 2 Reactor Vessel Intermediate Shell Plate W10201-4 (Longitudinal Orientation) 5-17

Figure 5-2 Charpy V-Notch Lateral Expansion vs. Temperature for H.B. Robinson Unit 2 Reactor Vessel Intermediate Shell Plate W10201-4 (Longitudinal Orientation) 5-18

Figure 5-3 Charpy V-Notch Percent Shear vs. Temperature for H.B. Robinson Unit 2 Reactor Vessel Intermediate Shell Plate W10201-4 (Longitudinal Orientation) 5-19

Figure 5-4 Charpy V-Notch Impact Energy vs. Temperature for H.B. Robinson Unit 2 Reactor Vessel Surveillance Weld Metal 5-20

Figure 5-5 Charpy V-Notch Lateral Expansion vs. Temperature for H.B. Robinson Unit 2 Reactor Vessel Surveillance Weld Metal 5-21

Figure 5-6 Charpy V-Notch Percent Shear vs. Temperature for H.B. Robinson Unit 2 Reactor Vessel Surveillance Weld Metal 5-22

Figure 5-7 Charpy V-Notch Impact Energy vs. Temperature for H.B. Robinson Unit 2 Reactor Vessel Heat Affected Zone Material 5-23

Figure 5-8 Charpy V-Notch Lateral Expansion vs. Temperature for H.B. Robinson Unit 2 Reactor Vessel Heat Affected Zone Material 5-24

Figure 5-9 Charpy V-Notch Percent Shear vs. Temperature for H.B. Robinson Unit 2 Reactor Vessel Heat Affected Zone Material 5-25

Figure 5-10 Charpy V-Notch Impact Energy vs. Temperature for H.B. Robinson Unit 2 Reactor Vessel Correlation Monitor Material 5-26

Figure 5-11 Charpy V-Notch Lateral Expansion vs. Temperature for H.B. Robinson Unit 2 Reactor Vessel Correlation Monitor Material 5-27

Figure 5-12 Charpy V-Notch Percent Shear vs. Temperature for H.B. Robinson Unit 2 Reactor Vessel Correlation Monitor Material 5-28

LIST OF FIGURES (CONTINUED)

Figure 5-13 Charpy Impact Specimen Fracture Surfaces for H.B. Robinson Unit 2 Reactor Vessel Intermediate Shell Plate W10201-4 (Longitudinal Orientation) 5-29

Figure 5-14 Charpy Impact Specimen Fracture Surfaces for H.B. Robinson Unit 2 Reactor Vessel Weld Metal Specimens 5-30

Figure 5-15 Charpy Impact Specimen Fracture Surfaces for H.B. Robinson Unit 2 Reactor Vessel Heat Affected Zone (HAZ) 5-31

Figure 5-16 Charpy Impact Specimen Fracture Surfaces for H.B. Robinson Unit 2 Reactor Vessel Correlation Monitor Material 5-32

Figure 5-17 Tensile Properties for H.B. Robinson Unit 2 Reactor Vessel Intermediate Shell Plate W10201-4 (Transverse Orientation) 5-33

Figure 5-18 Tensile Properties for H.B. Robinson Unit 2 Reactor Vessel Weld Metal 5-34

Figure 5-19 Fractured Tensile Specimens from H.B. Robinson Unit 2 Reactor Vessel Intermediate Shell Plate W10201-4 (Transverse Orientation) 5-35

Figure 5-20 Fractured Tensile Specimens from H.B. Robinson Unit 2 Reactor Vessel Weld Metal.. 5-36

Figure 5-21 Engineering Stress-Strain Curves for Intermediate Shell Plate W10201-4 Tensile Specimens C6 and C7 (Transverse Orientation) 5-37

Figure 5-22 Engineering Stress-Strain Curve for Weld Metal Tensile Specimens W1 and W2 5-38

PREFACE

This report has been technically reviewed and verified by:

Reviewer:

Sections 1 through 5, 7, 8, Appendices A, B and C	J.H. Ledger	JH Ledger
Section 6	S.L. Anderson	S.L. Anderson

EXECUTIVE SUMMARY

The purpose of this report is to document the results of the testing of surveillance capsule X from H.B. Robinson Unit 2. Capsule X was removed at 20.39 EFPY and post irradiation mechanical tests of the Charpy V-notch and tensile specimens was performed, along with a fluence evaluation based methodology and nuclear data including recently released neutron transport and dosimetry cross-section libraries derived from the ENDF/B-VI database. The calculated peak clad base/metal vessel fluence after 20.39 EFPY of plant operation was 2.76×10^{19} n/cm^2 and the surveillance Capsule X calculated fluence was 4.49×10^{19} n/cm^2. A brief summary of the Charpy V-notch testing results can be found in Section 1 and the updated capsule removal schedule can be found in Section 7. A supplement to this report is a credibility evaluation, which can be found in Appendix D, that shows the H.B. Robinson Unit 2 surveillance weld data, while including all surveillance data for weld heat W5214, is credible. Of the three surveillance plates, only intermediate shell plate W10201-5 was found to be credible.

1 SUMMARY OF RESULTS

The analysis of the reactor vessel materials contained in surveillance capsule X the fourth capsule to be removed from the H.B. Robinson Unit 2 reactor pressure vessel, led to the following conclusions: (General Note: Temperatures are reported to two significant digits only to match CVGraph output.)

- The capsule received an average fast neutron calculated fluence (E > 1.0 MeV) of 4.49 x 10^{19} n/cm^2 after 20.39 effective full power years (EFPY) of plant operation.

- Irradiation of the reactor vessel intermediate shell plate W10201-4 Charpy specimens, oriented with the longitudinal axis of the specimen parallel to the major working direction of the plate (longitudinal orientation), to 4.49 x 10^{19} n/cm^2 (E> 1.0MeV) resulted in a 30 ft-lb transition temperature increase of 104.73°F and a 50 ft-lb transition temperature increase of 98.68°F. This results in an irradiated 30 ft-lb transition temperature of 86.55°F and an irradiated 50 ft-lb transition temperature of 116.04°F for the longitudinally oriented specimens

- Irradiation of the weld metal Charpy specimens to 4.49 x 10^{19} n/cm^2 (E> 1.0MeV) resulted in a 30 ft-lb transition temperature increase of 265.93°F and a 50 ft-lb transition temperature increase of 251.74°F. This results in an irradiated 30 ft-lb transition temperature of 179.64°F and an irradiated 50 ft-lb transition temperature of 211.38°F.

- Irradiation of the weld Heat-Affected-Zone (HAZ) metal Charpy specimens to 4.49 x 10^{19} n/cm^2 (E > 1.0 MeV) resulted in a 30 ft-lb transition temperature increase of 210.13°F and a 50 ft-lb transition temperature increase of 216.59°F. This results in an irradiated 30 ft-lb transition temperature of 100.47°F and an irradiated 50 ft-lb transition temperature of 150.54°F.

- Irradiation of the correlation monitor material Charpy specimens to 4.49 x 10^{19} n/cm^2 (E > 1.0 MeV) resulted in a 30 ft-lb transition temperature increase of 125.21°F which resulted in an irradiated 30 ft-lb transition temperature of 188.15°F. The tested specimens did not reach the 50 ft-lb transition temperature.

- The average upper shelf energy of the intermediate shell plate W10201-4 (longitudinal orientation) resulted in an average energy decrease of 1 ft-lb after irradiation to 4.49 x 10^{19} n/cm^2 (E> 1.0 MeV). This results in an irradiated average upper shelf energy of 94 ft-lb for the longitudinally oriented specimens.

- The average upper shelf energy of the weld metal Charpy specimens resulted in an average energy decrease of 33 ft-lb after irradiation to 4.49 x 10^{19} n/cm^2 (E> 1.0 MeV). Hence, this results in an irradiated average upper shelf energy of 80 ft-lb for the weld metal specimens.

- The average upper shelf energy of the weld HAZ metal Charpy specimens resulted in an average energy decrease of 24 ft-lb after irradiation to 4.49 x 10^{19} n/cm^2 (E > 1.0 MeV). Hence, this results in an irradiated average upper shelf energy of 105 ft-lb for the weld HAZ metal.

- The average upper shelf energy of the correlation monitor material Charpy specimens resulted in no energy decrease after irradiation to 4.49×10^{19} n/cm^2 (E > 1.0 MeV). Hence, this results in an irradiated average upper shelf energy of 42 ft-lb for the correlation monitor material.

- A comparison of the H.B. Robinson Unit 2 reactor vessel beltline material test results with the Regulatory Guide 1.99, Revision 2[1], predictions led to the following conclusions:

  - The measured 30 ft-lb shift in transition temperature values of the intermediate shell plate W10201-4 contained in capsule X (longitudinal) is greater than the Regulatory Guide 1.99, Revision 2, predictions. However, the shift value is less than two sigma allowance by Regulatory Guide 1.99, Revision 2.

  - The measured 30 ft-lb shift in transition temperature values of the weld metal contained in capsule X (longitudinal) is less than the Regulatory Guide 1.99, Revision 2, predictions.

  - The measured percent decrease in upper shelf energy of the Capsule X surveillance material is less than the Regulatory Guide 1.99, Revision 2, predictions.

- The peak calculated end-of-license (29 EFPY) neutron fluence (E> 1.0 MeV) at the peak vessel location approximately 4 inches above the core midplane for the H.B. Robinson Unit 2 reactor vessel using the Regulatory Guide 1.99, Revision 2 attenuation formula (ie. Equation # 3 in the guide; $f_{(depth\ x)} = f_{surface} * e^{(-0.24x)}$) is as follows:

Calculated:	Vessel inner radius	=	3.67×10^{19} n/cm^2
	Vessel 1/4 thickness	=	2.10×10^{19} n/cm^2
	Vessel 3/4 thickness	=	6.87×10^{18} n/cm^2

- The credibility evaluation of the H.B. Robinson Unit 2 surveillance program presented in Appendix D of this report indicates that the surveillance results for intermediate shell plate W10201-5 and the weld metal are credible. Intermediate Shell Plates W10201-4 and W10201-6 were found not to comply with credibility criteria #3 of the Regulatory guide 1.99, Revision 2.

- The beltline is defined as portions of the vessel exposed to a fluence of 1×10^{17} n/cm^2. Per Table 6-18 the lower portion of one inlet and one outlet nozzle see a fluence of slightly greater than 1×10^{17} n/cm^2. Thus, the nozzles are considered in the beltline and will be addressed when evaluating PTS and PT Curves. However, it should be noted here that based on the magnitude of the fluence, the nozzles or the nozzle weld will not become the limiting material in the H.B. Robinson Vessel.

2 INTRODUCTION

This report presents the results of the examination of Capsule X, the fourth capsule to be removed from the reactor in the continuing surveillance program which monitors the effects of neutron irradiation on the H.B. Robinson Unit 2 reactor pressure vessel materials under actual operating conditions.

The surveillance program for the Carolina Power and Light Company H.B. Robinson Unit 2 reactor pressure vessel materials was designed and recommended by the Westinghouse Electric Company. A description of the surveillance program and the preirradiation mechanical properties of the reactor vessel materials is presented in WCAP-7373, "Carolina Power and Light co. H.B. Robinson Unit No. 2 Reactor Vessel Radiation Surveillance Program"[3]. The surveillance program was planned to cover the 40-year design life of the reactor pressure vessel and was based on ASTM E185-66, "Recommended Practice for Surveillance Tests on Structural Materials in Nuclear Reactors". Capsule X was removed from the reactor after 20.39 EFPY of exposure and shipped to the Westinghouse Science and Technology Center Hot Cell Facility, where the postirradiation mechanical testing of the Charpy V-notch impact and tensile surveillance specimens was performed.

This report summarizes the testing of and the post-irradiation data obtained from surveillance capsule X, removed from the H.B. Robinson Unit 2 reactor vessel and discusses the analysis of the data.

3 BACKGROUND

The ability of the large steel pressure vessel containing the reactor core and its primary coolant to resist fracture constitutes an important factor in ensuring safety in the nuclear industry. The beltline region of the reactor pressure vessel is the most critical region of the vessel because it is subjected to significant fast neutron bombardment. The overall effects of fast neutron irradiation on the mechanical properties of low alloy, ferritic pressure vessel steels such as A302 Grade B (base material of the Carolina Power and Light Company H.B. Robinson Unit 2 reactor pressure vessel beltline) are well documented in the literature. Generally, low alloy ferritic materials show an increase in hardness and tensile properties and a decrease in ductility and toughness during high-energy irradiation.

A method for ensuring the integrity of reactor pressure vessels has been presented in "Fracture Toughness Criteria for Protection Against Failure," Appendix G to Section XI of the ASME Boiler and Pressure Vessel Code[4]. The method uses fracture mechanics concepts and is based on the reference nil-ductility transition temperature (RT_{NDT}).

RT_{NDT} is defined as the greater of either the drop weight nil-ductility transition temperature (NDTT per ASTM E-208[5]) or the temperature 60°F less than the 50 ft-lb (and 35-mil lateral expansion) temperature as determined from Charpy specimens oriented perpendicular (transverse) to the major working direction of the plate. The RT_{NDT} of a given material is used to index that material to a reference stress intensity factor curve (K_{Ia} curve) which appears in Appendix G to the ASME Code[4]. The K_{Ia} curve is a lower bound of dynamic, crack arrest, and static fracture toughness results obtained from several heats of pressure vessel steel. When a given material is indexed to the K_{Ia} curve, allowable stress intensity factors can be obtained for this material as a function of temperature. Allowable operating limits can then be determined utilizing these allowable stress intensity factors. Note that Code Case N-641 now allows the use of the K_{Ic} curve as an alternative to the K_{Ia} curve.

RT_{NDT} and, in turn, the operating limits of nuclear power plants can be adjusted to account for the effects of radiation on the reactor vessel material properties. The changes in mechanical properties of a given reactor pressure vessel steel, due to irradiation, can be monitored by a reactor surveillance program, such as the H.B. Robinson Unit 2 reactor vessel radiation surveillance program[3], in which a surveillance capsule is periodically removed from the operating nuclear reactor and the encapsulated specimens tested. The increase in the average Charpy V-notch 30 ft-lb temperature (ΔRT_{NDT}) due to irradiation is added to the initial RT_{NDT}, along with a margin (M) to cover uncertainties, to adjust the RT_{NDT} (ART) for radiation embrittlement. This ART (RT_{NDT} initial + M + ΔRT_{NDT}) is used to index the material to the K_{Ia} curve and, in turn, to set operating limits for the nuclear power plant that take into account the effects of irradiation on the reactor vessel materials.

4 DESCRIPTION OF PROGRAM

Eight surveillance capsules for monitoring the effects of neutron exposure on the H.B. Robinson Unit 2 reactor pressure vessel core region (beltline) materials were inserted in the reactor vessel prior to initial plant start-up. The capsules were positioned in the reactor vessel between the thermal shield and the vessel wall at locations shown in Figure 4-1. The vertical center of the capsules is opposite the vertical center of the core. It should be noted that Capsules "X" and "U" were relocated to the "T" and "S" positions after cycle 8

Capsule X was removed after 20.39 effective full power years (EFPY) of plant operation. This capsule contained Charpy V-notch impact and tensile specimens made from reactor vessel intermediate shell plate W10201-4, submerged arc weld metal representative of the beltline region girth weld seam, and heat-affected-zone (HAZ) metal. This capsule also contained Charpy V-notch specimens from the 6-inch thick ASTM correlation monitor material (A302 Grade B).

Test specimens obtained from intermediate shell plate W10201-4 (after the thermal heat treatment and forming of the plate) was taken at least one plate thickness from the quenched ends of the plate. All test specimens were machined from the 1/4 thickness location of the plate. All plate Charpy V-notch specimens were oriented with the longitudinal axis of the specimen parallel to the major rolling direction of the plate (longitudinal orientation). Charpy V-notch impact specimens from the weld metal were oriented with the longitudinal axis of the specimen transverse to the weld with the notch oriented in the direction of the weld.

Tensile specimens from the plate materials were machined with the longitudinal axis of the specimen transverse to the major rolling direction of the plate. Tensile specimens from the weld metal were oriented with the longitudinal axis of the specimen transverse to the weld direction.

Capsule X contained dosimeter pure copper, nickel, and aluminum-cobalt (cadmium-shielded and unshielded).

The capsule contained thermal monitors made from four low-melting-point eutectic alloys and sealed in glass capsules. These thermal monitors were used to define the maximum temperature attained by the test specimens during irradiation. The composition of the four eutectic alloys and their melting points are:

2.5% Ag, 97.5% Pb	Melting Point 579°F (304°C)
1.75% Ag, 0.75% Sn, 97.5% Pb	Melting Point 590°F (310°C)

The arrangement of the various mechanical test specimens, dosimeters and thermal monitors contained in capsule X is shown in Figure 4-2.

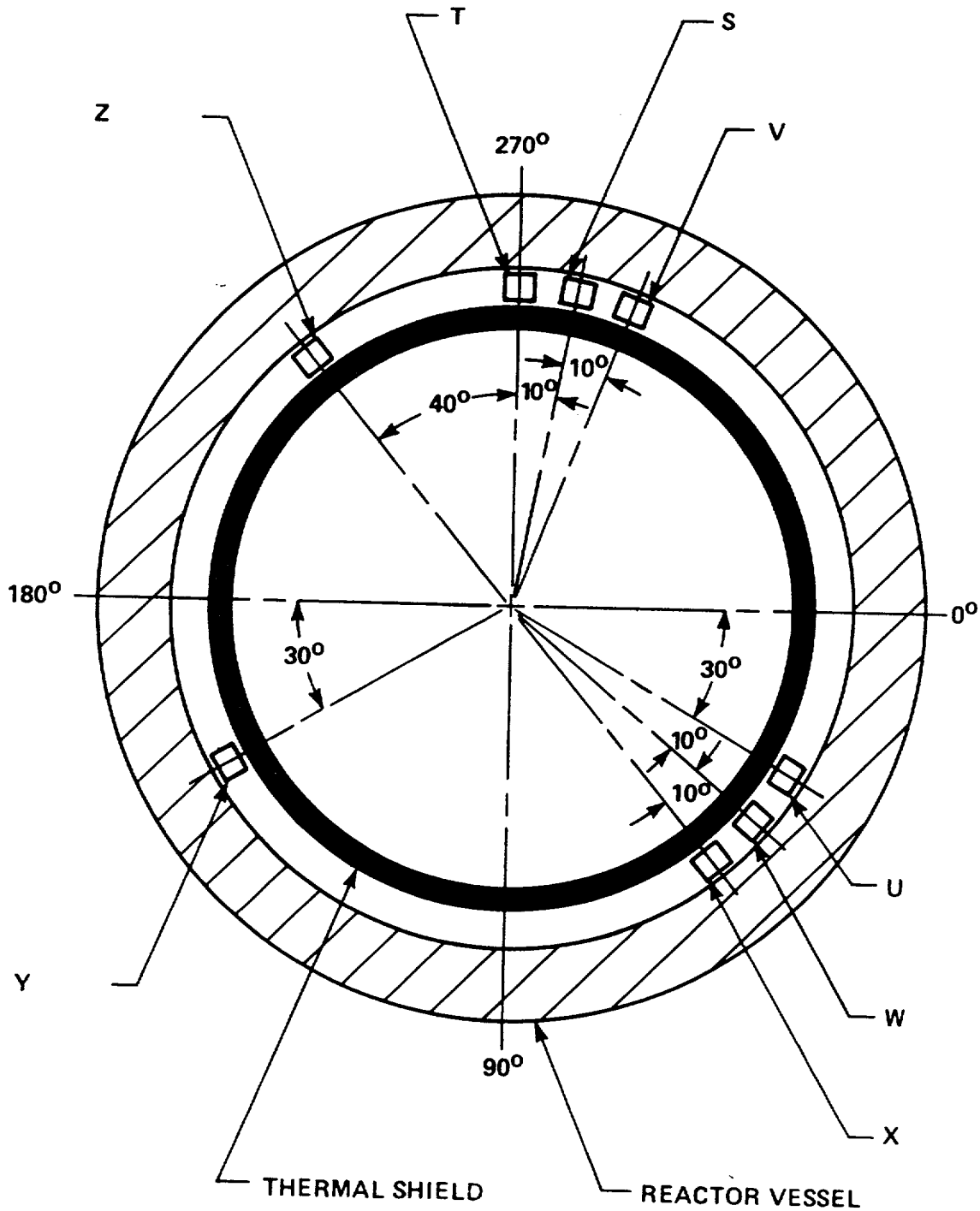

Figure 4-1. Arrangement of Surveillance Capsules in the H.B. Robinson Unit 2 Reactor Vessel

SPECIMEN NUMBERING CODE

C – PLATE W10201-4
W – WELD METAL
H – HEAT-AFFECTED-ZONE
R – CORRELATION MONITOR MATERIAL

SURVEILLANCE CAPSULE X

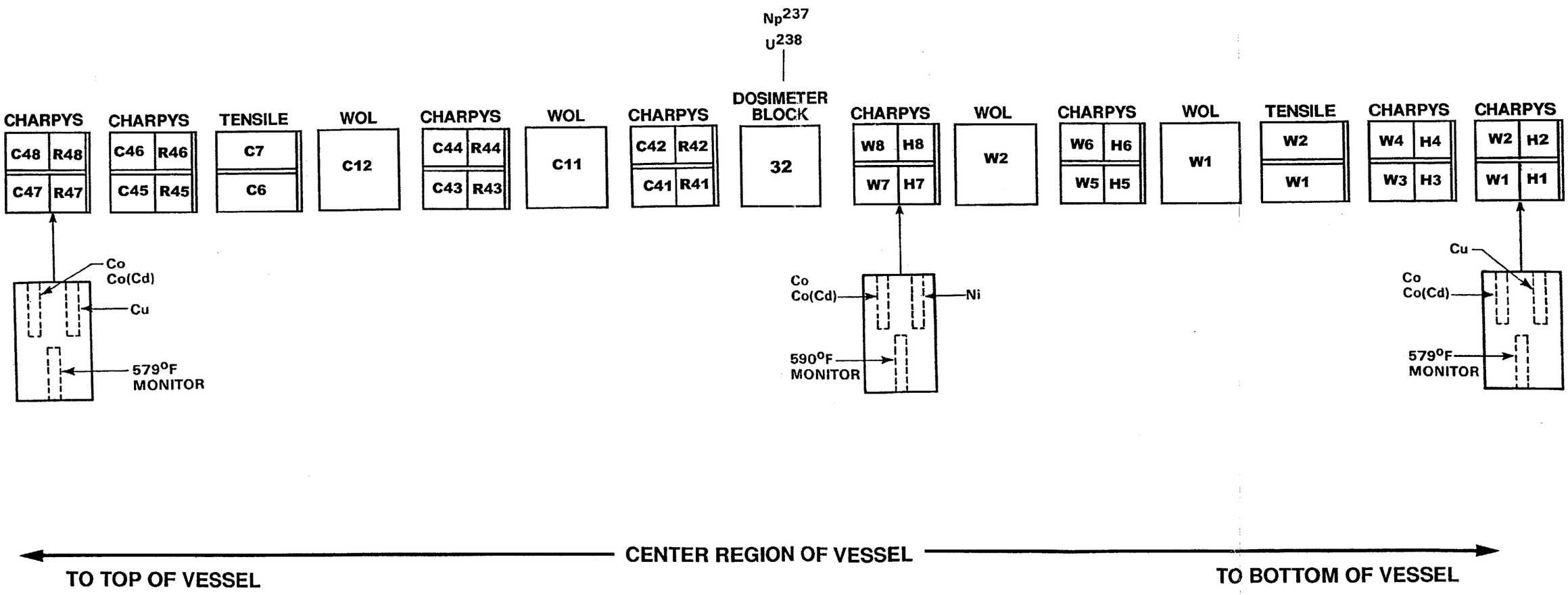

Figure 4-2 Capsule X Diagram Showing the Location of Specimens, Thermal Monitors and Dosimeters

Table 4-1 Chemical Composition (wt %) and Heat Treatment of Material for the H.B. Robinson Unit 2 Reactor Vessel Surveillance Material[a]

Chemical Composition

Element	Plate W10201-4	Plate W10201-5	Plate W10201-6	Weld Metal	Correlation Monitor Material
C	0.19	0.20	0.19	0.16	0.24
Mn	1.35	1.29	1.32	0.98	1.34
P	0007	0.010	0.010	0.021	0.011
S	0.019	0.021	0.015	0.014	0.023
Si	0.23	0.22	0.19	0.34	0.23
Mo	0.48	0.46	0.49	0.46	0.51
Cu	0.12	0.10	0.09	0.34	0.20
V	---	---	---	0.001	---
Ni	---	---	---	0.66	0.18
Cr	---	---	---	0.024	0.11
Co	---	---	---	---	---

Heat Treatment

Plate W10201-4,	1550°F to 1600°F, 4 hours, Water Quench
Plate W10201-5, &	1200°F to 1250°F, 4 hours, Air Cooled
Plate W10201-6	1125°F to 1175°F, 15 1/2 hours, Furnace cooled to 600°F
Weld Metal	1125°F to 1175°F, 30 hours, Furnace cooled to 600°F
Correlation Monitor	1650°F, 4 hours, Water Quenched 1200°F – 6 hours, Air Cooled

Notes:

a) The data given in this column (originally) is from WCAP-7373 & WCAP-10304.

5 TESTING OF SPECIMENS FROM CAPSULE X

5.1 OVERVIEW

The post-irradiation mechanical testing of the Charpy V-notch impact specimens and tensile specimens was performed in the Remote Metallographic Facility (RMF) at the Westinghouse Science and Technology Department. Testing was performed in accordance with 10CFR50, Appendices G and H[2], ASTM Specification E185-82[7], and Westinghouse Procedure RMF 8402, Revision 2 as modified by Westinghouse RMF Procedures 8102, Revision 1, and 8103, Revision 1.

Upon receipt of the capsule at the hot cell laboratory, the specimens and spacer blocks were carefully removed, inspected for identification number, and checked against the master lists in WCAP-7373[3]. No discrepancies were found.

Examination of the two low-melting point 579°F (304°C) and 590°F (310°C) eutectic alloys indicated no melting of either type of thermal monitor. Based on this examination, the maximum temperature to which the test specimens were exposed to was less than 579°F (304°F).

The Charpy impact tests were performed per ASTM Specification E23-98[8] and RMF Procedure 8103, Revision 1, on a Tinius-Olsen Model 74, 358J machine. The tup (striker) of the Charpy impact test machine is instrumented with a GRC 930-I instrumentation system, feeding information into an IBM compatible computer. With this system, load-time and energy-time signals can be recorded in addition to the standard measurement of Charpy energy (E_D). From the load-time curve (Appendix A), the load of general yielding (P_{GY}), the time to general yielding (t_{GY}), the maximum load (P_M), and the time to maximum load (t_M) can be determined. Under some test conditions, a sharp drop in load indicative of fast fracture was observed. The load at which fast fracture was initiated is identified as the fast fracture load (P_F), and the load at which fast fracture terminated is identified as the arrest load (P_A). The energy at maximum load (E_M) was determined by comparing the energy-time record and the load-time record. The energy at maximum load is approximately equivalent to the energy required to initiate a crack in the specimen. Therefore, the propagation energy for the crack (E_p) is the difference between the total energy to fracture (E_D) and the energy at maximum load (E_M).

The yield stress (σ_Y) was calculated from the three-point bend formula having the following expression:

$$\sigma_Y = (P_{GY} * L) / [B * (W - a)^2 * C] \quad (1)$$

where:
- L = distance between the specimen supports in the impact machine
- B = the width of the specimen measured parallel to the notch
- W = height of the specimen, measured perpendicularly to the notch
- a = notch depth

The constant C is dependent on the notch flank angle (ϕ), notch root radius (ρ) and the type of loading (i.e., pure bending or three-point bending). In three-point bending, for a Charpy specimen in which ϕ= 45° and ρ = 0.010 inch, Equation 1 is valid with C = 1.21. Therefore, (for L = 4W),

$$\sigma_y = (P_{GY} * L) / [B * (W - a)^2 * 1.21] = (3.33 * P_{GY} * W) / [B * (W - a)^2] \quad (2)$$

For the Charpy specimen, B = 0.394 inch, W = 0.394 inch and a = 0.079 inch. Equation 2 then reduces to:

$$\sigma_y = 33.3 * P_{GY} \quad (3)$$

where σ_y is in units of psi and P_{GY} is in units of lbs. The flow stress was calculated from the average of the yield and maximum loads, also using the three-point bend formula.

The symbol A in columns 4, 5, and 6 of Tables 5-5 through 5-8 is the cross-section area under the notch of the Charpy specimens:

$$A = B * (W - a) = 0.1241 \text{sq.in.} \quad (4)$$

Percent shear was determined from post-fracture photographs using the ratio-of-areas methods in compliance with ASTM Specification E23-98 and A370-97a[9]. The lateral expansion was measured using a dial gage rig similar to that shown in the same specification.

Tensile tests were performed on a 20,000-pound Instron, split-console test machine (Model 1115) per ASTM Specification E8-99[10] and E21-92[11], and RMF Procedure 8102, Revision 1. All pull rods, grips, and pins were made of Inconel 718. The upper pull rod was connected through a universal joint to improve axiality of loading. The tests were conducted at a constant crosshead speed of 0.05 inches per minute throughout the test.

Extension measurements were made with a linear variable displacement transducer extensometer. The extensometer knife edges were spring-loaded to the specimen and operated through specimen failure. The extensometer gage length was 1.00 inch. The extensometer is rated as Class B-2 per ASTM E83-93[12].

Elevated test temperatures were obtained with a three-zone electric resistance split-tube furnace with a 9-inch hot zone. All tests were conducted in air. Because of the difficulty in remotely attaching a thermocouple directly to the specimen, the following procedure was used to monitor specimen temperatures. Chromel-Alumel thermocouples were positioned at the center and at each end of the gage section of a dummy specimen and in each tensile machine griper. In the test configuration, with a slight load on the specimen, a plot of specimen temperature versus upper and lower tensile machine griper and controller temperatures was developed over the range from room temperature to 550°F. During the actual testing, the grip temperatures were used to obtain desired specimen temperatures. Experiments have indicated that this method is accurate to ±2°F.

The yield load, ultimate load, fracture load, total elongation, and uniform elongation were determined directly from the load-extension curve. The yield strength, ultimate strength, and fracture strength were calculated using the original cross-sectional area. The final diameter and final gage length were determined from post-fracture photographs. The fracture area used to calculate the fracture stress (true stress at fracture) and percent reduction in area was computed using the final diameter measurement.

5.2 CHARPY V-NOTCH IMPACT TEST RESULTS

The results of the Charpy V-notch impact tests performed on the various materials contained in capsule X, which received a fluence of 4.49 x 10^{19} n/cm^2 (E > 1.0 MeV) in 20.39 EFPY of operation, are presented in Tables 5-1 through 5-8, and are compared with unirradiated results as shown in Figures 5-1 through 5-12.

The transition temperature increases and upper shelf energy decreases for the capsule X materials are summarized in Table 5-9. These results led to the following conclusions:

Irradiation of the reactor vessel intermediate shell plate W10201-4 Charpy specimens, oriented with the longitudinal axis of the specimen parallel to the major working direction of the plate (longitudinal orientation), to 4.49 x 10^{19} n/cm^2 (E> 1.0MeV) resulted in a 30 ft-lb transition temperature increase of 104.73°F and a 50 ft-lb transition temperature increase of 98.68°F. This results in an irradiated 30 ft-lb transition temperature of 86.55°F and an irradiated 50 ft-lb transition temperature of 116.04°F for the longitudinally oriented specimens

Irradiation of the weld metal Charpy specimens to 4.49 x 10^{19} n/cm^2 (E> 1.0MeV) resulted in a 30 ft-lb transition temperature increase of 265.93°F and a 50 ft-lb transition temperature increase of 251.74°F. This results in an irradiated 30 ft-lb transition temperature of 179.64°F and an irradiated 50 ft-lb transition temperature of 211.38°F.

Irradiation of the weld Heat-Affected-Zone (HAZ) metal Charpy specimens to 4.49 x 10^{19} n/cm^2 (E > 1.0 MeV) resulted in a 30 ft-lb transition temperature increase of 210.13°F and a 50 ft-lb transition temperature increase of 216.59°F. This results in an irradiated 30 ft-lb transition temperature of 100.47°F and an irradiated 50 ft-lb transition temperature of 150.54°F.

Irradiation of the correlation monitor material Charpy specimens to 4.49 x 10^{19} n/cm^2 (E > 1.0 MeV) resulted in a 30 ft-lb transition temperature increase of 125.21°F which resulted in an irradiated 30 ft-lb transition temperature of 188.15°F. The tested specimens did not reach the 50 ft-lb transition temperature.

The average upper shelf energy of the intermediate shell plate W10201-4 (longitudinal orientation) resulted in an average energy decrease of 1 ft-lb after irradiation to 4.49 x 10^{19} n/cm^2 (E> 1.0 MeV). This results in an irradiated average upper shelf energy of 94 ft-lb for the longitudinally oriented specimens.

The average upper shelf energy of the weld metal Charpy specimens resulted in an average energy decrease of 33 ft-lb after irradiation to 4.49 x 10^{19} n/cm^2 (E> 1.0 MeV). Hence, this results in an irradiated average upper shelf energy of 80 ft-lb for the weld metal specimens.

The average upper shelf energy of the weld HAZ metal Charpy specimens resulted in an average energy decrease of 24 ft-lb after irradiation to 4.49 x 10^{19} n/cm^2 (E > 1.0 MeV). Hence, this results in an irradiated average upper shelf energy of 105 ft-lb for the weld HAZ metal.

The average upper shelf energy of the correlation monitor material Charpy specimens resulted in no energy decrease after irradiation to 4.49 x 10^{19} n/cm^2 (E > 1.0 MeV). Hence, this results in an irradiated average upper shelf energy of 42 ft-lb for the correlation monitor material.

A comparison of the H.B. Robinson Unit 2 reactor vessel beltline material test results with the Regulatory Guide 1.99, Revision 2[1], predictions led to the following conclusions:

- The measured 30 ft-lb shift in transition temperature values of the intermediate shell plate W10201-4 contained in capsule X (longitudinal) is greater than the Regulatory Guide 1.99, Revision 2, predictions. However, the shift value is less than two sigma allowance by Regulatory Guide 1.99, Revision 2.

- The measured 30 ft-lb shift in transition temperature values of the weld metal contained in capsule X (longitudinal) is less than the Regulatory Guide 1.99, Revision 2, predictions.

- The measured percent decrease in upper shelf energy of the Capsule X surveillance material is less than the Regulatory Guide 1.99, Revision 2, predictions.

The fracture appearance of each irradiated Charpy specimen from the various surveillance capsule X materials is shown in Figures 5-13 through 5-16 and show an increasingly ductile or tougher appearance with increasing test temperature.

The load-time records for individual instrumented Charpy specimen tests are shown in Appendix A.

The Charpy V-notch data presented in this report is based on a re-plot of all capsule data using CVGRAPH, Version 4.1, which is a hyperbolic tangent curve-fitting program. Hence, Appendix C contains a comparison of the Charpy V-notch shift results for each surveillance material (hand-fitting versus hyperbolic tangent curve-fitting). Additionally, Appendix B presents the CVGRAPH, Version 4.1, Charpy V-notch plots and the program input data.

5.3 TENSILE TEST RESULTS

The results of the tensile tests performed on the various materials contained in capsule X irradiated to 4.49×10^{19} n/cm^2 (E > 1.0 MeV) are presented in Table 5-11 and are compared with unirradiated results as shown in Figures 5-17 and 5-18.

The results of the tensile tests performed on the intermediate shell plate W10201-4 (transverse orientation) indicated that irradiation to 4.49×10^{19} n/cm^2 (E> 1.0 MeV) caused an approximate increase of 9 to 10 ksi in the 0.2 percent offset yield strength and approximately a 7 to 9 ksi increase in the ultimate tensile strength when compared to unirradiated data[1] (Figure 5-17).

The results of the tensile tests performed on the surveillance weld metal indicated that irradiation to 4.49×10^{19} n/cm^2 (E > 1.0 MeV) caused a 28 to 30 ksi increase in the 0.2 percent offset yield strength and a 22 to 28 ksi increase in the ultimate tensile strength when compared to unirradiated data (Figure 5-18).

The fractured tensile specimens for the intermediate shell plate W10201-4 material are shown in Figure 5-19, while the fractured tensile specimens for the surveillance weld metal are shown in Figures 5-20, respectively.

The engineering stress-strain curves for the tensile tests are shown in Figures 5-21 and 5-22.

Table 5-1 Charpy V-notch Data for the H.B. Robinson Unit 2 Intermediate Shell Plate W10201-4 Irradiated to a Fluence of 4.49 x 10^{19} n/cm^2 (E> 1.0 MeV) (Longitudinal Orientation)

Sample	Temperature		Impact Energy		Lateral Expansion		Shear
Number	F	C	ft-lbs	Joules	mils	mm	%
C42	25	-4	11	15	5	0.13	10
C44	80	27	37	50	25	0.64	25
C48	100	38	22	30	18	0.46	20
C45	125	52	62	84	40	1.02	50
C46	150	66	73	99	45	1.14	60
C41	250	121	99	134	60	1.52	100
C43	325	163	92	125	57	1.45	100
C47	350	177	91	123	57	1.45	100

Table 5-2 Charpy V-notch Data for the H.B. Robinson Unit 2 Surveillance Weld Metal Irradiated to a Fluence of 4.49 x 10^{19} n/cm^2 (E> 1.0 MeV)

Sample	Temperature		Impact Energy		Lateral Expansion		Shear
Number	F	C	ft-lbs	Joules	mils	mm	%
W3	0	-18	4	5	0	0.00	0
W2	100	38	14	19	4	0.10	15
W6	175	79	28	38	16	0.41	35
W4	200	93	38	52	22	0.56	40
W8	250	121	74	100	49	1.24	100
W7	350	177	78	106	51	1.30	100
W5	375	191	85	115	56	1.42	100
W1	425	218	82	111	54	1.37	100

Table 5-3 Charpy V-notch Data for the H.B. Robinson Unit 2 Heat Affected Zone (HAZ) Material Irradiated to a Fluence of 4.49 x 10^{19} n/cm^2 (E> 1.0 MeV)

Sample	Temperature		Impact Energy		Lateral Expansion		Shear
Number	F	C	ft-lbs	Joules	mils	mm	%
H2	-50	-46	25	34	12	0.30	15
H7	0	-18	18	24	6	0.15	5
H6	25	-4	13	18	3	0.08	5
H5	100	38	24	33	9	0.23	25
H4	150	66	46	62	28	0.71	55
H3	250	121	90	122	63	1.60	100
H8	375	191	120	163	74	1.88	100
H1	400	204	106	144	59	1.50	100

Table 5-4 Charpy V-notch Data for the H.B. Robinson Unit 2 Correlation Monitor Material Irradiated to a Fluence of 4.49 x 10^{19} n/cm^2 (E> 1.0 MeV)

Sample	Temperature		Impact Energy		Lateral Expansion		Shear
Number	F	C	ft-lbs	Joules	mils	mm	%
R41	30	-1	2	3	0	0.00	5
R45	100	38	25	34	14	0.36	40
R48	150	66	18	24	10	0.25	30
R43	200	93	27	37	17	0.43	65
R46	225	107	38	52	28	0.71	95
R47	300	149	43	58	31	0.79	100
R42	325	163	44	60	29	0.74	100
R44	425	218	39	53	30	0.76	100

Table 5-5 Instrumented Charpy Impact Test Results for the H.B. Robinson Unit 2 Intermediate Shell Plate W10201-4 Irradiated to a Fluence of 4.49 x 10^{19} n/cm^2 (E>1.0 MeV) (Longitudinal Orientation)

Sample No.	Test Temp. (°F)	Charpy Energy E_D (ft-lb)	Normalized Energies (ft-lb/in^2)			Yield Load P_{GY} (lb)	Time to Yield t_{GY} (msec)	Max. Load P_M (lb)	Time to Max. T_m (msec)	Fast Fract. Load P_F (lb)	Arrest Load P_A (lb)	Yield Stress S_Y (ksi)	Flow Stress (ksi)
			Charpy E_D/A	Max. E_M/A	Prop. E_p/A								
C42	25	11	89	44	45	3745	0.17	3788	0.18	3783	0	125	125
C44	80	37	298	202	97	3589	0.17	4268	0.48	4159	454.73	120	131
C48	100	22	177	32	146	3098	0.16	3102	0.16	3098	1022.55	103	103
C45	125	62	500	219	280	3429	0.17	4218	0.53	3822	1125	114	127
C46	150	73	588	205	384	3469	0.17	4164	0.50	3467	1559	116	127
C41	250	99	798	281	517	3227	0.17	4074	0.67	n/a	n/a	107	122
C43	325	92	741	207	534	3225	0.17	4015	0.53	n/a	n/a	107	121
C47	350	91	733	185	548	3214	0.17	3862	0.49	n/a	n/a	107	118

Table 5-6 Instrumented Charpy Impact Test Results for the H.B. Robinson Unit 2 Surveillance Weld Metal Irradiated to a Fluence of 4.49 x 10^{19} n/cm^2 (E>1.0 MeV)

Sample No.	Test Temp. (°F)	Charpy Energy E_D (ft-lb)	Normalized Energies (ft-lb/in^2)			Yield Load P_{GY} (lb)	Time to Yield t_{GY} (msec)	Max. Load P_M (lb)	Time to Max. T_m (msec)	Fast Fract. Load P_F (lb)	Arrest Load P_A (lb)	Yield Stress S_Y (ksi)	Flow Stress (ksi)
			Charpy E_D/A	Max. E_M/A	Prop. E_p/A								
W3	0	4	32	17	15	2201	0.12	2214	0.13	2201	0	73	74
W2	100	14	113	70	43	4204	0.17	4615	0.22	4593	0	140	147
W6	175	28	226	71	155	3994	0.17	4380	0.23	4194	707	133	139
W4	200	38	306	213	93	3967	0.17	4582	0.47	4482	1090	132	142
W8	250	74	596	223	373	3898	0.17	4535	0.49	n/a	n/a	130	140
W7	350	78	628	231	397	3808	0.17	4450	0.52	n/a	n/a	127	138
W5	375	85	685	230	455	3873	0.17	4512	0.51	n/a	n/a	129	140
W1	425	82	661	211	450	3477	0.17	4201	0.51	n/a	n/a	116	128

Table 5-7 Instrumented Charpy Impact Test Results for the H.B. Robinson Unit 2 Heat Affected Zone (HAZ) Material Irradiated to a Fluence of 4.49 x 10^{19} n/cm^2 (E>1.0 MeV)

Sample No.	Test Temp. (°F)	Charpy Energy E_D (ft-lb)	Normalized Energies (ft-lb/in^2)			Yield Load P_{GY} (lb)	Time to Yield t_{GY} (msec)	Max. Load P_M (lb)	Time to Max. T_m (msec)	Fast Fract. Load P_F (lb)	Arrest Load P_A (lb)	Yield Stress S_Y (ksi)	Flow Stress (ksi)
			Charpy E_D/A	Max. E_M/A	Prop. E_p/A								
H2	-50	25	201	74	128	4351	0.17	4747	0.22	4539	0	145	151
H7	0	18	145	71	74	4172	0.17	4593	0.22	4403	0	139	146
H6	25	13	105	66	39	4326	0.17	4654	0.21	4652	0	144	150
H5	100	24	193	68	126	4068	0.17	4406	0.22	4267	171	135	141
H4	150	46	371	197	173	3860	0.17	4454	0.46	4384	2065	129	138
H3	250	90	725	306	420	3460	0.16	4353	0.67	n/a	n/a	115	130
H8	375	120	967	294	673	3477	0.17	4266	0.67	n/a	n/a	116	129
H1	400	106	854	301	554	3540	0.17	4246	0.68	n/a	n/a	118	130

Table 5-8 Instrumented Charpy Impact Test Results for the H.B. Robinson Unit 2 Correlation Monitor Material Irradiated to a Fluence of 4.49 x 10^{19} n/cm^2 (E>1.0 MeV)

Sample No.	Test Temp. (°F)	Charpy Energy E_D (ft-lb)	Normalized Energies (ft-lb/in^2)			Yield Load P_{GY} (lb)	Time to Yield t_{GY} (msec)	Max. Load P_M (lb)	Time to Max. T_m (msec)	Fast Fract. Load P_F (lb)	Arrest Load P_A (lb)	Yield Stress S_Y (ksi)	Flow Stress (ksi)
			Charpy E_D/A	Max. E_M/A	Prop. E_p/A								
R41	30	2	16	8	8	1155	0.11	1165	0.1	1155	0	38	39
R45	100	25	201	71	131	3886	0.17	4248	0.23	4092	896	129	135
R48	150	18	145	62	83	3749	0.17	4061	0.22	4057	605	125	130
R43	200	27	218	68	149	3669	0.17	4028	0.23	3917	1858	122	128
R46	225	38	306	121	185	3728	0.17	4108	0.33	3965	2009	124	130
R47	300	43	346	142	204	3231	0.18	4048	0.4	n/a	n/a	108	121
R42	325	44	355	153	202	3620	0.17	4156	0.39	n/a	n/a	121	129
R44	425	39	314	68	246	3428	0.17	3744	0.24	n/a	n/a	114	119

Table 5-9 Effect of Irradiation to 4.49 x 10^{19} n/cm^2 (E>1.0 MeV) on the Notch Toughness Properties of the H.B. Robinson Unit 2 Reactor Vessel Surveillance Materials

Material	Average 30 (ft-lb)[a] Transition Temperature (°F)			Average 35 mil Lateral[b] Expansion Temperature (°F)			Average 50 ft-lb[a] Transition Temperature (°F)			Average Energy Absorption[a] at Full Shear (ft-lb)		
	Unirradiated	Irradiated	ΔT	Unirradiated	Irradiated	ΔT	Unirradiated	Irradiated	ΔT	Unirradiated	Irradiated	ΔE
Intermediate Shell Plate W10201-4 (Longitudinal)	-18.17	86.55	104.73	-3.32	120.96	124.28	17.35	116.04	98.68	95	94	-1
Weld Metal	-86.29	179.64	265.93	-60.64	219.24	279.89	-40.35	211.38	251.74	113	80	-33
HAZ Metal	-109.66	100.47	210.13	-84.08	164.51	248.60	-66.04	150.54	216.59	129	105	-24
Correlation Monitor Material	62.94	188.15	125.21	- - -	- - -	- - -	- - -	- - -	- - -	39	42	+3

a. "Average" is defined as the value read from the curve fit through the data points of the Charpy tests (see Figures 5-1, 5-4, 5-7 and 5-10).

b. "Average" is defined as the value read from the curve fit through the data points of the Charpy tests (see Figures 5-2, 5-5, 5-8 and 5-11)

Table 5-10 Comparison of the H.B. Robinson Unit 2 Surveillance Material 30 ft-lb Transition Temperature Shifts and Upper Shelf Energy Decreases with Regulatory Guide 1.99, Revision 2, Predictions

Material	Capsule	Fluence ($x\ 10^{19}$ n/cm^2)	30 ft-lb Transition Temperature Shift		Upper Shelf Energy Decrease	
			Predicted (°F) [(a)]	Measured (°F) [(b)]	Predicted (%) [(a)]	Measured (%) [(c)]
Inter. Shell Plate W10201-4 (Longitudinal)	S	0.479	45.39	32.51	18	10
	X	4.49	78.86	104.73	30	1
Surveillance Program Weld Metal	V	0.530	179.17	209.32	39	38
	T	3.87	293.68	288.15	52	46
	X	4.49	300.64	265.93	54	29
Heat Affected Zone Material	V	0.530	- -	59.21	- - -	26
	T	3.87	- -	(d)	- - -	24
	X	4.49	- -	210.13	- - -	19
Correlation Monitor Material	S	0.479	- -	72.79	- - -	3
	V	0.530	- -	69.39	- - -	5
	T	3.87	- -	156.83	- - -	5
	X	4.49	- -	125.21	- - -	0

Notes:

(a) Based on Regulatory Guide 1.99, Revision 2, methodology using the mean weight percent values of copper and nickel of the surveillance material.

(b) Calculated using measured Charpy data plotted using CVGRAPH, Version 4.1 (See Appendix B)

(c) Values are based on the definition of upper shelf energy given in ASTM E185-82.

(d) Only 2 specimens were tested from capsule T to confirm the upper shelf energy, thus, there is insufficient data to determine the measured 30 ft-lb shift.

Table 5-11 Tensile Specimens From Intermediate Shell Course Plate W10201-4 and Weld Material

Sample Number	Sample Material	Test Temperature (°F)	0.2% Yield Strength (ksi)	Ultimate Strength (ksi)	Fracture Load (kip)	Fracture Stress (ksi)	Fracture Strength (ksi)	Uniform Elongation (%)	Total Elongation (%)	Reduction in Area (%)
C 6	PLATE	200	69.3	87.6	2.80	123.4	57.0	9.9	19.3	54
C 7	PLATE	550	66.2	89.6	3.80	138.4	77.4	10.5	17.1	44
W 1	WELD	275	91.2	105.3	3.75	186.5	76.4	9.5	19.8	59
W 2	WELD	550	87.6	101.7	4.10	166.6	83.5	8.3	16.8	50

INTERMEDIATE SHELL PLATE W10201-4 (LONG.)

CVGRAPH 4.1 Hyperbolic Tangent Curve Printed at 13:57:18 on 10-23-2001

Results

Curve	Fluence	LSE	d-LSE	USE	d-USE	T @ 30	d-T @ 30	T @ 50	d-T @ 50
1	0	2.19	0	95	0	-18.17	0	17.35	0
2	0	2.19	0	85	-10	14.33	32.51	60.2	42.84
3	0	2.19	0	94	-1	86.55	104.73	116.04	98.68

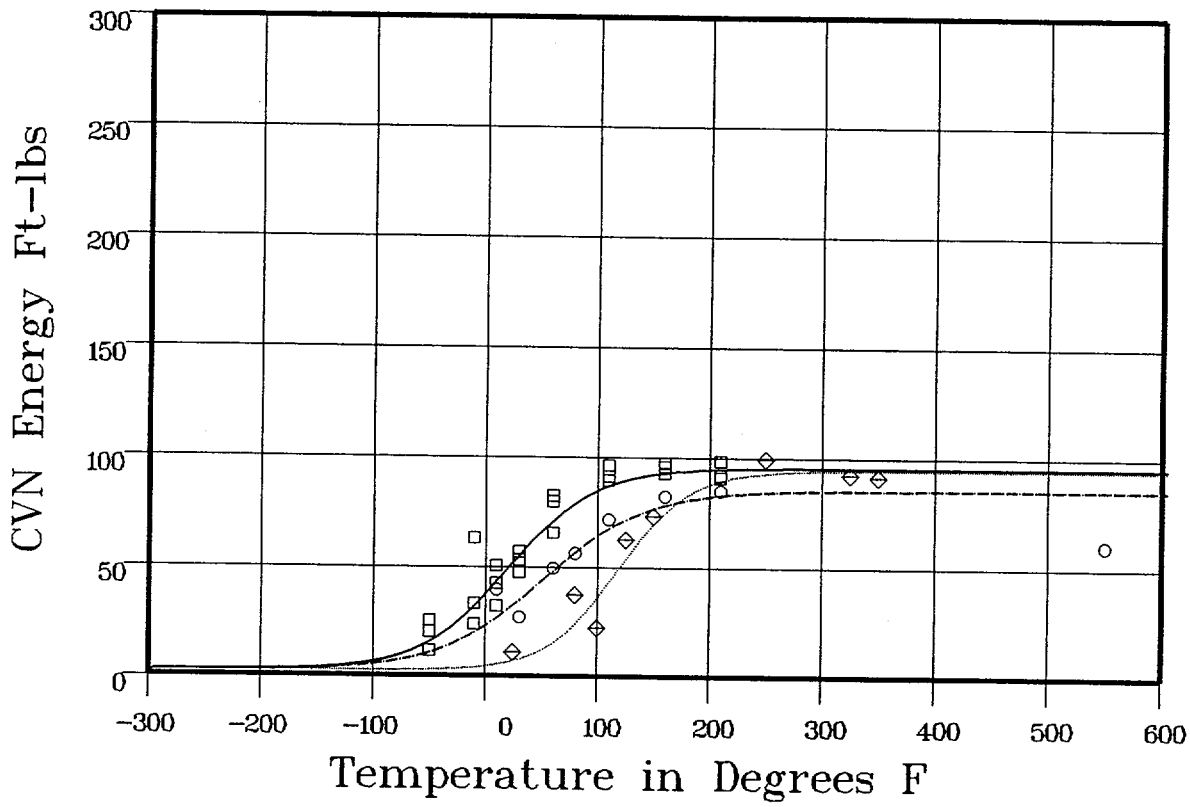

Curve Legend

1 ——— 2 ---------- 3 ———

Data Set(s) Plotted

Curve	Plant	Capsule	Material	Ori.	Heat#
1	HB2	UNIRR	PLATE SA302B	LT	A-6604-1
2	HB2	S	PLATE SA302B	LT	A-6604-1
3	HB2	X	PLATE SA302B	LT	A-6604-1

Figure 5-1 **Charpy V-Notch Impact Energy vs. Temperature for H.B. Robinson Unit 2 Reactor Vessel Intermediate Shell Plate W10201-4 (Longitudinal Orientation)**

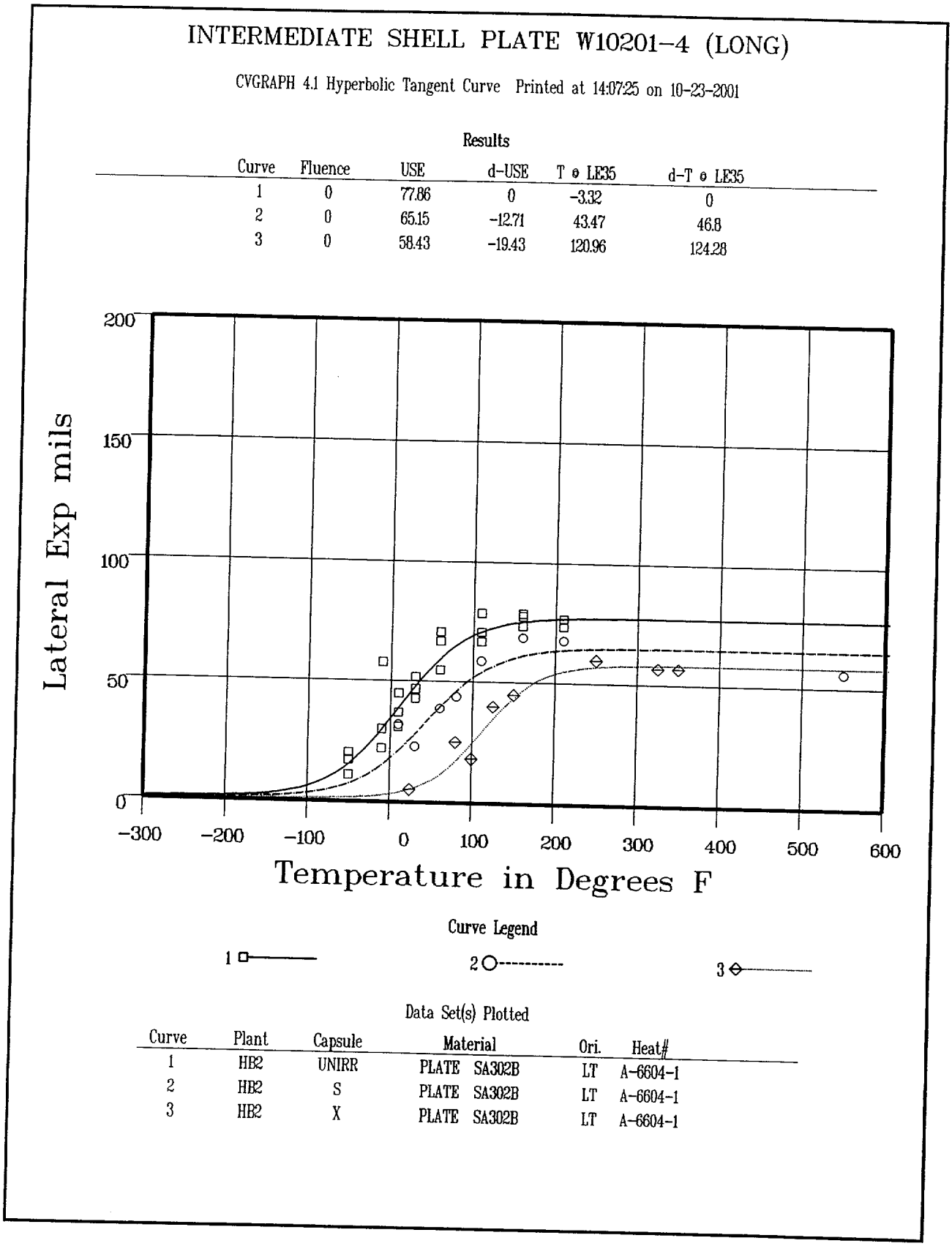

Figure 5-2 **Charpy V-Notch Lateral Expansion vs. Temperature for H.B. Robinson Unit 2 Reactor Vessel Intermediate Shell Plate W10201-4 (Longitudinal Orientation)**

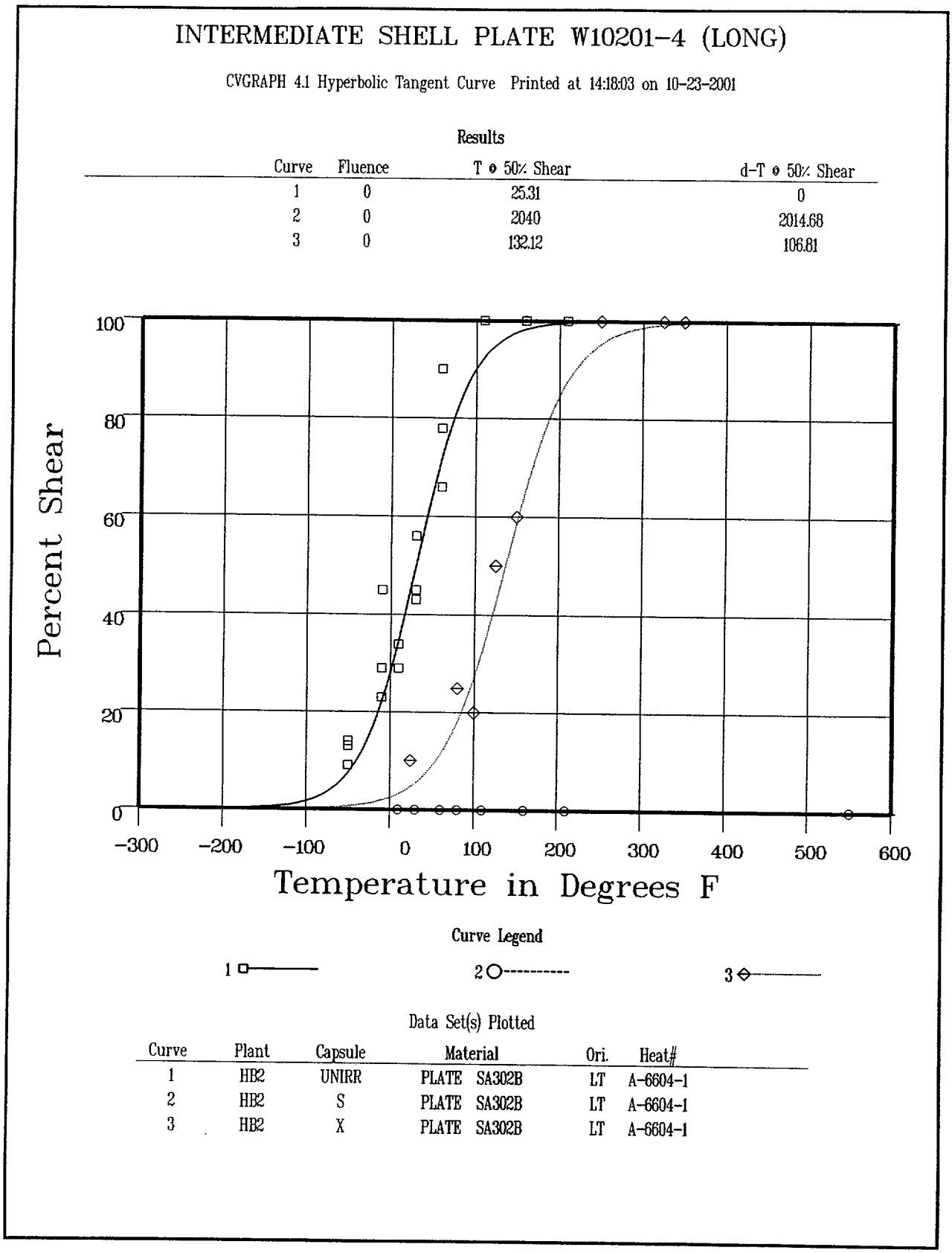

Figure 5-3 **Charpy V-Notch Percent Shear vs. Temperature for H.B. Robinson Unit 2 Reactor Vessel Intermediate Shell Plate W10201-4 (Longitudinal Orientation)**

SURVELLIANCE PROGRAM WELD MATERIAL

CVGRAPH 4.1 Hyperbolic Tangent Curve Printed at 09:54:57 on 10-24-2001

Results

Curve	Fluence	LSE	d-LSE	USE	d-USE	T @ 30	d-T @ 30	T @ 50	d-T @ 50
1	0	2.19	0	113	0	-86.29	0	-40.35	0
2	0	2.19	0	70	-43	123.02	209.32	214.59	254.94
3	0	2.2	0	61	-52	201.86	288.15	205.94	246.3
4	0	2.19	0	80	-33	179.64	265.93	211.38	251.74

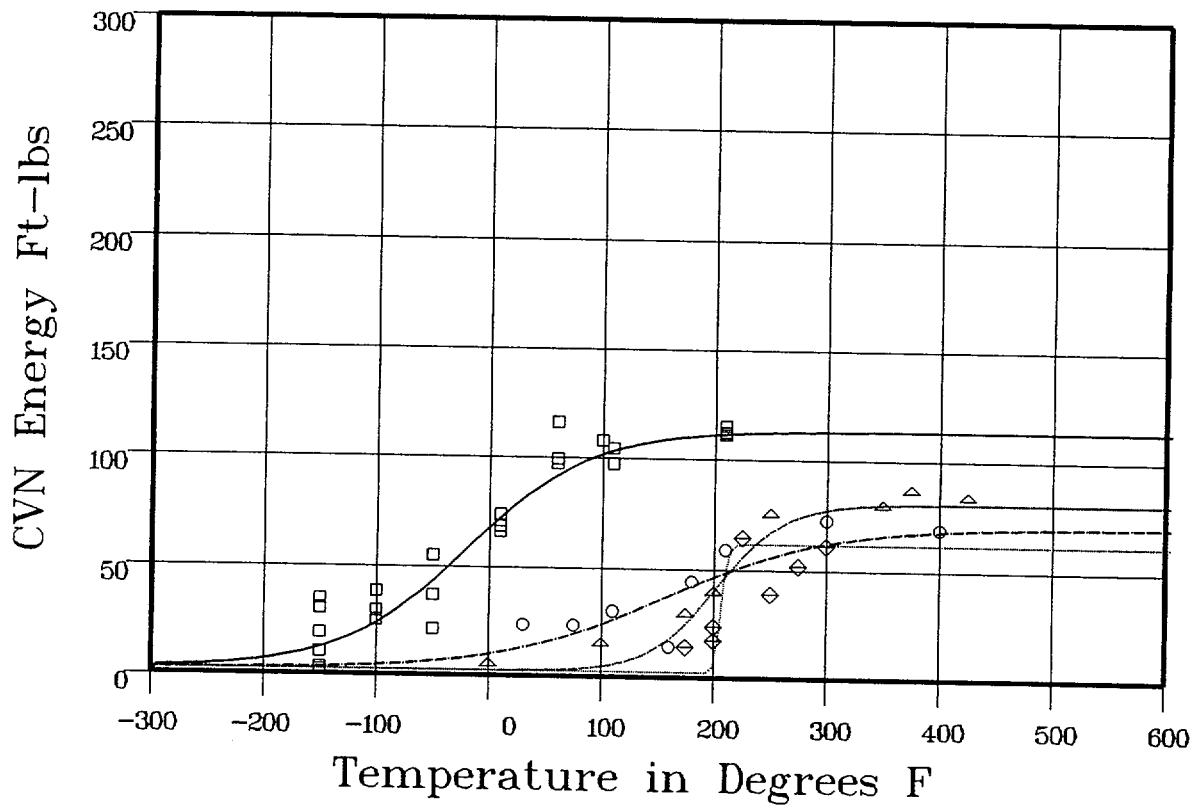

Curve Legend

1 □——— 2 ○---------- 3 ◇——— 4 △———

Data Set(s) Plotted

Curve	Plant	Capsule	Material	Ori.	Heat#
1	HB2	UNIRR	WELD N/A		W5214
2	HB2	V	WELD N/A		W5214
3	HB2	T	WELD N/A		W5214
4	HB2	X	WELD N/A		W5214

Figure 5-4 **Charpy V-Notch Impact Energy vs. Temperature for H.B. Robinson Unit 2 Reactor Vessel Surveillance Weld Metal**

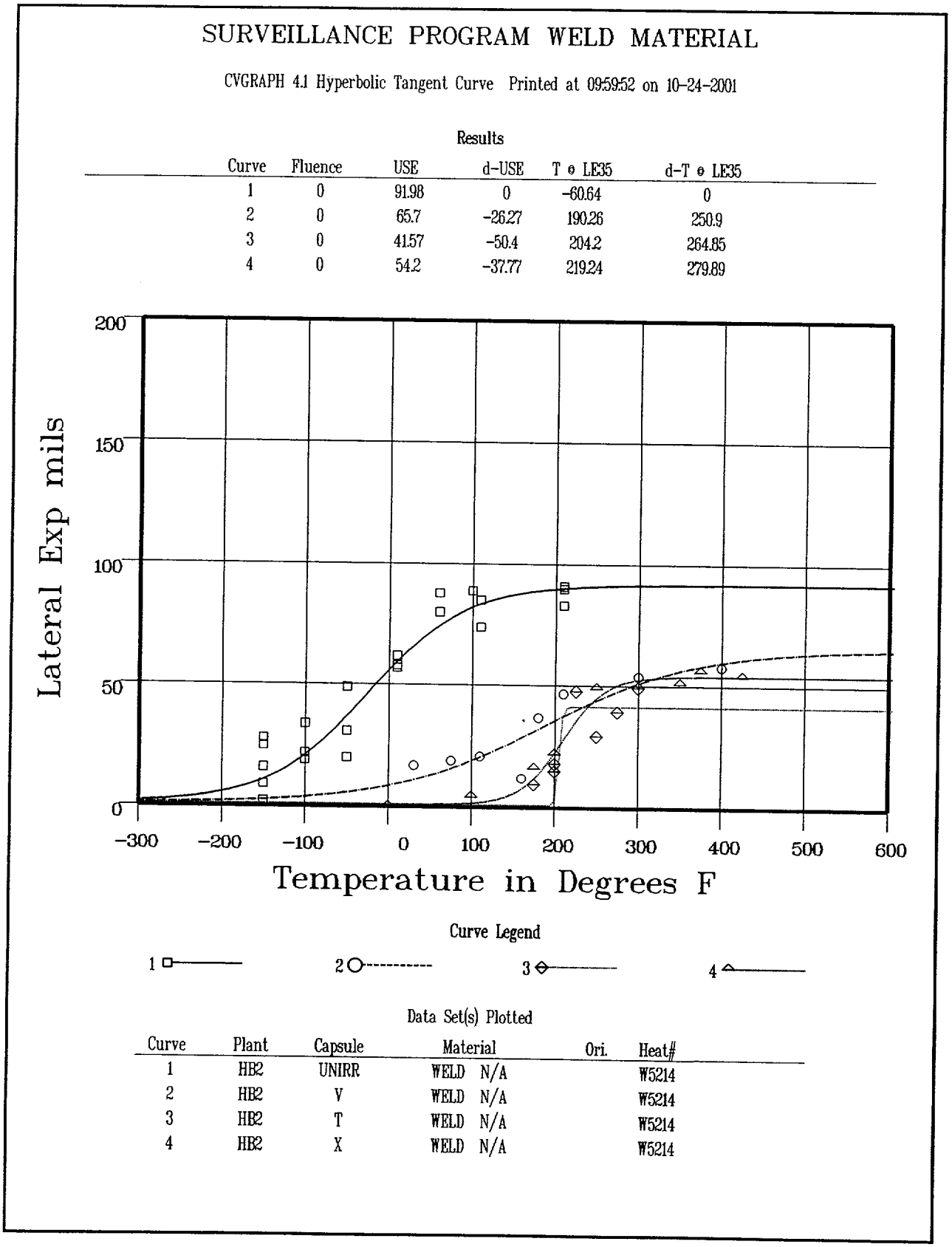

Figure 5-5 **Charpy V-Notch Lateral Expansion vs. Temperature for H.B. Robinson Unit 2 Reactor Vessel Surveillance Weld Metal**

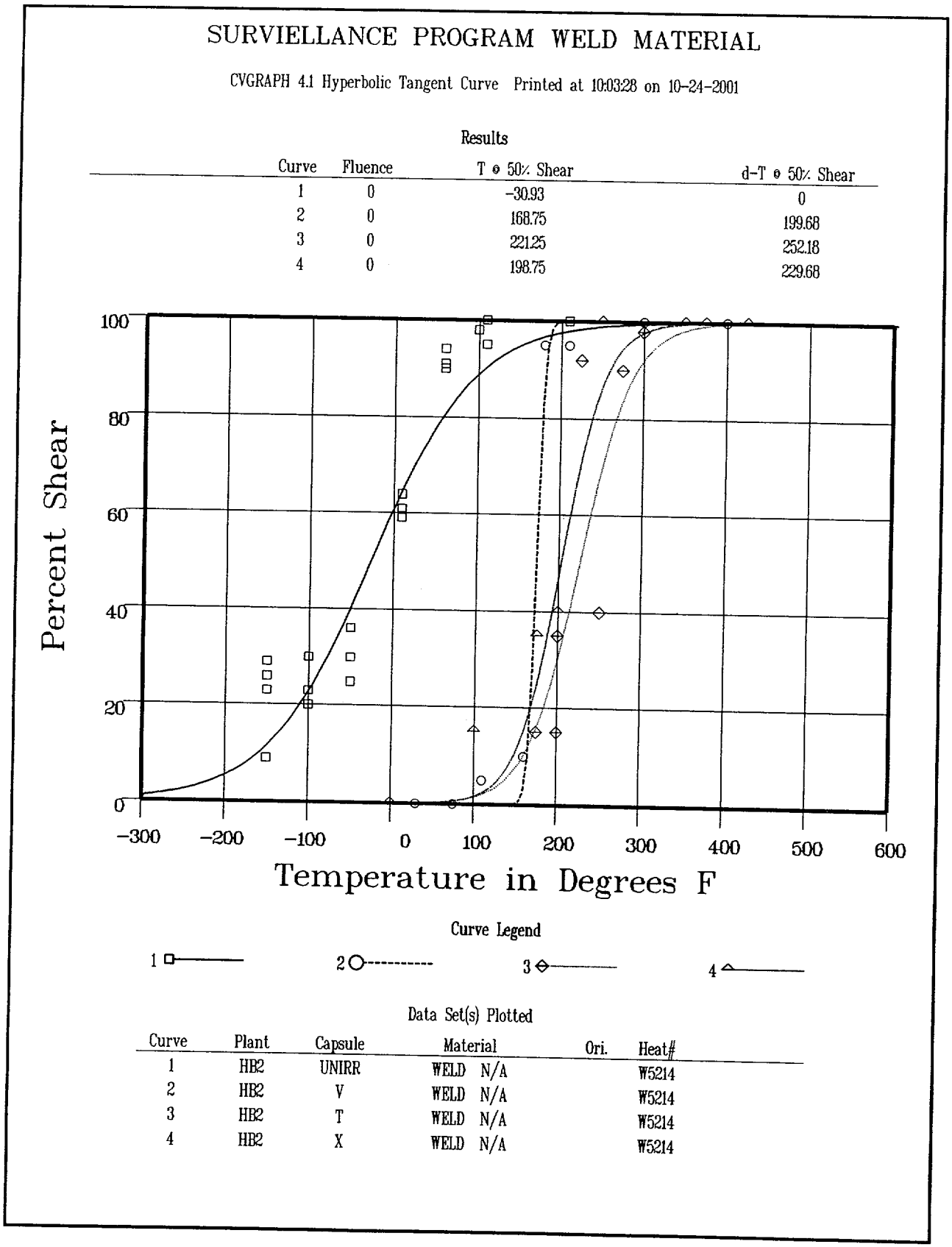

Figure 5-6 **Charpy V-Notch Percent Shear vs. Temperature for H.B. Robinson Unit 2 Reactor Vessel Surveillance Weld Metal**

HEAT AFFECTED ZONE

CVGRAPH 4.1 Hyperbolic Tangent Curve Printed at 10:36:17 on 10-24-2001

Results

Curve	Fluence	LSE	d-LSE	USE	d-USE	T @ 30	d-T @ 30	T @ 50	d-T @ 50
1	0	2.19	0	129	0	-109.66	0	-66.04	0
2	0	2.19	0	96	-33	-50.44	59.21	-.75	65.28
3	0	2.19	0	105	-24	100.47	210.13	150.54	216.59

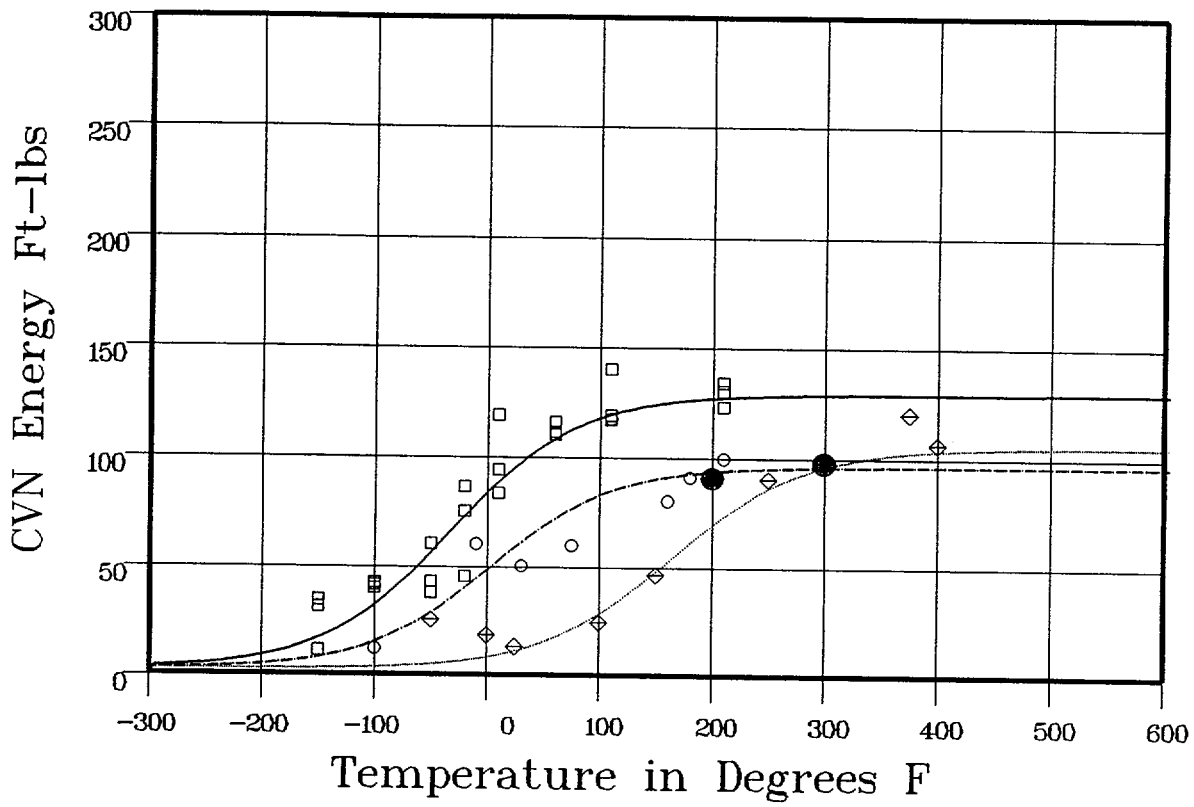

Curve Legend

1 □——— 2 ○---------- 3 ◇——— 4 ●———

Data Set(s) Plotted

Curve	Plant	Capsule	Material	Ori.	Heat#
1	HB2	UNIRR	HEAT AFF'D ZONE SA302B		A-6623-1
2	HB2	V	HEAT AFF'D ZONE SA302B		A-6623-1
3	HB2	X	HEAT AFF'D ZONE SA302B		A-6623-1
4	HB2	T	HEAT AFF'D ZONE SA302B		A-6623-1

Figure 5-7 **Charpy V-Notch Impact Energy vs. Temperature for H.B. Robinson Unit 2 Reactor Vessel Heat Affected Zone Material**

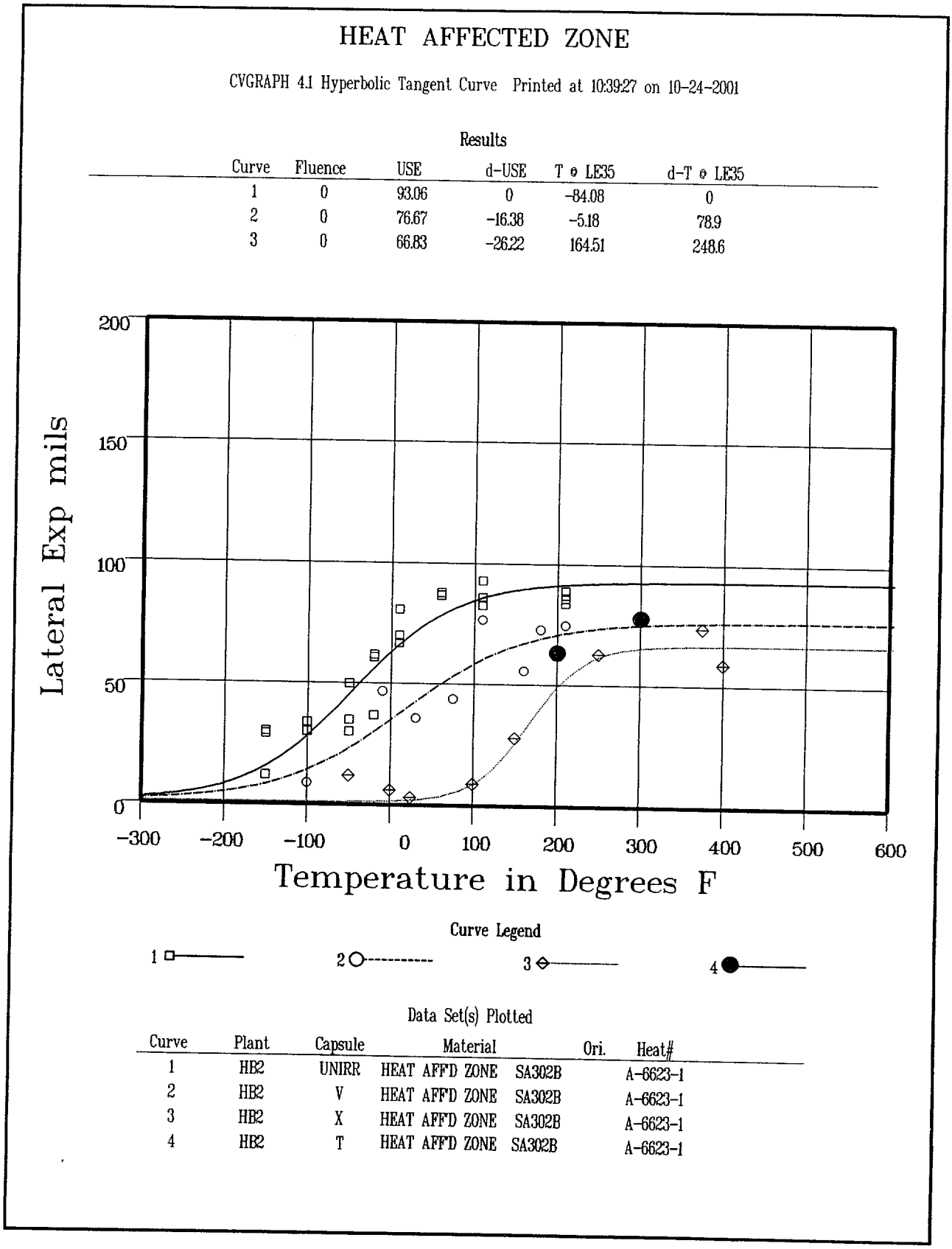

Figure 5-8 **Charpy V-Notch Lateral Expansion vs. Temperature for H.B. Robinson Unit 2 Reactor Vessel Heat Affected Zone Material**

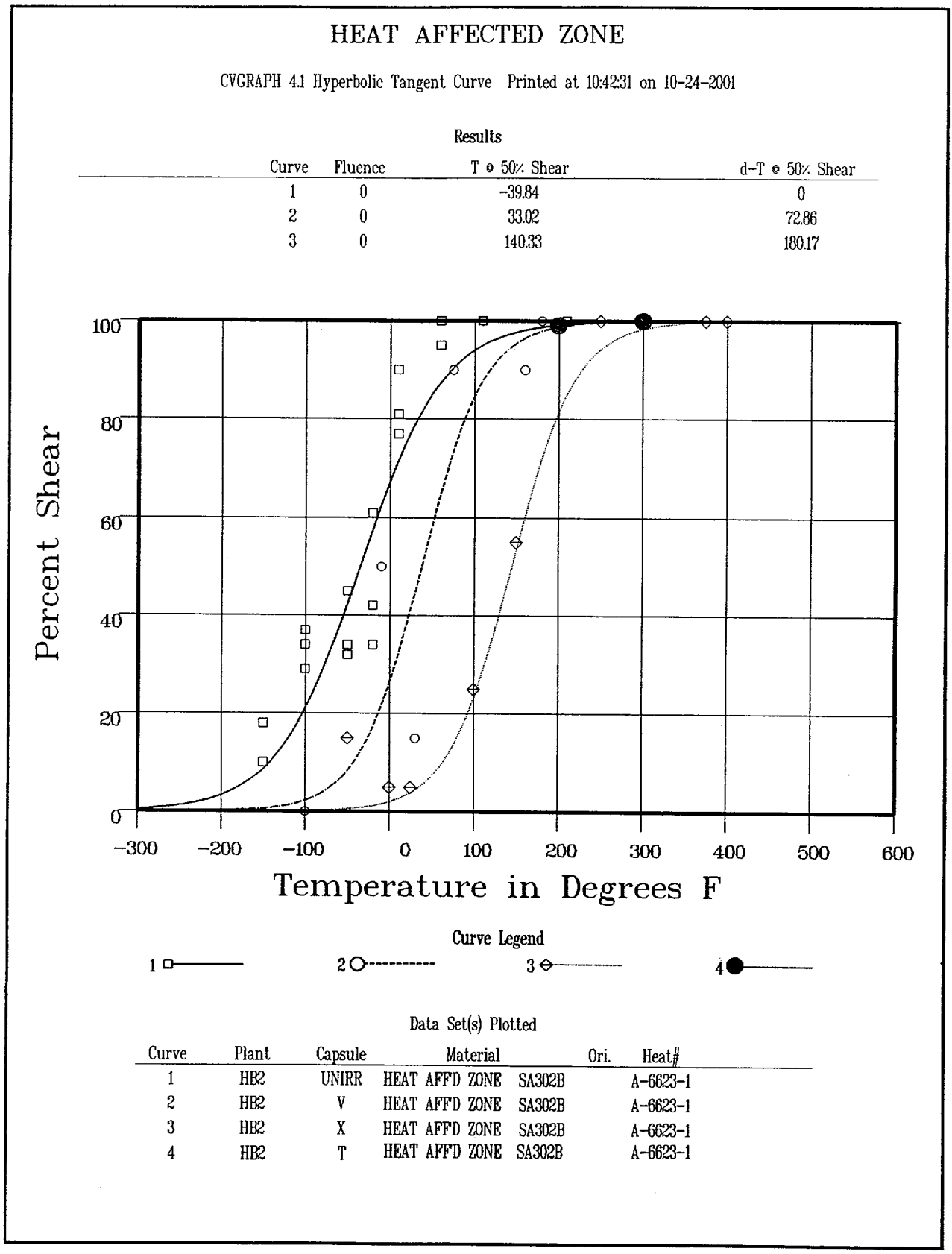

Figure 5-9 **Charpy V-Notch Percent Shear vs. Temperature for H.B. Robinson Unit 2 Reactor Vessel Heat Affected Zone Material**

CORRELATION MONITOR (SRM)

CVGRAPH 4.1 Hyperbolic Tangent Curve Printed at 13:39:15 on 10-24-2001

Results

Curve	Fluence	LSE	d-LSE	USE	d-USE	T @ 30	d-T @ 30	T @ 50	d-T @ 50
1	0	2.2	0	39	0	62.94	0		
2	0	2.2	0	38	-1	135.73	72.79		
3	0	2.2	0	37	-2	132.33	69.39		
4	0	2.2	0	37	-2	219.77	156.83		
5	0	2.2	0	42	3	188.15	125.21		

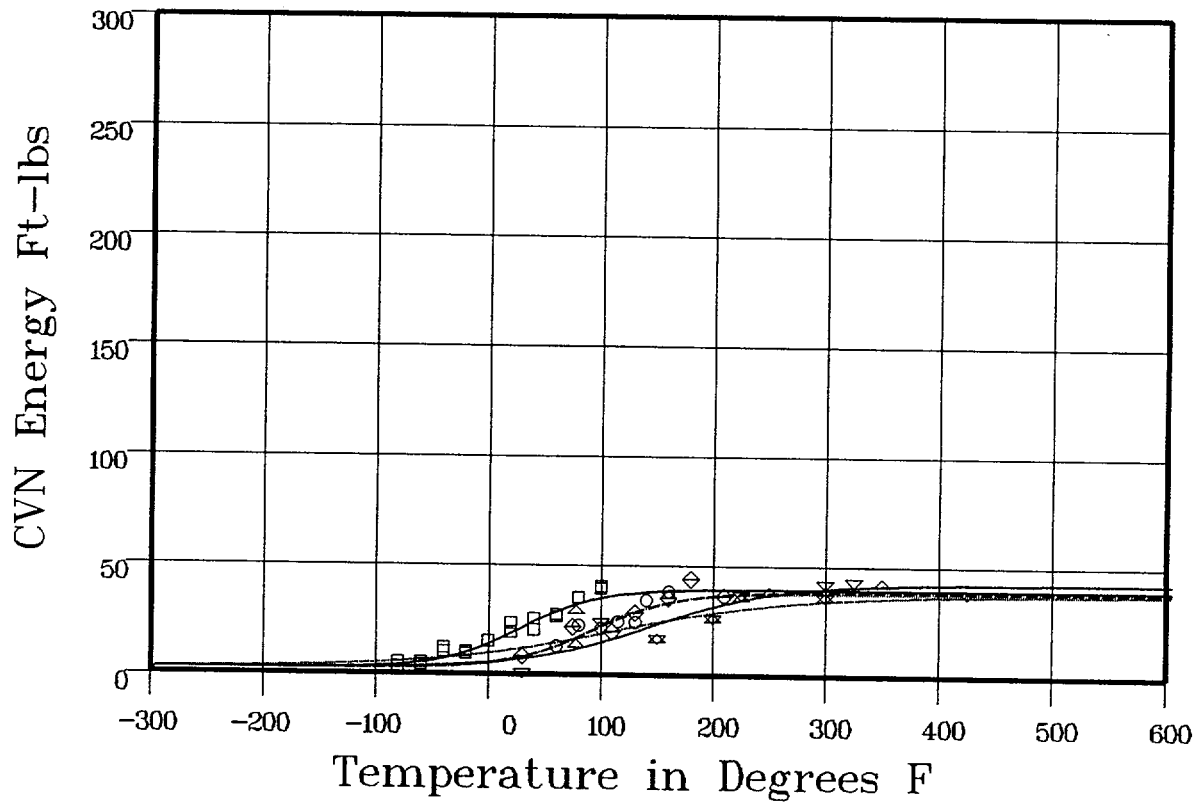

Curve Legend

1 □——— 2 ○---------- 3 ◇——— 4 △——— 5 ▽———

Data Set(s) Plotted

Curve	Plant	Capsule	Material	Ori.	Heat#
1	HB2	UNIRR	SRM SA302B	TL	
2	HB2	S	SRM SA302B	TL	
3	HB2	V	SRM SA302B	TL	
4	HB2	T	SRM SA302B	TL	
5	HB2	X	SRM SA302B	TL	

Figure 5-10 Charpy V-Notch Impact Energy vs. Temperature for H.B. Robinson Unit 2 Reactor Vessel Correlation Monitor Material

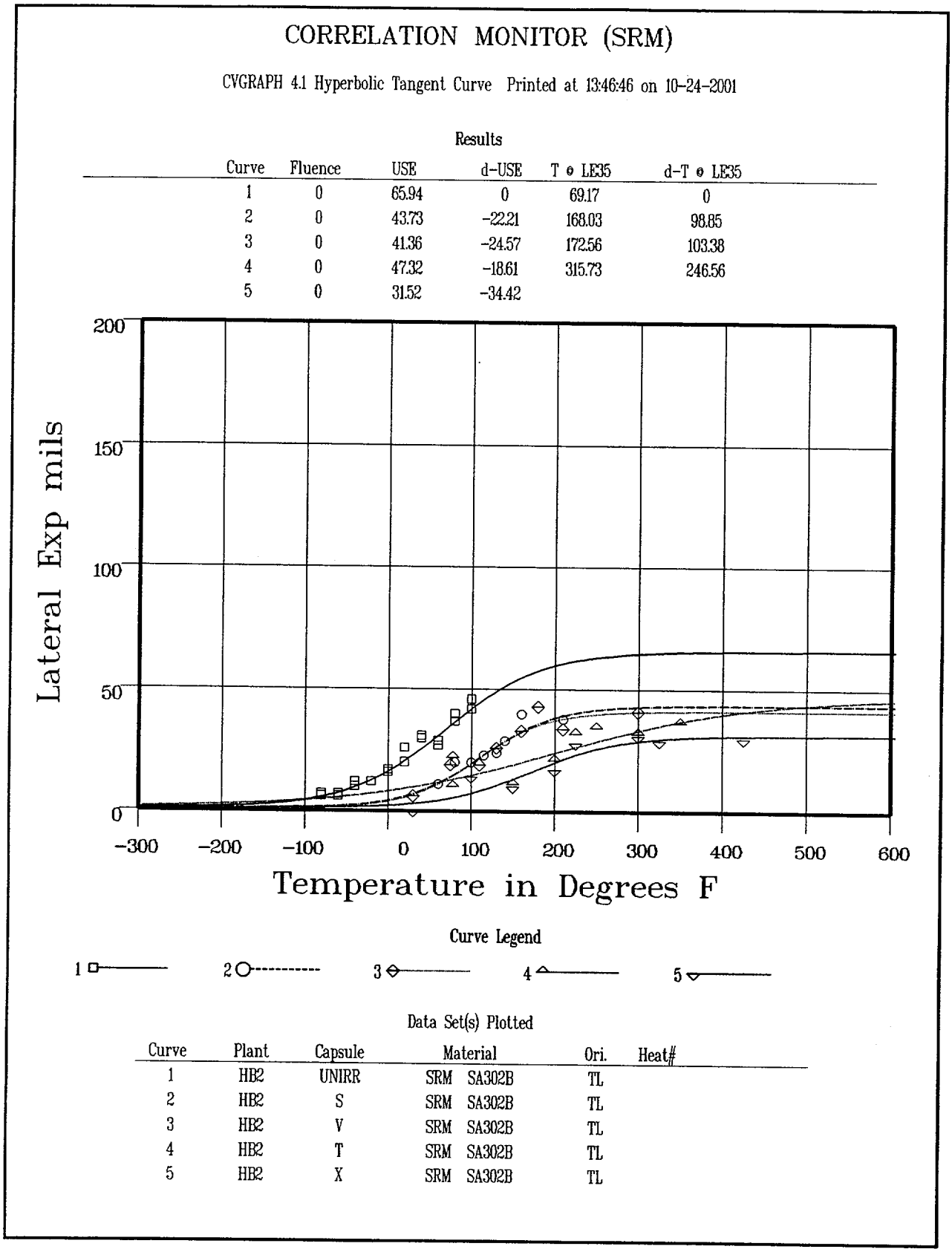

Figure 5-11 **Charpy V-Notch Lateral Expansion vs. Temperature for H.B. Robinson Unit 2 Reactor Vessel Correlation Monitor Material**

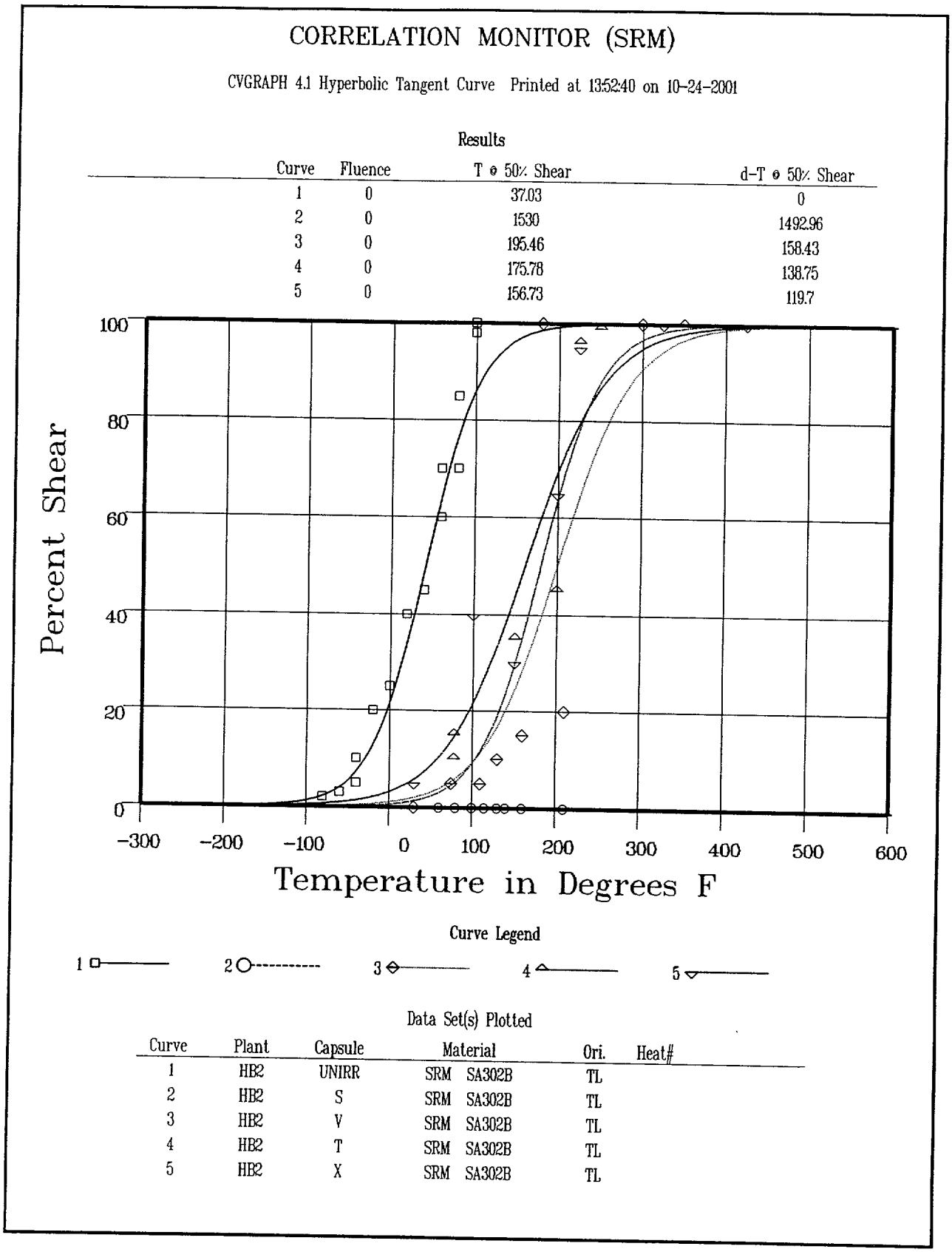

Figure 5-12 **Charpy V-Notch Percent Shear vs. Temperature for H.B. Robinson Unit 2 Reactor Vessel Correlation Monitor Material**

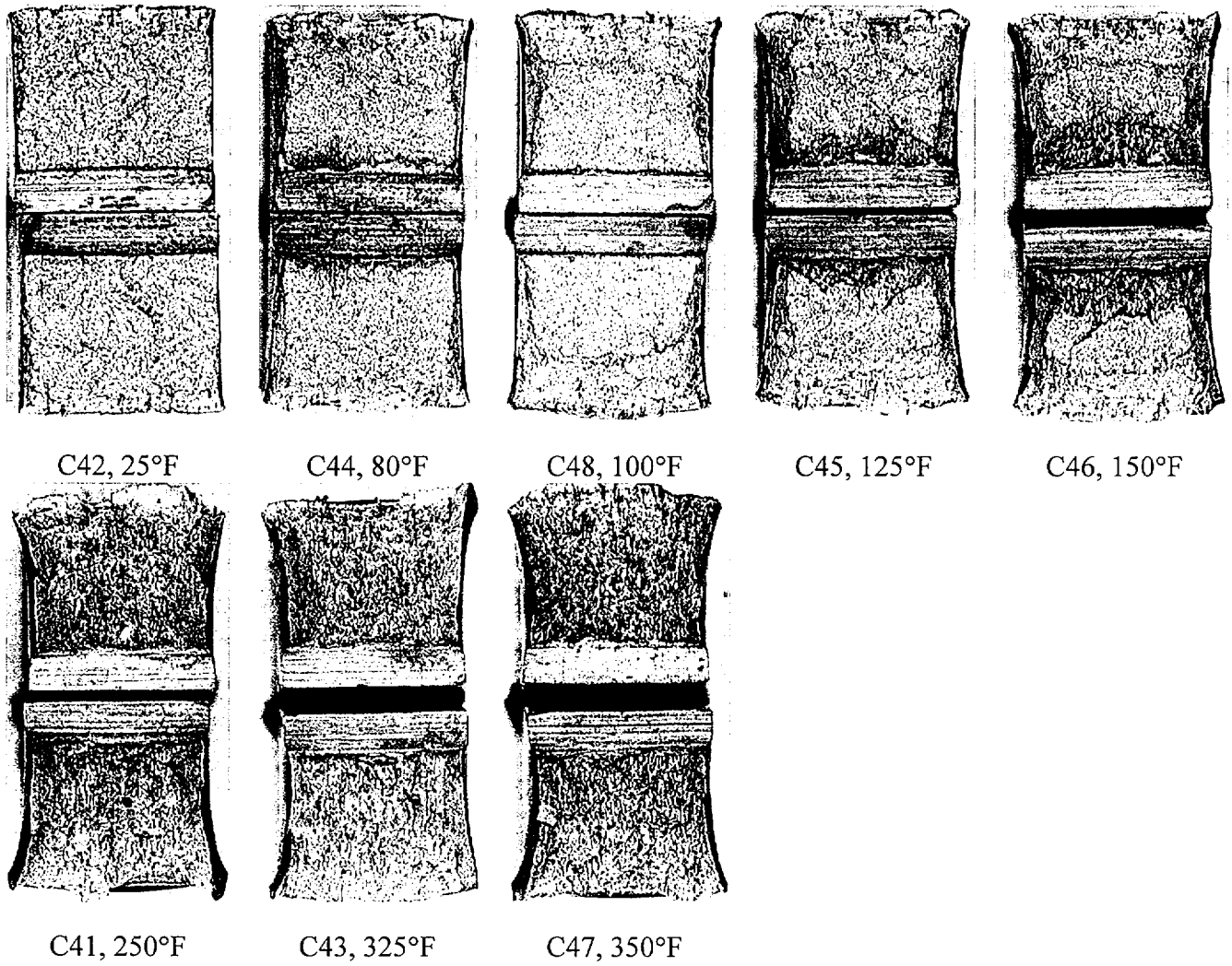

Figure 5-13 Charpy Impact Specimen Fracture Surfaces for H.B. Robinson Unit 2 Reactor Vessel Intermediate Shell Plate W10201-4 (Longitudinal Orientation)

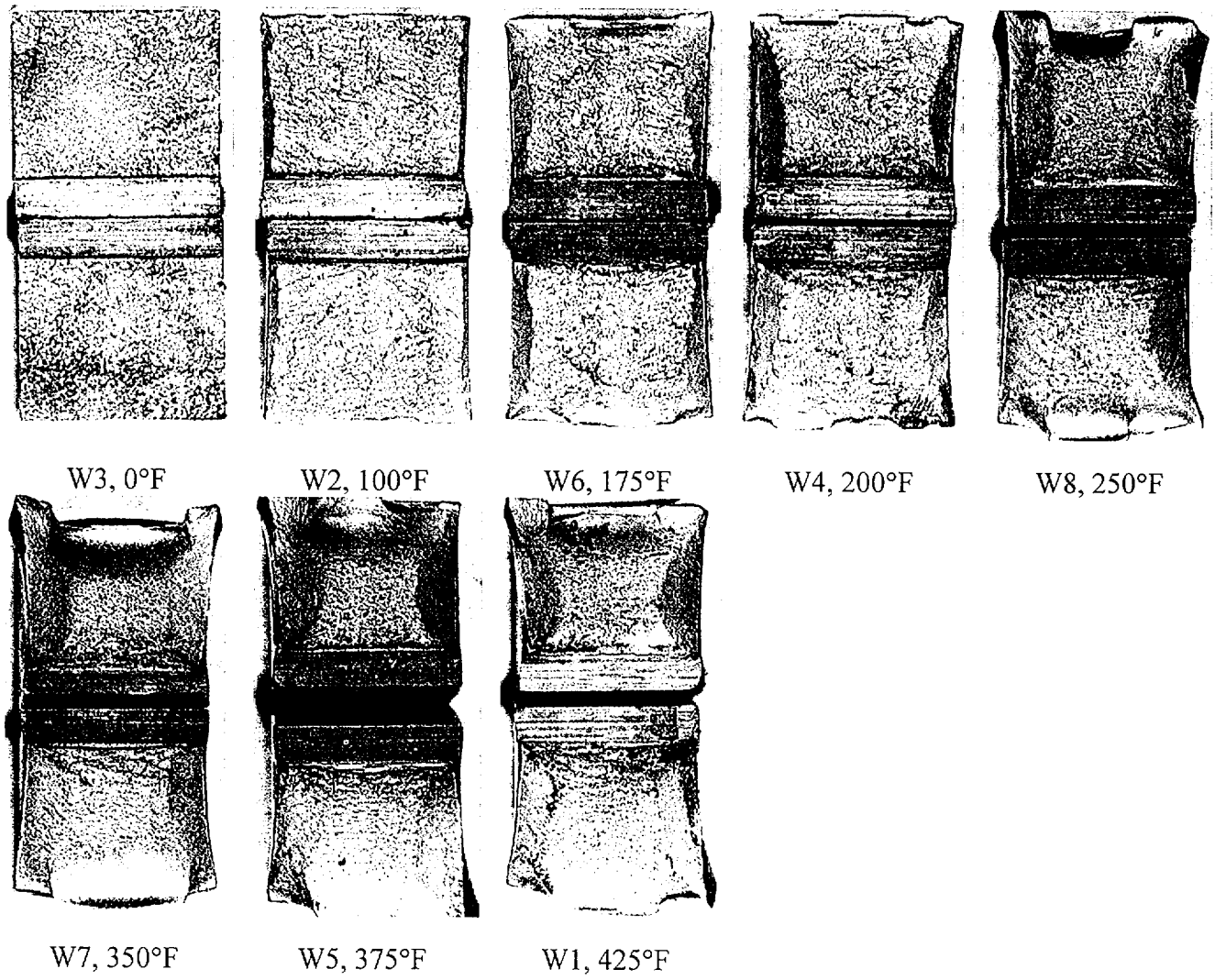

Figure 5-14 Charpy Impact Specimen Fracture Surfaces for H.B. Robinson Unit 2 Reactor Vessel Weld Metal Specimens

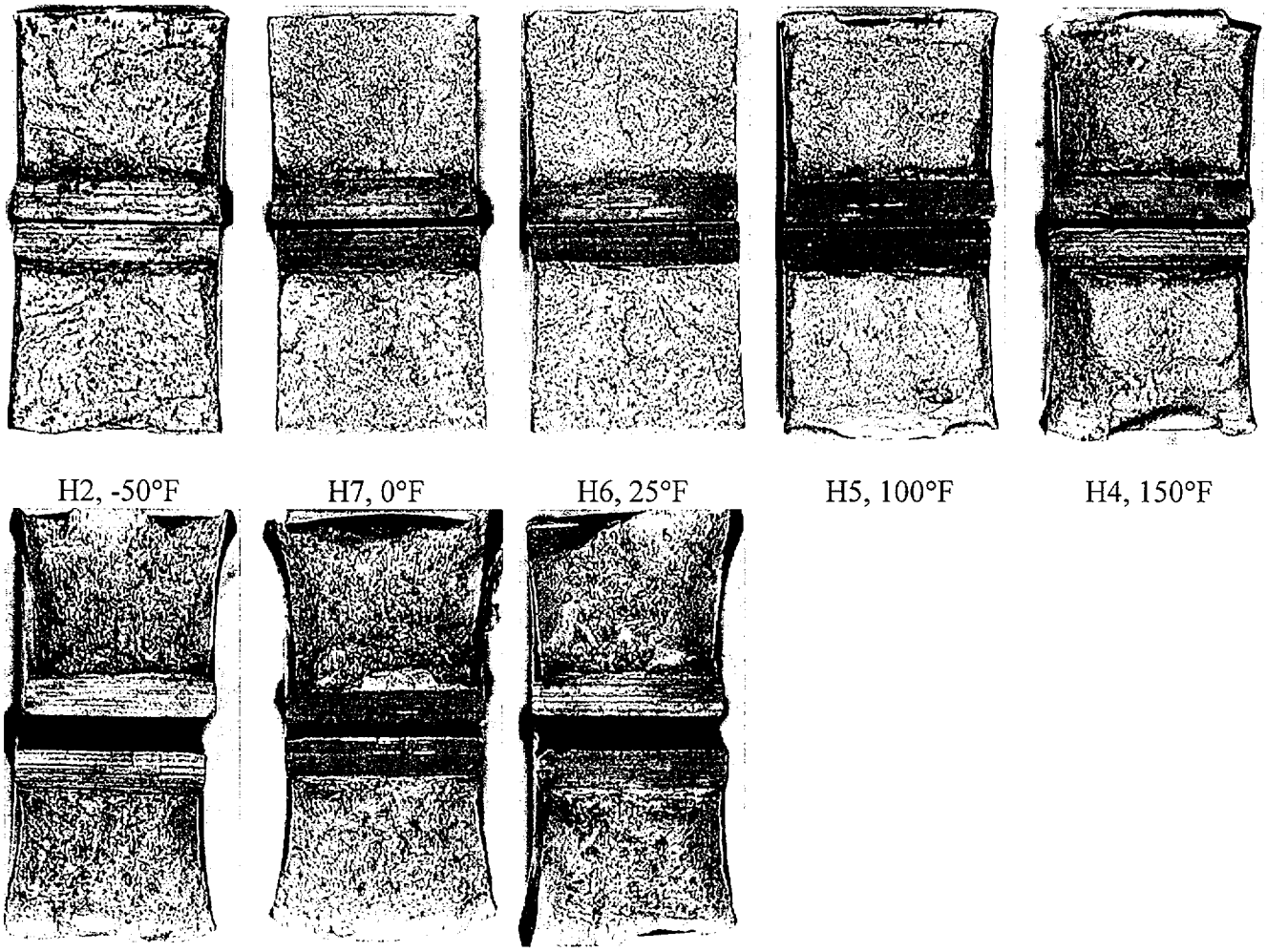

Figure 5-15 Charpy Impact Specimen Fracture Surfaces for St. Lucie Unit 2 Reactor Vessel Heat Affected Zone (HAZ)

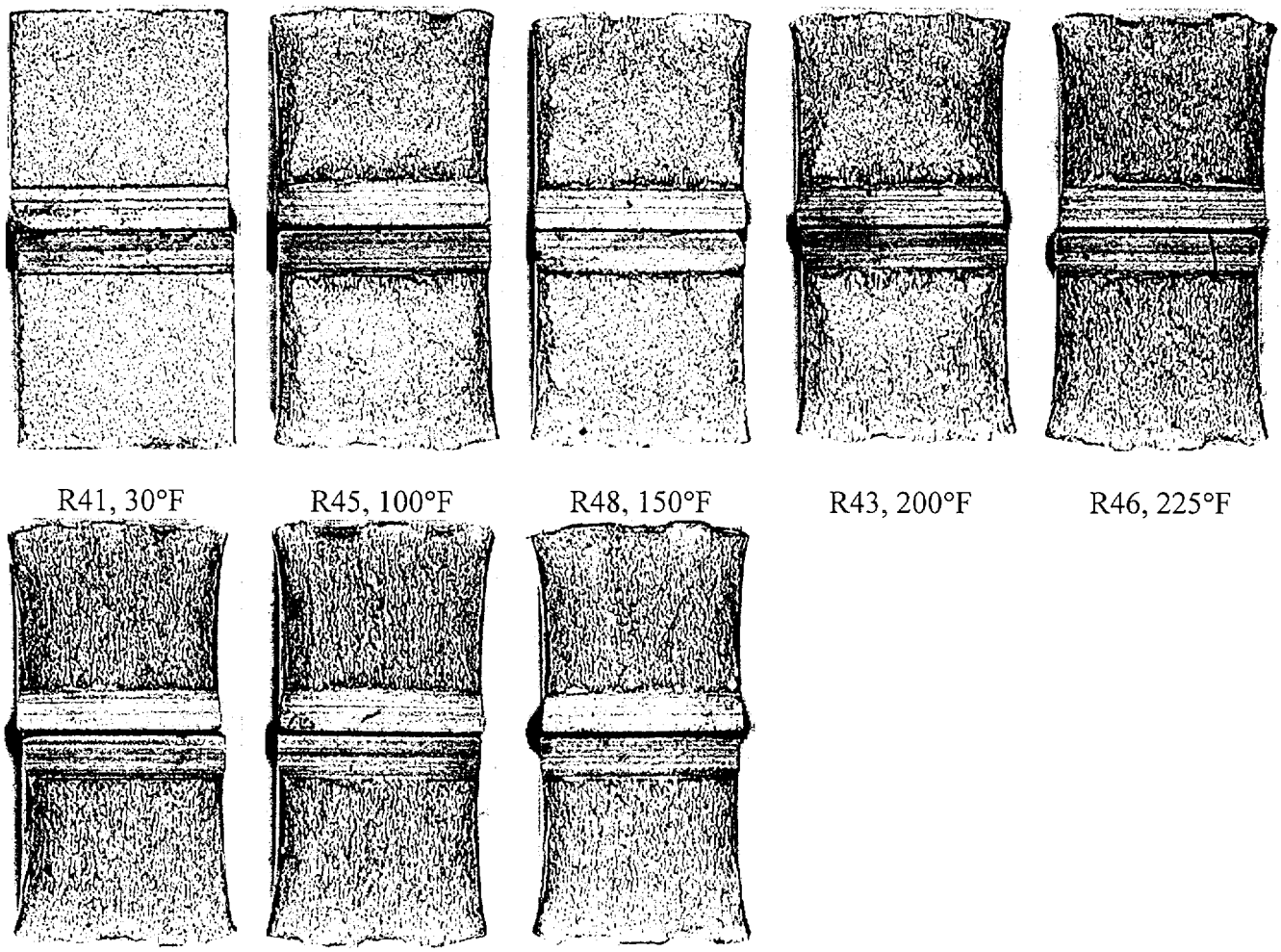

Figure 5-16 Charpy Impact Specimen Fracture Surfaces for H.B. Robinson Unit 2 Reactor Vessel Correlation Monitor Material

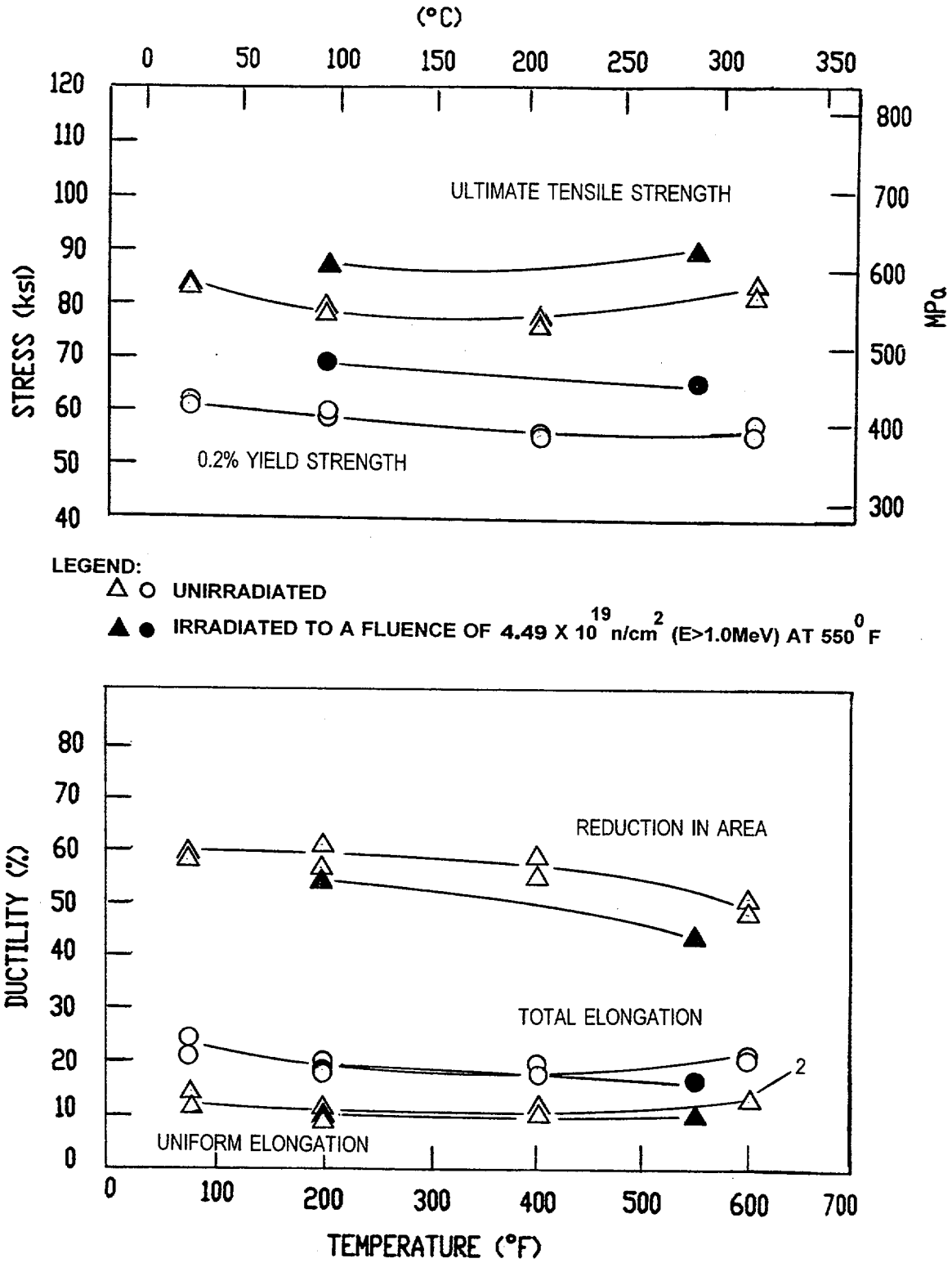

Figure 5-17 **Tensile Properties for H.B. Robinson Unit 2 Reactor Vessel Intermediate Shell Plate W10201-4 (Transverse Orientation)**

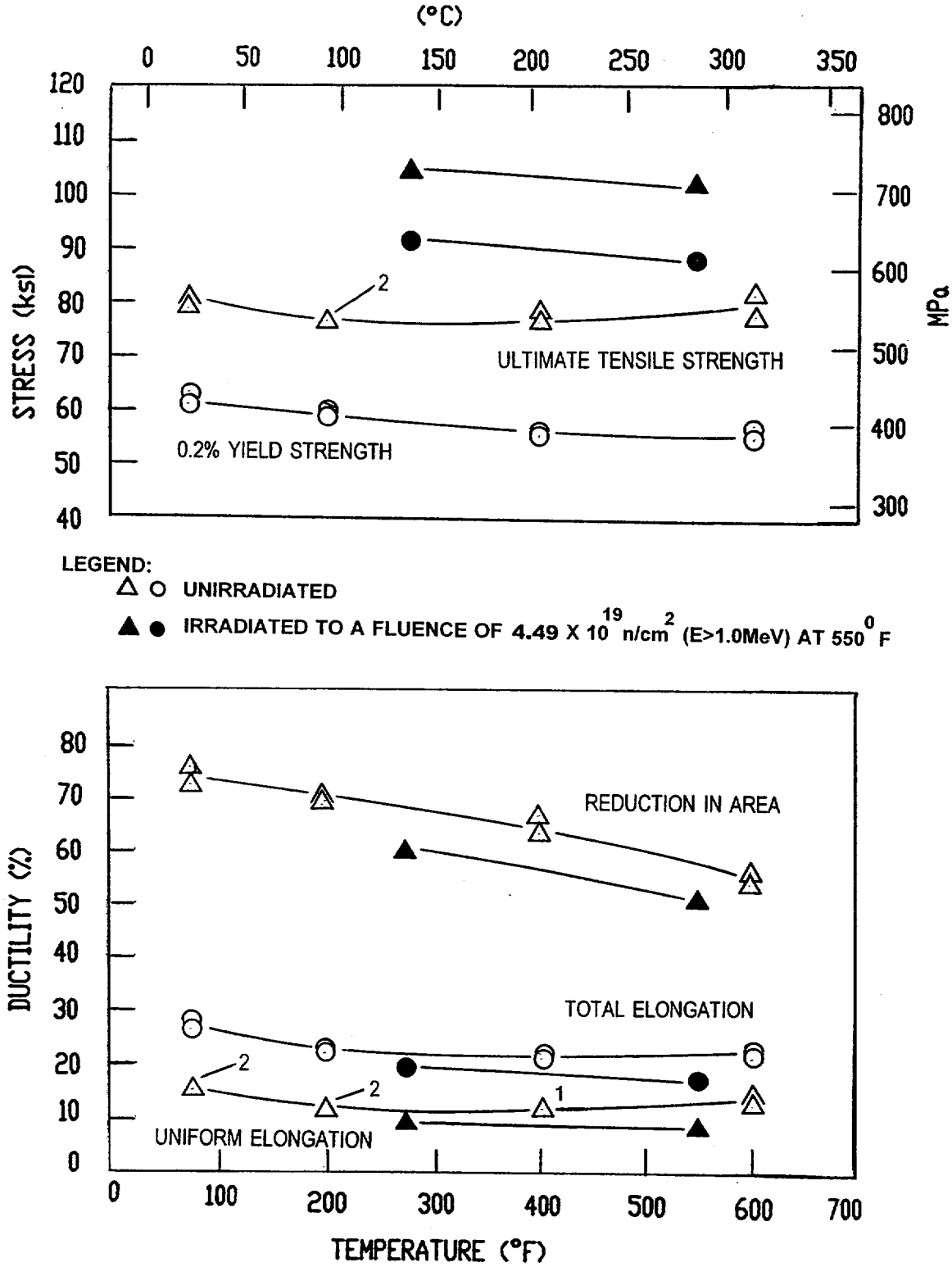

Figure 5-18 Tensile Properties for H.B. Robinson Unit 2 Reactor Vessel Weld Metal

Specimen C6 Tested at 200°F

Specimen C7 Tested at 550°F

Figure 5-19 Fractured Tensile Specimens from H.B. Robinson Unit 2 Reactor Vessel Intermediate Shell Plate W10201-4 (Transverse Orientation)

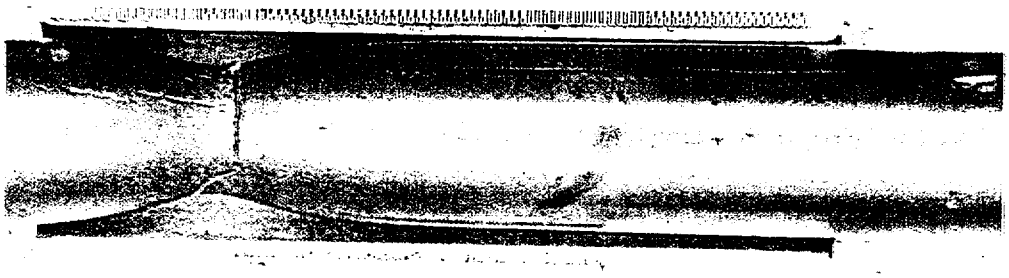

Specimen W1 Tested at 275°F

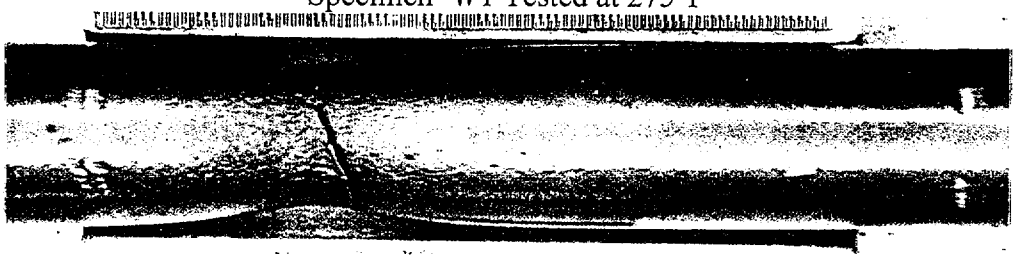

Specimen W2 Tested at 550°F

Figure 5-20 Fractured Tensile Specimens from H.B. Robinson Unit 2 Reactor Vessel Weld Metal

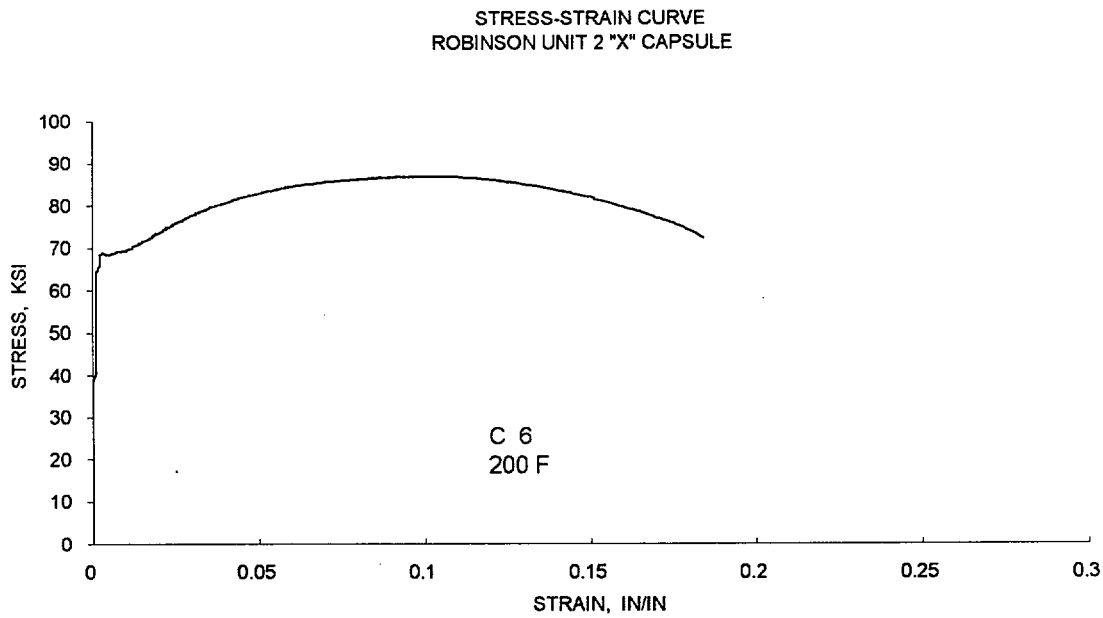

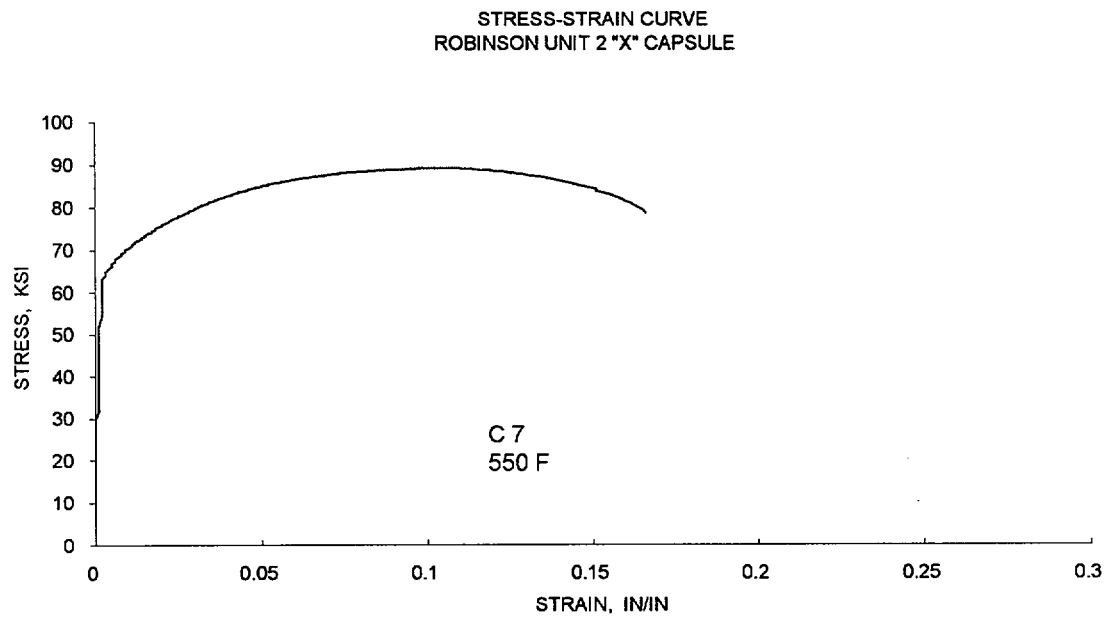

Figure 5-21 Engineering Stress-Strain Curves for Intermediate Shell Plate W10201-4 Tensile Specimens C6 and C7 (Transverse Orientation)

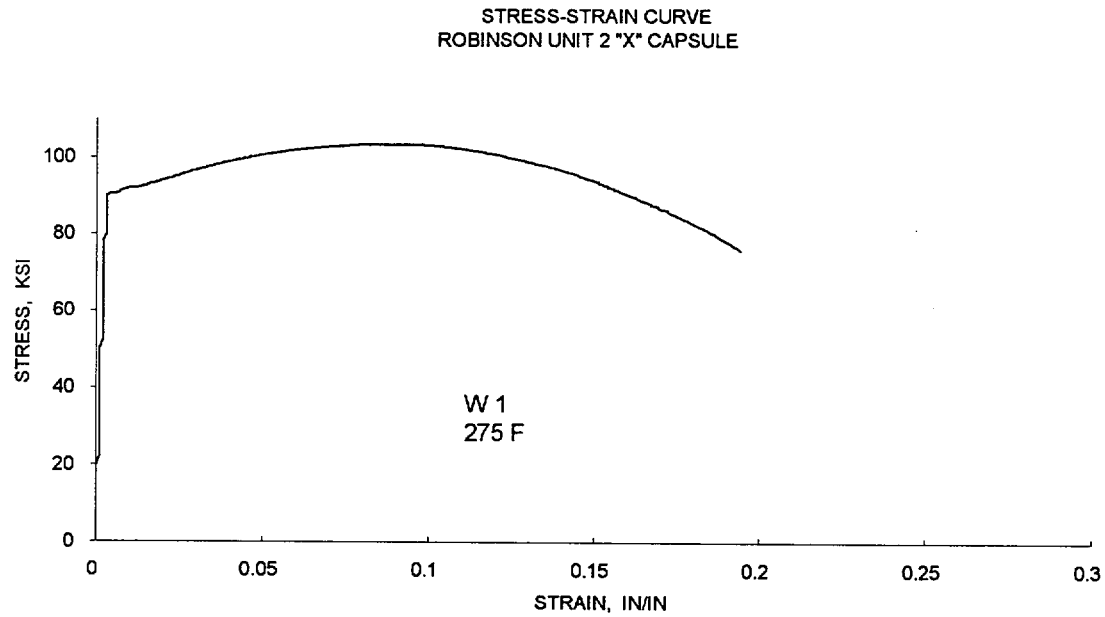

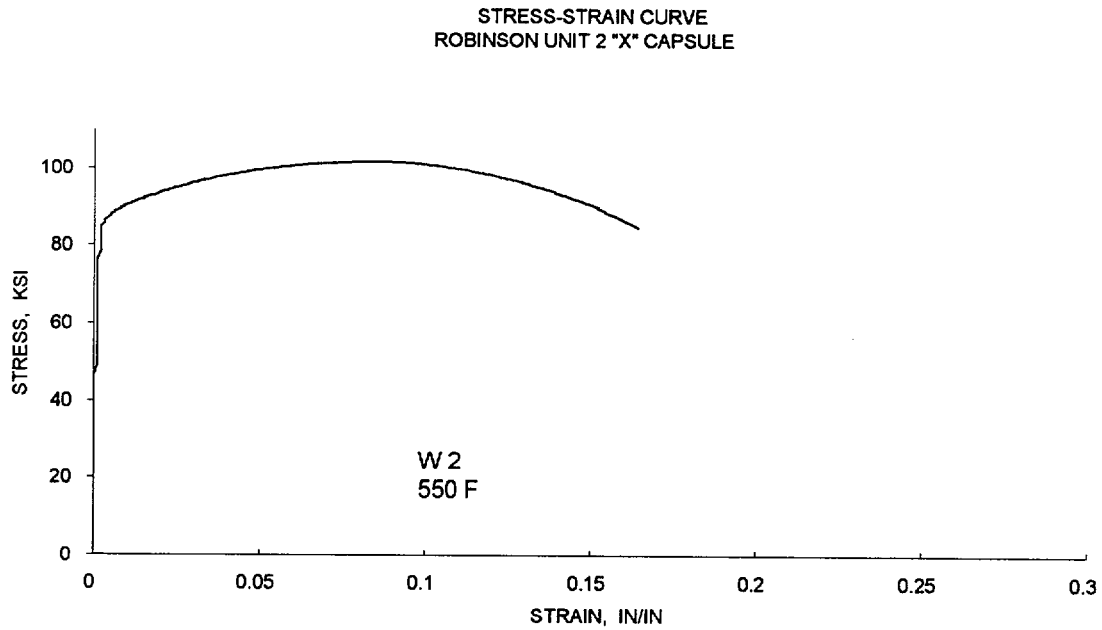

Figure 5-22 Engineering Stress-Strain Curves Weld Metal Tensile Specimens W1 and W2

6 RADIATION ANALYSIS AND NEUTRON DOSIMETRY

6.1 INTRODUCTION

This section describes a discrete ordinates S_n transport analysis performed for the H. B. Robinson Unit 2 reactor to determine the neutron radiation environment within the reactor pressure vessel and surveillance capsules. In this evaluation, fast neutron exposure parameters in terms of fast neutron fluence (E > 1.0 MeV) and iron atom displacements (dpa) were established on a plant and fuel cycle specific basis for the first 21 reactor operating cycles. In addition, neutron dosimetry sensor sets from Surveillance Capsules S, V, T, and X withdrawn from the H. B. Robinson Unit 2 reactor at the conclusion of fuel cycles 1, 3, 8, and 20, respectively, were analyzed using current dosimetry evaluation methodology. Comparisons of the results of these dosimetry evaluations with the analytical predictions provided a validation of the plant specific neutron transport calculations. These validated calculations were then used to provide projections of the neutron exposure of the reactor pressure vessel for operating periods extending to 50 Effective Full Power Years (EFPY). These projections conservatively account for an assumed plant uprating, from 2300 MWt to 2335 MWt, beginning with the operation of the twenty second fuel cycle.

The use of fast neutron fluence (E > 1.0 MeV) to correlate measured material property changes to the neutron exposure of the material has traditionally been accepted for the development of damage trend curves as well as for the implementation of trend curve data to assess the condition of the vessel. In recent years, however, it has been suggested that an exposure model that accounts for differences in neutron energy spectra between surveillance capsule locations and positions within the vessel wall could lead to an improvement in the uncertainties associated with damage trend curves and improved accuracy in the evaluation of damage gradients through the reactor vessel wall.

Because of this potential shift away from a threshold fluence toward an energy dependent damage function for data correlation, ASTM Standard Practice E853, "Analysis and Interpretation of Light-Water Reactor Surveillance Results,"[13] recommends reporting displacements per iron atom (dpa) along with fluence (E > 1.0 MeV) to provide a database for future reference. The energy dependent dpa function to be used for this evaluation is specified in ASTM Standard Practice E693, "Characterizing Neutron Exposures in Iron and Low Alloy Steels in Terms of Displacements per Atom."[14] The application of the dpa parameter to the assessment of embrittlement gradients through the thickness of the reactor vessel wall has already been promulgated in Revision 2 to Regulatory Guide 1.99, "Radiation Embrittlement of Reactor Vessel Materials."[1] Recently a new standard dpa cross section has been developed based on ENDF/B-VI cross sections.[15] If the new standard was used, minor changes in calculated dpa values would be obtained. As tabulated in Reference 15, this would result in about a 0.3% decrease in dpa at the reactor vessel surface, a 1.7% increase at the 1/4T position, and a 3.7% increase at the 3/4T position for the H. B. Robinson reactor vessel. Since the correlations used for embrittlement extrapolation and Regulatory Guide 1.99 are based on the earlier ENDF/B-IV dpa cross section, the results in this report are also based on the older standard.

All of the calculations and dosimetry evaluations described in this section were based on the latest available nuclear cross-section data derived from ENDF/B-VI and made use of the latest available calculational tools. Furthermore, the neutron transport and dosimetry evaluation methodologies follow the guidance and meet the requirements of Regulatory Guide 1.190, "Calculational and Dosimetry Methods for Determining Pressure Vessel Neutron Fluence."[16] Additionally, the methods used to develop the calculated pressure vessel fluence are consistent with the NRC approved methodology described in WCAP-14040-NP-A, "Methodology Used to Develop Cold Overpressure Mitigating System Setpoints and RCS Heatup and Cooldown Limit Curves," January 1996.[17] The specific calculational methods applied are also consistent with those described in WCAP-15557, "Qualification of the Westinghouse Pressure Vessel Neutron Fluence Evaluation Methodology."[18]

6.2 DISCRETE ORDINATES ANALYSIS

A plan view of the H. B. Robinson Unit 2 reactor geometry at the core midplane is shown in Figure 4-1. Eight irradiation capsules attached to the thermal shield were included in the reactor design that constitutes the reactor vessel surveillance program. The capsules were located at azimuthal angles of 270° (0° from the core cardinal axis), 280° (10° from the core cardinal axis), 290° (20° from the core cardinal axis), 30° and 150° (30° from the core cardinal axes), and 40°, 50°, and 230° (40° from the core cardinal axes) as shown in Figure 4-1. The stainless steel specimen containers are 1-inch square by 36 inches in height. The containers are positioned axially such that the test specimens are centered on the core midplane, thus spanning the central 3 feet of the 12-foot high reactor core.

From a neutronic standpoint, the surveillance capsules and associated support structures are significant. The presence of these materials has a marked effect on both the spatial distribution of neutron flux and the neutron energy spectrum in the water annulus between the thermal shield and the reactor vessel. In order to determine the neutron environment at the test specimen location, the capsules themselves must be included in the analytical model.

The fast neutron exposure evaluations for the H. B. Robinson Unit 2 surveillance capsules and reactor vessel were based on a series of fuel cycle specific forward transport calculations that were combined using the following three-dimensional flux synthesis technique:

$$\phi(r,\theta,z) = [\phi(r,\theta)] * [\phi(r,z)]/[\phi(r)]$$

where $\phi(r,\theta,z)$ is the synthesized three-dimensional neutron flux distribution, $\phi(r,\theta)$ is the transport solution in r,θ geometry, $\phi(r,z)$ is the two-dimensional solution for a cylindrical reactor model using the actual axial core power distribution, and $\phi(r)$ is the one-dimensional solution for a cylindrical reactor model using the same source per unit height as that used in the r,θ two-dimensional calculation. This synthesis procedure was carried out for each operating cycle at H. B. Robinson Unit 2.

The synthesis procedure for H. B. Robinson Unit 2 was complicated by the use of partial length shield assemblies (PLSA) beginning in fuel cycle 10. These assemblies are designed to provide a reduction in exposure to the lower circumferential weld. The PLSA are located in the three outer row positions near each of the core cardinal axes where the fluence maximum is located. The fuel pins in the PLSA contain of lower enrichment fuel pellets in the top 8.5 feet of the core region and contain stainless steel rods in the lower 3.5 feet instead of fuel. The PLSA assemblies are irradiated at these locations for a total of six cycles.

To perform the synthesis with the assymetry introduced by the PLSA, the core source is divided into two axial regions and two sets of calculations are performed. For the top region, the flux is given by

$$\phi_t(r,\theta,z) = [\phi_t(r,\theta)] * [\phi_t(r,z)]/[\phi_t(r)].$$

In this region, the axial source is set to zero in the lower 3.5 feet of the core. In the PLSA region, the flux is given by

$$\phi_p(r,\theta,z) = [\phi_p(r,\theta)] * [\phi_p(r,z)]/[\phi_p(r)].$$

In the PLSA region, the axial source is set to zero in the upper 8.5 feet of the core. The total source is then given by the sum of the two parts:

$$\phi(r,\theta,z) = \phi_t(r,\theta,z) + \phi_p(r,\theta,z).$$

For the H. B. Robinson Unit 2 calculations, a one octant r,θ model was developed since the reactor core is octant symmetric. This r,θ model includes the core, the reactor internals, the thermal shield -- including explicit representations of the surveillance capsules at 0°, 10°, 20°, 30°, and 40°, the pressure vessel cladding and vessel wall, the insulation external to the pressure vessel, and the primary biological shield wall. The r,θ model was utilized to perform both the surveillance capsule dosimetry evaluations, and subsequent comparisons with calculated results, and to generate the maximum fluence levels at the pressure vessel wall. The inclusion of all the capsules in a single octant does not represent a real case, since no octant has capsules at all positions, but the perturbation between capsules is negligible. However, the capsules do reduce the fluence to the vessel by 5 to 7% at nearby vessel locations. This perturbation was examined by running several cases with and without capsules, and appropriate corrections were made to obtain the maximum vessel exposure which occurs at locations where no capsules are present.

In developing the analytical model, nominal design dimensions were employed for the various structural components. Likewise, water temperatures, and hence, coolant densities in the reactor core and downcomer regions of the reactor were taken to be representative of full power operating conditions. The coolant densities were treated on a fuel cycle specific basis for cycles 8 and 9 which ran at a reduced power. (The power was reduced for part of cycle 8 and all of cycle 9 due to steam generator limitations). The reactor core itself was treated as a homogeneous mixture of fuel, cladding, water, and miscellaneous core structures such as fuel assembly grids, guide tubes, et cetera. The r,θ geometric mesh description of the reactor model consisted of 161 radial by 107 azimuthal intervals. Mesh sizes were chosen to assure that proper convergence of the inner iterations was achieved on a point-wise basis. The point-wise inner iteration flux convergence criterion utilized in the r,θ calculations was set at a value of 0.001.

For the top region (fuel cycles 10 to 21) the appropriate radial and azimuthal source distribution was used and included the power produced in this axial region by each fuel assembly. For the PLSA region, the source averaged over the bottom 3.5 feet of the core was used and the source in the PLSA assemblies was set to zero.

The r,z model used for the H. B. Robinson Unit 2 calculations extended radially from the centerline of the reactor core out to a location within the primary biological shield and over an axial span from an elevation 1-foot below the active fuel to 1-foot above the active fuel. As in the case of the r,θ model, nominal design dimensions and full power coolant densities were employed in the calculations. In this case, the homogenous core region was treated as an equivalent cylinder with a volume equal to that of the active core zone. The stainless steel former plates located between the core baffle and core barrel regions were also explicitly included in the model. The r,z geometric mesh description of the reactor model consisted of 158 radial by 110 axial intervals. As in the case of the r,θ calculations, mesh sizes were chosen to assure that proper convergence of the inner iterations was achieved on a point-wise basis. The point-wise inner iteration flux convergence criterion utilized in the r,z calculations was also set at a value of 0.001.

The r,z neutron source for the cycles with PLSA was handled as follows. In the calculation for the top region, the source was set to zero in the bottom 3.5 feet of the core. In the calculation for the bottom 3.5 feet, the source in the top 8.5 feet was set to zero. The appropriate radial source distribution for each region was used in each case. It should be noted that the r,z geometrical model was similar for each of the two regions with the only difference being a composition change in the annular region corresponding to the outer row of assemblies to represent the substitution of stainless steel for fuel.

The one-dimensional radial model used in the synthesis procedure consisted of the same 158 radial mesh intervals included in the r,z model. Thus, radial synthesis factors could be determined on a mesh-wise basis throughout the entire geometry.

The core power distributions used in the plant specific transport analysis were mostly taken from an information package supplied by the H. B. Robinson Unit 2 plant staff[19] and H. B. Robinson Unit 2 fuel cycle design reports.[20, 21] For the first fuel cycle, a generic axial power distribution for three loop plants was used.[22] The data extracted from these reports represented cycle dependent fuel assembly enrichments, burn-ups, and axial power distributions. This information was used to develop spatial and energy dependent core source distributions averaged over each individual fuel cycle. Therefore, the results from the neutron transport calculations provided data in terms of fuel cycle averaged neutron flux, which when multiplied by the appropriate fuel cycle length, generated the incremental fast neutron exposure for each fuel cycle. In constructing these core source distributions, the energy distribution of the source was based on an appropriate fission split for uranium and plutonium isotopes based on the initial enrichment and burn-up history of individual fuel assemblies. From these assembly dependent fission splits, composite values of energy release per fission, neutron yield per fission, and fission spectrum were determined.

All of the transport calculations supporting this analysis were carried out using the DORT discrete ordinates code Version 3.1[23] and the BUGLE-96 cross-section library.[24] The BUGLE-96 library provides a 67 group coupled neutron-gamma ray cross-section data set produced specifically for light water reactor (LWR) applications. In these analyses, anisotropic scattering was treated with a P_5 legendre expansion and angular discretization was modeled with an S_{16} order of angular quadrature. Energy and space dependent core power distributions, as well as system operating temperatures, were treated on a fuel cycle specific basis.

Selected results from the neutron transport analyses are provided in Tables 6-1 through 6-4. The data listed in these tables establish the means for absolute comparisons of analysis and measurement for the Capsules S, V, T, and X irradiation and provide the calculated neutron exposure of the pressure vessel wall for the first 21 fuel cycles. In Table 6-1, the calculated exposure rates and integrated exposures, expressed in terms of both neutron fluence ($E > 1.0$ MeV) and dpa, are given at the radial and azimuthal center of the five different azimuthally symmetric surveillance capsule positions (0°, 10°, 20°, 30° and 40°). These data, calculated at the axial midplane of the active core, are meant to establish the exposure of the surveillance capsules withdrawn to date and to provide data for an absolute comparison of measurement with calculation. Similar information is provided in Table 6-2 for the reactor vessel inner radius. The vessel data given in Table 6-2 calculated at the axial location of the maximum neutron exposure at each of six azimuthal locations. Again, both fluence ($E > 1.0$ MeV) and dpa data are provided. It is important to note that the data for the vessel inner radius were taken at the clad/base metal interface, and thus, represent the maximum calculated exposure levels of the vessel plates. The axial position of maximum exposure rate varies from cycle to cycle, and therefore the integrated exposure cannot be directly derived from the cycle exposure rates in this table. However, the difference is very small since the flux level is nearly flat in the axial region encompassing the various cycle maxima and the reactor axial midplane.

Radial gradient information applicable to $\phi(E > 1.0$ MeV) and dpa/sec are given in Tables 6-3 and 6-4, respectively. The data, based on the cumulative exposure through cycle 20, are presented on a relative basis for each exposure parameter at six azimuthal locations. Exposure distributions through the vessel wall may be obtained by multiplying the calculated exposure at the vessel inner radius by the gradient data listed in Tables 6-3 and 6-4.

6.3 NEUTRON DOSIMETRY

6.3.1 Sensor Reaction Rate Determinations

In this section, the results of the evaluations of the four neutron sensor sets withdrawn to date as a part of the H. B. Robinson Unit 2 Reactor Vessel Materials Surveillance Program are presented. The capsule designation, location within the reactor, and time of withdrawal of each of these dosimetry sets were as follows:

Capsule ID	Azimuthal Location	Withdrawal Time	Irradiation Time [EFPY]
S	10	End of Cycle 1	1.28
V	20	End of Cycle 3	3.18
T	0	End of Cycle 8	7.27
X	40, 0	End of Cycle 20	20.39

The azimuthal locations included in the above tabulation represent the first octant equivalent azimuthal angle of the geometric center of the respective surveillance capsules. Capsule X was irradiated at the 40° location for the first 8 cycles and was then moved to the 0° location.

The passive neutron sensors included in the evaluations of Surveillance Capsules S, V, T, and X are summarized as follows:

Sensor Material	Reaction of Interest	Capsule S	Capsule V	Capsule T	Capsule X
Copper	$^{63}Cu(n,\alpha)^{60}Co$	X	X	X	X
Iron	$^{54}Fe(n,p)^{54}Mn$	X	X	X	X
Nickel	$^{58}Ni(n,p)^{58}Co$	X	X	X	X
Uranium-238	$^{238}U(n,f)^{137}Cs$	none	**	X	X
Neptunium-237	$^{237}Np(n,f)^{137}Cs$	none	**	X	X
Cobalt-Aluminum*	$^{59}Co(n,\gamma)^{60}Co$	X	X	X	X

* The cobalt-aluminum measurements for this plant include both bare wire and cadmium-covered sensors.
** The fission reaction data for this capsule are regarded as in error and were not used.

The copper, nickel, and cobalt-aluminum monitors, in wire form, were placed in holes drilled in spacers at several radial locations within the test specimen array. Iron wires were not included in these capsules, but iron activation measurements were made on samples taken from Charpy bars. As a result, it was necessary to apply gradient corrections to these measured reaction rates in order to index all of the sensor measurements to the radial center of the respective surveillance capsules. Since the cadmium-shielded uranium and neptunium

fission monitors were accommodated within the dosimeter block centered at the radial, azimuthal, and axial center of the material test specimen array, gradient corrections were not required for the fission monitor reaction rates. Pertinent physical and nuclear characteristics of the passive neutron sensors are listed in Table 6-5.

The use of passive monitors such as those listed above does not yield a direct measure of the energy dependent neutron flux at the point of interest. Rather, the activation or fission process is a measure of the integrated effect that the time and energy dependent neutron flux has on the target material over the course of the irradiation period. An accurate assessment of the average neutron flux level incident on the various monitors may be derived from the activation measurements only if the irradiation parameters are well known. In particular, the following variables are of interest:

- the measured specific activity of each monitor,
- the physical characteristics of each monitor,
- the operating history of the reactor,
- the energy response of each monitor, and
- the neutron energy spectrum at the monitor location.

The radiometric counting of the neutron sensors from capsules S and V was carried out at the Southwest Research Institute [25, 26]. These data are less reliable than more modern data, and corrections were made to some of the data in the Westinghouse Surveillance Capsule Neutron Fluence Evaluation[27], carried out in 1994. For capsule S, two Cu reaction rate measurements were made that were inconsistent. In the present analysis, the top Cu measurement was discarded and the bottom measurement, which appears to be consistent with the other data sets, was used. For capsule V, the iron reaction rate was decreased by dividing by 1.15 as recommended in Reference 27. The analysis of capsule T was carried out at the Westinghouse Analytical Services Laboratory at the Waltz Mill Site and results are reported in Reference 28. The radiometric counting of the sensors from capsule X was completed at the Antech Analytical Laboratory, also located at the Waltz Mill Site.[29] For capsules T and X, the radiometric counting followed established ASTM procedures. Following sample preparation and weighing, the specific activity of each sensor was determined by means of a high-resolution gamma spectrometer. For the copper, iron, nickel, and cobalt-aluminum sensors, these analyses were performed by direct counting of each of the individual samples. In the case of the uranium and neptunium fission sensors, the analyses were carried out by direct counting preceded by dissolution and chemical separation of cesium from the sensor material.

The irradiation history of the reactor over the irradiation periods experienced by Capsules S, V, T, and X was based on the reported monthly power generation of H. B. Robinson Unit 2 from initial reactor startup through the end of the dosimetry evaluation period. For the sensor sets utilized in the surveillance capsules, the half-lives of the product isotopes are long enough that a monthly histogram describing reactor operation has proven to be an adequate representation for use in radioactive decay corrections for the reactions of interest in the exposure evaluations. The irradiation history applicable to Capsules S, V, T, and X is given in Table 6-6.

Having the measured specific activities, the physical characteristics of the sensors, and the operating history of the reactor, reaction rates referenced to full-power operation were determined from the following equation:

$$R = \frac{A}{N_0 F Y \Sigma \frac{P_j}{P_{ref}} C_j [1 - e^{-\lambda t_j}] [e^{-\lambda t_d}]}$$

where:

R	=	Reaction rate averaged over the irradiation period and referenced to operation at a core power level of P_{ref} (rps/nucleus).
A	=	Measured specific activity (dps/gm).
N_0	=	Number of target element atoms per gram of sensor.
F	=	Weight fraction of the target isotope in the sensor material.
Y	=	Number of product atoms produced per reaction.
P_j	=	Average core power level during irradiation period j (MW).
P_{ref}	=	Maximum or reference power level of the reactor (MW).
C_j	=	Calculated ratio of $\phi(E > 1.0$ MeV) during irradiation period j to the time weighted average $\phi(E > 1.0$ MeV) over the entire irradiation period.
λ	=	Decay constant of the product isotope (1/sec).
t_j	=	Length of irradiation period j (sec).
t_d	=	Decay time following irradiation period j (sec).

and the summation is carried out over the total number of monthly intervals comprising the irradiation period.

In the equation describing the reaction rate calculation, the ratio $[P_j]/[P_{ref}]$ accounts for month-by-month variation of reactor core power level within any given fuel cycle as well as over multiple fuel cycles. The ratio C_j, which was calculated for each fuel cycle using the transport methodology discussed in Section 6.2, accounts for the change in sensor reaction rates caused by variations in flux level induced by changes in core spatial power distributions from fuel cycle to fuel cycle. For a single-cycle irradiation, C_j is normally taken to be 1.0. However, for multiple-cycle irradiations, particularly those employing low leakage fuel management, the additional C_j term should be employed. The impact of changing flux levels for constant power operation can be quite significant for sensor sets that have been irradiated for many cycles in a reactor that has transitioned from non-low leakage to low leakage fuel management or for sensor sets contained in surveillance capsules that have been moved from one capsule location to another. The fuel cycle specific neutron flux values along with the computed values for C_j are listed in Table 6-7. These flux values represent the cycle dependent results at the radial and azimuthal center of the respective capsules at the axial elevation of the active fuel midplane.

Normally, the neutron spectrum at the capsule location is relatively constant and thus a single set of C_j values can be used for all the dosimeter reactions. In the case of Capsule X, however, the change in position creates a change in the spectrum that was taken into account in the analysis. For this capsule, C_j was determined separately for each individual reaction.

Prior to using the measured reaction rates in the least-squares evaluations of the dosimetry sensor sets, additional corrections were made to the ^{238}U measurements to account for the presence of ^{235}U impurities in the sensors as well as to adjust for the build-in of plutonium isotopes over the course of the irradiation. Corrections were also made to the ^{238}U and ^{237}Np sensor reaction rates to account for gamma ray induced

fission reactions that occurred over the course of the capsule irradiations. The correction factors applied to the H. B. Robinson Unit 2 fission sensor reaction rates are summarized as follows:

Correction	Capsule T	Capsule X
^{235}U Impurity/Pu Build-in	0.747	0.727
^{238}U(γ,f)	0.956	0.956
Net ^{238}U Correction	0.714	0.695
^{237}Np(γ,f)	0.984	0.984

These factors were applied in a multiplicative fashion to the decay corrected uranium and neptunium fission sensor reaction rates.

Results of the sensor reaction rate determinations for Capsules S, V, T, and X are given in Table 6-8. In Table 6-8, the measured specific activities, decay corrected saturated specific activities, and computed reaction rates for each sensor indexed to the radial center of the capsule are listed. The fission sensor reaction rates are listed both with and without the applied corrections for ^{238}U impurities, plutonium build-in, and gamma ray induced fission effects.

6.3.2 Least Squares Evaluation of Sensor Sets

Least squares adjustment methods provide the capability of combining the measurement data with the corresponding neutron transport calculations resulting in a Best Estimate neutron energy spectrum with associated uncertainties. Best Estimates for key exposure parameters such as $\phi(E > 1.0\ \text{MeV})$ or dpa/s along with their uncertainties are then easily obtained from the adjusted spectrum. In general, the least squares methods, as applied to surveillance capsule dosimetry evaluations, act to reconcile the measured sensor reaction rate data, dosimetry reaction cross-sections, and the calculated neutron energy spectrum within their respective uncertainties. For example,

$$R_i \pm \delta_{R_i} = \sum_g (\sigma_{ig} \pm \delta_{\sigma_{ig}})(\phi_g \pm \delta_{\phi_g})$$

relates a set of measured reaction rates, R_i, to a single neutron spectrum, ϕ_g, through the multigroup dosimeter reaction cross-section, σ_{ig}, each with an uncertainty δ. The primary objective of the least squares evaluation is to produce unbiased estimates of the neutron exposure parameters at the location of the measurement.

For the least squares evaluation of the H. B. Robinson Unit 2 surveillance capsule dosimetry, the FERRET code[30] was employed to combine the results of the plant specific neutron transport calculations and sensor set reaction rate measurements to determine best-estimate values of exposure parameters ($\phi(E > 1.0\ \text{MeV})$ and dpa) along with associated uncertainties for the four in-vessel capsules withdrawn to date.

The application of the least squares methodology requires the following input:

1 - The calculated neutron energy spectrum and associated uncertainties at the measurement location.

2 - The measured reaction rates and associated uncertainty for each sensor contained in the multiple foil set.

3 - The energy dependent dosimetry reaction cross-sections and associated uncertainties for each sensor contained in the multiple foil sensor set.

For the H. B. Robinson Unit 2 application, the calculated neutron spectrum was obtained from the results of plant specific neutron transport calculations described in Section 6.2 of this report. The sensor reaction rates were derived from the measured specific activities using the procedures described in Section 6.3.1. The dosimetry reaction cross-sections and uncertainties were obtained from the SNLRML dosimetry cross-section library[31]. The SNLRML library is an evaluated dosimetry reaction cross-section compilation recommended for use in LWR evaluations by ASTM Standard E1018, "Application of ASTM Evaluated Cross-Section Data File, Matrix E 706 (IIB)".[32]

The uncertainties associated with the measured reaction rates, dosimetry cross-sections, and calculated neutron spectrum were input to the least squares procedure in the form of variances and covariances. The assignment of the input uncertainties followed the guidance provided in ASTM Standard E 944, "Application of Neutron Spectrum Adjustment Methods in Reactor Surveillance."[33]

The following provides a summary of the uncertainties associated with the least squares evaluation of the

H. B. Robinson Unit 2 surveillance capsule sensor sets.

Reaction Rate Uncertainties

The overall uncertainty associated with the measured reaction rates includes components due to the basic measurement process, irradiation history corrections, and corrections for competing reactions. A high level of accuracy in the reaction rate determinations is assured by utilizing laboratory procedures that conform to the ASTM National Consensus Standards for reaction rate determinations for each sensor type.

After combining all of these uncertainty components, the sensor reaction rates derived from the counting and data evaluation procedures were assigned the following net uncertainties for input to the least squares evaluation:

Reaction	Uncertainty
$^{63}Cu(n,\alpha)^{60}Co$	5%
$^{54}Fe(n,p)^{54}Mn$	5%
$^{58}Ni(n,p)^{58}Co$	5%
$^{238}U(n,f)^{137}Cs$	10%
$^{237}Np(n,f)^{137}Cs$	10%
$^{59}Co(n,\gamma)^{60}Co$	5%

These uncertainties are given at the 1σ level.

Dosimetry Cross-Section Uncertainties

The reaction rate cross-sections used in the least squares evaluations were taken from the SNLRML library. This data library provides reaction cross-sections and associated uncertainties, including covariances, for 66 dosimetry sensors in common use. Both cross-sections and uncertainties are provided in a fine multigroup structure for use in least squares adjustment applications. These cross-sections were compiled from the most recent cross-section evaluations and they have been tested with respect to their accuracy and consistency for least squares evaluations. Further, the library has been empirically tested for use in fission spectra determination as well as in the fluence and energy characterization of 14 MeV neutron sources.

For sensors included in the H. B. Robinson Unit 2 surveillance program, the following uncertainties in the fission spectrum averaged cross-sections are provided in the SNLRML documentation package.

Reaction	Uncertainty
$^{63}Cu(n,\alpha)^{60}Co$	4.08-4.16%
$^{54}Fe(n,p)^{54}Mn$	3.05-3.11%
$^{58}Ni(n,p)^{58}Co$	4.49-4.56%
$^{238}U(n,f)^{137}Cs$	0.54-0.64%
$^{237}Np(n,f)^{137}Cs$	10.32-10.97%
$^{59}Co(n,\gamma)^{60}Co$	0.79-3.59%

These tabulated ranges provide an indication of the dosimetry cross-section uncertainties associated with the sensor sets used in LWR irradiations.

Calculated Neutron Spectrum

The neutron spectra input to the least squares adjustment procedure were obtained directly from the results of plant specific transport calculations for each surveillance capsule irradiation period and location. The spectrum for each capsule was input in an absolute sense (rather than as simply a relative spectral shape). Therefore, within the constraints of the assigned uncertainties, the calculated data were treated equally with the measurements.

While the uncertainties associated with the reaction rates were obtained from the measurement procedures and counting benchmarks and the dosimetry cross-section uncertainties were supplied directly with the SNLRML library, the uncertainty matrix for the calculated spectrum was constructed from the following relationship:

$$M_{gg'} = R_n^2 + R_g * R_{g'} * P_{gg'}$$

where R_n specifies an overall fractional normalization uncertainty and the fractional uncertainties R_g and $R_{g'}$ specify additional random groupwise uncertainties that are correlated with a correlation matrix given by:

$$P_{gg'} = [1-\theta]\delta_{gg'} + \theta\, e^{-H}$$

where

$$H = \frac{(g-g')^2}{2\gamma^2}$$

The first term in the correlation matrix equation specifies purely random uncertainties, while the second term describes the short-range correlations over a group range γ (θ specifies the strength of the latter term). The value of δ is 1.0 when g = g', and is 0.0 otherwise.

The set of parameters defining the input covariance matrix for the H. B. Robinson Unit 2 calculated spectra was as follows:

Flux Normalization Uncertainty (R_n)	15%
Flux Group Uncertainties (R_g, $R_{g'}$)	
(E > 0.0055 MeV)	15%
(0.68 eV < E < 0.0055 MeV)	29%
(E < 0.68 eV)	52%
Short Range Correlation (θ)	
(E > 0.0055 MeV)	0.9
(0.68 eV < E < 0.0055 MeV)	0.5
(E < 0.68 eV)	0.5
Flux Group Correlation Range (γ)	
(E > 0.0055 MeV)	6
(0.68 eV < E < 0.0055 MeV)	3
(E < 0.68 eV)	2

6.3.3 Comparisons of Measurements and Calculations

Results of the least squares evaluations of the dosimetry from the four H. B. Robinson Unit 2 surveillance capsules withdrawn to date are provided in Tables 6-9 and 6-10. In Table 6-9, measured, calculated, and best-estimate values for sensor reaction rates are given for each capsule. Also provided in this tabulation are ratios of the measured reaction rates to both the calculated and least squares adjusted reaction rates. These ratios of M/C and M/BE illustrate the consistency of the fit of the calculated neutron energy spectra to the measured reaction rates both before and after adjustment. In Table 6-10, comparison of the calculated and best estimate values of neutron flux (E > 1.0 MeV) and iron atom displacement rate are tabulated along with the C/BE ratios observed for each of the capsules.

The data comparisons provided in Tables 6-9 and 6-10 show that the adjustments to the calculated spectra are relatively small and well within the assigned uncertainties for the calculated spectra, measured sensor reaction rates, and dosimetry reaction cross-sections. Further, these results indicate that the use of the least squares evaluation results in a reduction in the uncertainties associated with the exposure of the surveillance capsules. From Section 6.4 of this report, it may be noted that the uncertainty associated with the unadjusted calculation of neutron fluence (E > 1.0 MeV) and iron atom displacements at the surveillance capsule locations is specified as 12% at the 1σ level. From Table 6-10, it is noted that the corresponding uncertainties associated with the least squares adjusted exposure parameters have been reduced to 6-8% for neutron flux (E > 1.0 MeV) and 7-9% for iron atom displacement rate. Again, the uncertainties from the least squares evaluation are at the 1σ level.

Further comparisons of the measurement results with calculations are given in Tables 6-11 and 6-12. These comparisons are given on two levels. In Table 6-11, calculations of individual threshold sensor reaction rates are compared directly with the corresponding measurements. These threshold reaction rate comparisons provide a good evaluation of the accuracy of the fast neutron portion of the calculated energy spectra. In Table 6-12, calculations of fast neutron exposure rates in terms of $\phi(E > 1.0$ MeV) and dpa/s are compared with the best estimate results obtained from the least squares evaluation of the four capsule dosimetry results. These two levels of comparison yield consistent and similar results with all measurement-to-calculation comparisons falling well within the 20% limits specified as the acceptance criteria in Regulatory Guide 1.190.

In the case of the direct comparison of measured and calculated sensor reaction rates, the C/M comparisons for fast neutron reactions range from 0.76–1.13 for the samples included in the data set. The overall average C/M ratio for the entire set of H. B. Robinson Unit 2 data is 0.87 with an associated standard deviation of 11.4%.

In the comparisons of best estimate and calculated fast neutron exposure parameters, the corresponding C/BE ratios for the four capsule data set range from 0.81–0.95 for neutron flux ($E > 1.0$ MeV) and from 0.82 to 0.95 for iron atom displacement rate. The overall average C/BE ratios for neutron flux ($E > 1.0$ MeV) and iron atom displacement rate are 0.89 with a standard deviation of 7.9% and 0.89 with a standard deviation of 7.1%, respectively.

Based on these comparisons, it is concluded that the calculated fast neutron exposures provided in Section 6.4 of this report are validated for use in the assessment of the condition of the materials comprising the beltline region of the H. B. Robinson Unit 2 reactor pressure vessel.

6.4 PROJECTIONS OF REACTOR VESSEL EXPOSURE

The final results of the fluence evaluations performed for the four surveillance capsules withdrawn from the H. B. Robinson Unit 2 reactor are provided in Table 6-13. These assigned neutron exposure levels are based on the plant and fuel cycle specific neutron transport calculations performed for the H. B. Robinson Unit 2 reactor. As shown by the comparisons provided in Tables 6-11 and 6-12, the validity of these calculated fluence levels is demonstrated both by a direct comparison with measured sensor reaction rates as well by comparison with the least squares evaluation performed for each of the capsule dosimetry sets.

The corresponding calculated fast neutron fluence (E > 1.0 MeV) and dpa exposure values for the H. B. Robinson Unit 2 pressure vessel are provided in Table 6-14. As presented, these data represent the maximum exposure of the clad/base metal interface at azimuthal angles of at 0°, 10°, 20°, 30°, 40°, and 45°, relative to the core cardinal axes. The data tabulation includes the plant and fuel cycle specific calculated fluence at the end of the twentieth operating fuel cycle as well as projections for future operation to the end of cycle 21 and to 29, 30, 35, 40, 45, and 50 effective full power years. The projections were based on the assumption that the spatial power distributions averaged over fuel cycles 16 through 21 (these six cycles represent the exposure of a single set of PLSA) will be representative of future plant operation. The future projections also account for a 1.5% power uprate from 2300 MWt to 2335 MWt.

Similar calculated fluence projections are provided in Tables 6-15 and 6-16 for the H. B. Robinson Unit 2 circumferential welds. The upper circumferential weld is located 5.375 inches below the top of the fuel region and fluence and dpa for this weld are in Table 6-15. The lower circumferential weld is located at 21.75 inches above the bottom of the fuel. Fluence and dpa for this weld are in Table 6-16. This weld has a reduced fluence rate near 0° for cycles starting with 10 due to the PLSA. This reduction shifts the maximum fluence rate to this weld to angles between 20 and 30 degrees. However, due to the large fluence acquired in cycles 1 to 9 near 0°, the maximum fluence will be at 0° through 50 EFPY.

Data from Table 6-14 can also be used to determine the maximum exposure to the three intermediate shell vertical welds, which are located at angles of 10°, 20°, and 40° with respect to the cardinal axes. Similarly, the maximum exposure to the vertical welds in the upper shell (also located at 10°, 20°, and 40° with respect to the cardinal axes) can be taken from Table 6-15 and the maximum exposure to the vertical welds in the lower shell (located at 0°, 30°, and 30° with respect to the cardinal axes) can be taken from Table 6-16.

Updated lead factors for the H. B. Robinson Unit 2 surveillance capsules are provided in Table 6-17. The capsule lead factor is defined as the ratio of the calculated fluence (E > 1.0 MeV) at the geometric center of the surveillance capsule to the corresponding maximum calculated fluence at the pressure vessel clad/base metal interface. In Table 6-17, the lead factors for capsules that have been withdrawn from the reactor (S, V, T, and X) were based on the calculated fluence values for the irradiation period corresponding to the time of withdrawal for the individual capsules. For the capsules remaining in the reactor (U, Y, W, and Z), the lead factors correspond to the calculated fluence values at the end of cycle 20. For these four capsules, future lead factors are also given in Table 6-17 since these can be different from the past exposure.

In addition to the pressure vessel materials located adjacent to the active core region, nozzle components located in the vicinity of the azimuthal peak fluence will experience a neutron exposure (E > 1.0 MeV) greater than 1.0E+17 n/cm^2 during the extended operating periods. These components include the inlet and outlet nozzle structures as well as the circumferential welds connecting the nozzles to the vessel shell course. The portions of these materials experiencing fluence values greater than 1.0E+17 n/cm^2 are limited to small areas at the lowest extent of the nozzles and associated welds as well as to the inlet and outlet nozzles located near

the 0.0 degree azimuth. A summary of the maximum calculated neutron fluence applicable to the nozzle components is given in Table 6-18.

The uncertainty associated with the calculated neutron exposure of the H. B. Robinson Unit 2 surveillance capsule and reactor pressure vessel is based on the recommended approach provided in Regulatory Guide 1.190. In particular, the qualification of the methodology was carried out in the following four stages:

1 - Comparison of calculations with benchmark measurements from the Pool Critical Assembly (PCA) simulator at the Oak Ridge National Laboratory (ORNL).

2 - Comparisons of calculations with surveillance capsule and reactor cavity measurements from the H. B. Robinson power reactor benchmark experiment.

3 - An analytical sensitivity study addressing the uncertainty components resulting important input parameters applicable to the plant specific transport calculations used in the neutron exposure assessments.

4 - Comparisons of the plant specific calculations with all available dosimetry results from the H. B. Robinson Unit 2 surveillance program capsules.

The first phase of the methods qualification (PCA comparisons) addressed the adequacy of basic transport calculation and dosimetry evaluation techniques and associated cross-sections. This phase, however, did not test the accuracy of commercial core neutron source calculations nor did it address uncertainties in operational or geometric variables that impact power reactor calculations. The second phase of the qualification (H. B. Robinson comparisons) addressed uncertainties in these additional areas that are primarily methods related and would tend to apply generically to all fast neutron exposure evaluations. The third phase of the qualification (analytical sensitivity study) identified the potential uncertainties introduced into the overall evaluation due to calculational methods approximations as well as to a lack of knowledge relative to various plant specific input parameters. The overall calculational uncertainty applicable to the H. B. Robinson Unit 2 analysis was established from results of these three phases of the methods qualification.

The fourth phase of the uncertainty assessment (comparisons with H. B. Robinson Unit 2 capsule measurements) was used solely to demonstrate the validity of the transport calculations and to confirm the uncertainty estimates associated with the analytical results. The comparison was used only as a check and was not used in any way to modify the calculated surveillance capsule and pressure vessel neutron exposures.

The following summarizes the uncertainties developed from the first three phases of the methodology qualification. Additional information pertinent to these evaluations is provided in Reference 7.

	Capsule	Vessel IR
PCA Comparisons	3%	3%
H. B. Robinson Comparisons	3%	3%
Analytical Sensitivity Studies	10%	11%
Additional Uncertainty for Factors not Explicitly Evaluated	5%	5%
Net Calculational Uncertainty	12%	13%

The net calculational uncertainty was determined by combining the individual components in quadrature which assumes that each component of the uncertainty is random and uncorrelated. Therefore, no systematic bias was applied to the analytical results.

The plant specific measurement comparisons provided in Tables 6-11 and 6-12 support these uncertainty assessments for H. B. Robinson Unit 2.

Table 6-1

Calculated Neutron Exposure Rates And Integrated Exposures
At The Surveillance Capsule Center

Neutrons (E > 1.0 MeV)

Cycle	Cycle Length [EFPY]	Total Irradiation Time [EFPY]	Neutron Flux (E > 1.0 MeV) [n/cm^2-s]				
			0 Degrees	10 Degrees	20 Degrees	30 Degrees	40 Degrees
1	1.279	1.28	1.71E+11	1.19E+11	5.33E+10	4.10E+10	2.84E+10
2	0.814	2.09	1.70E+11	1.22E+11	5.65E+10	4.37E+10	2.94E+10
3	1.091	3.18	1.45E+11	1.01E+11	4.94E+10	3.98E+10	2.78E+10
4	0.791	3.97	1.92E+11	1.35E+11	5.75E+10	4.39E+10	3.05E+10
5	0.812	4.79	1.77E+11	1.26E+11	5.56E+10	4.23E+10	2.83E+10
6	0.840	5.63	1.70E+11	1.20E+11	5.39E+10	4.14E+10	2.77E+10
7	0.810	6.44	1.64E+11	1.17E+11	5.54E+10	4.29E+10	2.82E+10
8	0.835	7.27	1.67E+11	1.18E+11	5.31E+10	4.07E+10	2.69E+10
9	0.857	8.13	8.35E+10	6.10E+10	4.09E+10	3.67E+10	2.52E+10
10	0.871	9.00	1.05E+11	7.87E+10	5.49E+10	4.59E+10	2.72E+10
11	0.916	9.92	9.51E+10	7.53E+10	5.73E+10	4.77E+10	2.63E+10
12	0.982	10.90	8.93E+10	7.30E+10	5.98E+10	4.91E+10	2.62E+10
13	0.983	11.88	7.67E+10	6.44E+10	5.61E+10	4.78E+10	2.64E+10
14	0.996	12.88	7.60E+10	6.58E+10	6.02E+10	5.06E+10	2.68E+10
15	1.074	13.95	7.16E+10	6.31E+10	5.98E+10	5.01E+10	2.60E+10
16	1.076	15.03	1.28E+11	9.06E+10	4.01E+10	3.03E+10	2.36E+10
17	1.185	16.21	1.13E+11	8.15E+10	3.83E+10	2.78E+10	2.02E+10
18	1.346	17.56	1.02E+11	7.41E+10	3.73E+10	2.81E+10	1.92E+10
19	1.414	18.97	9.17E+10	6.72E+10	3.54E+10	2.82E+10	2.16E+10
20	1.420	20.39	8.00E+10	5.96E+10	3.32E+10	2.73E+10	2.18E+10
21	1.389	21.78	7.02E+10	5.37E+10	3.28E+10	2.71E+10	2.11E+10

Table 6-1 cont'd

Calculated Neutron Exposure Rates And Integrated Exposures
At The Surveillance Capsule Center

Neutrons (E > 1.0 MeV)

Cycle	Cycle Length [EFPY]	Total Irradiation Time [EFPY]	Neutron Fluence (E > 1.0 MeV) [n/cm^2]				
			0 Degrees	10 Degrees	20 Degrees	30 Degrees	40 Degrees
1	1.279	1.28	6.92E+18	4.79E+18	2.15E+18	1.65E+18	1.15E+18
2	0.814	2.09	1.13E+19	7.94E+18	3.60E+18	2.77E+18	1.90E+18
3	1.091	3.18	1.63E+19	1.14E+19	5.30E+18	4.14E+18	2.86E+18
4	0.791	3.97	2.11E+19	1.48E+19	6.74E+18	5.24E+18	3.62E+18
5	0.812	4.79	2.56E+19	1.80E+19	8.16E+18	6.32E+18	4.34E+18
6	0.840	5.63	3.01E+19	2.11E+19	9.59E+18	7.42E+18	5.08E+18
7	0.810	6.44	3.43E+19	2.41E+19	1.10E+19	8.52E+18	5.80E+18
8	0.835	7.27	3.87E+19	2.72E+19	1.24E+19	9.59E+18	6.51E+18
9	0.857	8.13	4.10E+19	2.89E+19	1.35E+19	1.06E+19	7.19E+18
10	0.871	9.00	4.38E+19	3.11E+19	1.50E+19	1.18E+19	7.94E+18
11	0.916	9.92	4.66E+19	3.32E+19	1.67E+19	1.32E+19	8.70E+18
12	0.982	10.90	4.93E+19	3.55E+19	1.85E+19	1.47E+19	9.51E+18
13	0.983	11.88	5.17E+19	3.75E+19	2.03E+19	1.62E+19	1.03E+19
14	0.996	12.88	5.41E+19	3.96E+19	2.22E+19	1.78E+19	1.12E+19
15	1.074	13.95	5.65E+19	4.17E+19	2.42E+19	1.95E+19	1.20E+19
16	1.076	15.03	6.09E+19	4.48E+19	2.56E+19	2.05E+19	1.29E+19
17	1.185	16.21	6.51E+19	4.78E+19	2.70E+19	2.16E+19	1.36E+19
18	1.346	17.56	6.94E+19	5.10E+19	2.86E+19	2.28E+19	1.44E+19
19	1.414	18.97	7.35E+19	5.40E+19	3.01E+19	2.40E+19	1.54E+19
20	1.420	20.39	7.71E+19	5.66E+19	3.16E+19	2.53E+19	1.64E+19
21	1.389	21.78	8.02E+19	5.90E+19	3.31E+19	2.64E+19	1.73E+19

Table 6-1 cont'd

Calculated Neutron Exposure Rates And Integrated Exposures
At The Surveillance Capsule Center

Iron Atom Displacements

Cycle	Cycle Length [EFPY]	Total Irradiation Time [EFPY]	Displacement Rate [dpa/s]				
			0 Degrees	10 Degrees	20 Degrees	30 Degrees	40 Degrees
1	1.279	1.28	2.91E-10	2.03E-10	8.75E-11	6.73E-11	4.61E-11
2	0.814	2.09	2.89E-10	2.09E-10	9.27E-11	7.17E-11	4.77E-11
3	1.091	3.18	2.46E-10	1.72E-10	8.10E-11	6.53E-11	4.51E-11
4	0.791	3.97	3.26E-10	2.30E-10	9.44E-11	7.21E-11	4.95E-11
5	0.812	4.79	3.00E-10	2.15E-10	9.14E-11	6.95E-11	4.59E-11
6	0.840	5.63	2.88E-10	2.05E-10	8.85E-11	6.80E-11	4.50E-11
7	0.810	6.44	2.78E-10	2.01E-10	9.09E-11	7.06E-11	4.58E-11
8	0.835	7.27	2.82E-10	2.01E-10	8.70E-11	6.68E-11	4.37E-11
9	0.857	8.13	1.40E-10	1.03E-10	6.63E-11	5.99E-11	4.06E-11
10	0.871	9.00	1.76E-10	1.34E-10	8.96E-11	7.53E-11	4.40E-11
11	0.916	9.92	1.60E-10	1.28E-10	9.35E-11	7.84E-11	4.26E-11
12	0.982	10.90	1.50E-10	1.24E-10	9.75E-11	8.07E-11	4.25E-11
13	0.983	11.88	1.29E-10	1.09E-10	9.15E-11	7.85E-11	4.28E-11
14	0.996	12.88	1.28E-10	1.11E-10	9.82E-11	8.32E-11	4.35E-11
15	1.074	13.95	1.20E-10	1.07E-10	9.74E-11	8.23E-11	4.22E-11
16	1.076	15.03	2.17E-10	1.54E-10	6.56E-11	4.95E-11	3.82E-11
17	1.185	16.21	1.91E-10	1.39E-10	6.27E-11	4.54E-11	3.27E-11
18	1.346	17.56	1.72E-10	1.26E-10	6.09E-11	4.60E-11	3.11E-11
19	1.414	18.97	1.54E-10	1.14E-10	5.78E-11	4.62E-11	3.49E-11
20	1.420	20.39	1.35E-10	1.01E-10	5.42E-11	4.47E-11	3.53E-11
21	1.389	21.78	1.18E-10	9.07E-11	5.35E-11	4.43E-11	3.42E-11

Table 6-1 cont'd

Calculated Neutron Exposure Rates And Integrated Exposures
At The Surveillance Capsule Center

Iron Atom Displacements

Cycle	Cycle Length [EFPY]	Total Irradiation Time [EFPY]	Displacements [dpa]				
			0 Degrees	10 Degrees	20 Degrees	30 Degrees	40 Degrees
1	1.279	1.28	1.17E-02	8.19E-03	3.53E-03	2.71E-03	1.86E-03
2	0.814	2.09	1.92E-02	1.36E-02	5.91E-03	4.56E-03	3.09E-03
3	1.091	3.18	2.76E-02	1.95E-02	8.70E-03	6.81E-03	4.64E-03
4	0.791	3.97	3.58E-02	2.52E-02	1.11E-02	8.61E-03	5.87E-03
5	0.812	4.79	4.34E-02	3.07E-02	1.34E-02	1.04E-02	7.05E-03
6	0.840	5.63	5.11E-02	3.62E-02	1.57E-02	1.22E-02	8.24E-03
7	0.810	6.44	5.82E-02	4.13E-02	1.81E-02	1.40E-02	9.41E-03
8	0.835	7.27	6.56E-02	4.66E-02	2.04E-02	1.58E-02	1.06E-02
9	0.857	8.13	6.94E-02	4.94E-02	2.22E-02	1.74E-02	1.17E-02
10	0.871	9.00	7.43E-02	5.30E-02	2.46E-02	1.94E-02	1.29E-02
11	0.916	9.92	7.89E-02	5.67E-02	2.73E-02	2.17E-02	1.41E-02
12	0.982	10.90	8.35E-02	6.06E-02	3.03E-02	2.42E-02	1.54E-02
13	0.983	11.88	8.75E-02	6.39E-02	3.32E-02	2.66E-02	1.67E-02
14	0.996	12.88	9.16E-02	6.74E-02	3.63E-02	2.93E-02	1.81E-02
15	1.074	13.95	9.56E-02	7.10E-02	3.96E-02	3.21E-02	1.95E-02
16	1.076	15.03	1.03E-01	7.63E-02	4.18E-02	3.37E-02	2.08E-02
17	1.185	16.21	1.10E-01	8.14E-02	4.41E-02	3.54E-02	2.21E-02
18	1.346	17.56	1.17E-01	8.68E-02	4.67E-02	3.74E-02	2.34E-02
19	1.414	18.97	1.24E-01	9.19E-02	4.93E-02	3.94E-02	2.49E-02
20	1.420	20.39	1.30E-01	9.64E-02	5.17E-02	4.14E-02	2.65E-02
21	1.389	21.78	1.35E-01	1.00E-01	5.41E-02	4.34E-02	2.80E-02

Table 6-2

Calculated Azimuthal Variation Of Maximum Exposure Rates
And Integrated Exposures At The Reactor Vessel
Clad/Base Metal Interface

Cycle	Cycle Length [EFPY]	Total Irradiation Time [EFPY]	Neutron Flux (E > 1.0 MeV) [n/cm^2-s]					
			0 Degrees	10 Degrees	20 Degrees	30 Degrees	40 Degrees	45 Degrees
1	1.279	1.28	6.23E+10	4.38E+10	2.16E+10	1.62E+10	1.17E+10	1.11E+10
2	0.814	2.09	6.07E+10	4.40E+10	2.23E+10	1.68E+10	1.19E+10	1.12E+10
3	1.091	3.18	5.14E+10	3.63E+10	1.94E+10	1.53E+10	1.12E+10	1.06E+10
4	0.791	3.97	6.96E+10	4.92E+10	2.32E+10	1.72E+10	1.25E+10	1.19E+10
5	0.812	4.79	6.37E+10	4.56E+10	2.23E+10	1.65E+10	1.16E+10	1.09E+10
6	0.840	5.63	6.16E+10	4.39E+10	2.17E+10	1.63E+10	1.14E+10	1.07E+10
7	0.810	6.44	5.92E+10	4.28E+10	2.21E+10	1.68E+10	1.16E+10	1.08E+10
8	0.835	7.27	5.90E+10	4.21E+10	2.09E+10	1.56E+10	1.08E+10	1.02E+10
9	0.857	8.13	2.92E+10	2.18E+10	1.55E+10	1.37E+10	9.90E+09	9.32E+09
10	0.871	9.00	3.76E+10	2.89E+10	2.12E+10	1.75E+10	1.11E+10	1.02E+10
11	0.916	9.92	3.44E+10	2.77E+10	2.21E+10	1.81E+10	1.08E+10	9.71E+09
12	0.982	10.90	3.25E+10	2.70E+10	2.30E+10	1.87E+10	1.08E+10	9.63E+09
13	0.983	11.88	2.81E+10	2.39E+10	2.16E+10	1.82E+10	1.08E+10	9.75E+09
14	0.996	12.88	2.78E+10	2.44E+10	2.30E+10	1.92E+10	1.10E+10	9.84E+09
15	1.074	13.95	2.63E+10	2.34E+10	2.29E+10	1.91E+10	1.08E+10	9.54E+09
16	1.076	15.03	4.61E+10	3.30E+10	1.61E+10	1.19E+10	9.58E+09	9.27E+09
17	1.185	16.21	4.07E+10	2.97E+10	1.53E+10	1.09E+10	8.20E+09	7.88E+09
18	1.346	17.56	3.69E+10	2.71E+10	1.48E+10	1.10E+10	7.85E+09	7.32E+09
19	1.414	18.97	3.32E+10	2.46E+10	1.40E+10	1.10E+10	8.74E+09	8.42E+09
20	1.420	20.39	2.93E+10	2.21E+10	1.33E+10	1.08E+10	8.89E+09	8.63E+09
21	1.389	21.78	2.56E+10	1.98E+10	1.29E+10	1.06E+10	8.56E+09	8.27E+09

Table 6-2 cont'd

Calculated Azimuthal Variation Of Maximum Exposure Rates
And Integrated Exposures At The Reactor Vessel
Clad/Base Metal Interface

Cycle	Cycle Length [EFPY]	Total Irradiation Time [EFPY]	Neutron Fluence (E > 1.0 MeV) [n/cm^2]					
			0 Degrees	10 Degrees	20 Degrees	30 Degrees	40 Degrees	45 Degrees
1	1.279	1.28	2.52E+18	1.77E+18	8.71E+17	6.53E+17	4.73E+17	4.49E+17
2	0.814	2.09	4.07E+18	2.90E+18	1.44E+18	1.09E+18	7.78E+17	7.35E+17
3	1.091	3.18	5.84E+18	4.15E+18	2.11E+18	1.61E+18	1.16E+18	1.10E+18
4	0.791	3.97	7.55E+18	5.36E+18	2.68E+18	2.03E+18	1.47E+18	1.39E+18
5	0.812	4.79	9.17E+18	6.52E+18	3.25E+18	2.46E+18	1.77E+18	1.67E+18
6	0.840	5.63	1.08E+19	7.67E+18	3.82E+18	2.88E+18	2.07E+18	1.95E+18
7	0.810	6.44	1.23E+19	8.76E+18	4.38E+18	3.31E+18	2.36E+18	2.23E+18
8	0.835	7.27	1.38E+19	9.86E+18	4.93E+18	3.72E+18	2.64E+18	2.49E+18
9	0.857	8.13	1.46E+19	1.05E+19	5.35E+18	4.09E+18	2.91E+18	2.74E+18
10	0.871	9.00	1.56E+19	1.12E+19	5.92E+18	4.56E+18	3.21E+18	3.02E+18
11	0.916	9.92	1.66E+19	1.20E+19	6.55E+18	5.08E+18	3.52E+18	3.30E+18
12	0.982	10.90	1.76E+19	1.28E+19	7.26E+18	5.66E+18	3.86E+18	3.60E+18
13	0.983	11.88	1.84E+19	1.35E+19	7.92E+18	6.22E+18	4.19E+18	3.90E+18
14	0.996	12.88	1.93E+19	1.43E+19	8.65E+18	6.83E+18	4.54E+18	4.21E+18
15	1.074	13.95	2.01E+19	1.51E+19	9.42E+18	7.47E+18	4.90E+18	4.53E+18
16	1.076	15.03	2.17E+19	1.62E+19	9.94E+18	7.87E+18	5.22E+18	4.84E+18
17	1.185	16.21	2.32E+19	1.73E+19	1.05E+19	8.27E+18	5.52E+18	5.13E+18
18	1.346	17.56	2.48E+19	1.84E+19	1.11E+19	8.73E+18	5.85E+18	5.44E+18
19	1.414	18.97	2.63E+19	1.95E+19	1.18E+19	9.22E+18	6.24E+18	5.81E+18
20	1.420	20.39	2.76E+19	2.05E+19	1.24E+19	9.69E+18	6.63E+18	6.19E+18
21	1.389	21.78	2.87E+19	2.14E+19	1.29E+19	1.02E+19	7.01E+18	6.56E+18

Note: At the end of Cycle 20, the maximum fast (E > 1.0 MeV) neutron fluence at the pressure vessel wall occurs at an axial elevation about 10 cm above the midplane of the active fuel for the 0°, 10°, and 20° azimuths and at about 37 cm below the midplane of the active fuel for the 30°, 40° and 45° azimuths. However, the axial distribution is quite flat around axial midplane and the maximum fluence value is within ~1% of the midplane value.

Table 6-2 cont'd

Calculated Azimuthal Variation Of Maximum Exposure Rates
And Integrated Exposures At The Reactor Vessel
Clad/Base Metal Interface

Cycle	Cycle Length [EFPY]	Total Irradiation Time [EFPY]	Iron Atom Displacement Rate [dpa/s]					
			0 Degrees	10 Degrees	20 Degrees	30 Degrees	40 Degrees	45 Degrees
1	1.279	1.28	1.03E-10	7.32E-11	3.56E-11	2.65E-11	1.92E-11	1.83E-11
2	0.814	2.09	1.00E-10	7.34E-11	3.67E-11	2.75E-11	1.94E-11	1.84E-11
3	1.091	3.18	8.49E-11	6.06E-11	3.19E-11	2.50E-11	1.82E-11	1.74E-11
4	0.791	3.97	1.15E-10	8.21E-11	3.83E-11	2.82E-11	2.04E-11	1.95E-11
5	0.812	4.79	1.05E-10	7.62E-11	3.67E-11	2.70E-11	1.89E-11	1.79E-11
6	0.840	5.63	1.02E-10	7.33E-11	3.58E-11	2.66E-11	1.87E-11	1.76E-11
7	0.810	6.44	9.78E-11	7.15E-11	3.65E-11	2.74E-11	1.89E-11	1.78E-11
8	0.835	7.27	9.73E-11	7.02E-11	3.44E-11	2.55E-11	1.77E-11	1.67E-11
9	0.857	8.13	4.76E-11	3.59E-11	2.52E-11	2.22E-11	1.61E-11	1.52E-11
10	0.871	9.00	6.18E-11	4.80E-11	3.47E-11	2.86E-11	1.81E-11	1.68E-11
11	0.916	9.92	5.67E-11	4.59E-11	3.61E-11	2.97E-11	1.76E-11	1.60E-11
12	0.982	10.90	5.34E-11	4.47E-11	3.75E-11	3.06E-11	1.77E-11	1.59E-11
13	0.983	11.88	4.61E-11	3.95E-11	3.52E-11	2.97E-11	1.77E-11	1.61E-11
14	0.996	12.88	4.58E-11	4.04E-11	3.76E-11	3.14E-11	1.81E-11	1.63E-11
15	1.074	13.95	4.33E-11	3.88E-11	3.72E-11	3.11E-11	1.76E-11	1.58E-11
16	1.076	15.03	7.60E-11	5.49E-11	2.64E-11	1.94E-11	1.56E-11	1.52E-11
17	1.185	16.21	6.70E-11	4.94E-11	2.51E-11	1.78E-11	1.34E-11	1.29E-11
18	1.346	17.56	6.06E-11	4.50E-11	2.43E-11	1.79E-11	1.28E-11	1.20E-11
19	1.414	18.97	5.45E-11	4.08E-11	2.30E-11	1.80E-11	1.42E-11	1.38E-11
20	1.420	20.39	4.81E-11	3.66E-11	2.17E-11	1.76E-11	1.45E-11	1.41E-11
21	1.389	21.78	4.20E-11	3.28E-11	2.12E-11	1.73E-11	1.39E-11	1.36E-11

Table 6-2 cont'd

Calculated Azimuthal Variation Of Maximum Exposure Rates
And Integrated Exposures At The Reactor Vessel
Clad/Base Metal Interface

Cycle	Cycle Length [EFPY]	Total Irradiation Time [EFPY]	Iron Atom Displacements [dpa]					
			0 Degrees	10 Degrees	20 Degrees	30 Degrees	40 Degrees	45 Degrees
1	1.279	1.28	4.16E-03	2.95E-03	1.44E-03	1.07E-03	7.73E-04	7.37E-04
2	0.814	2.09	6.73E-03	4.84E-03	2.38E-03	1.78E-03	1.27E-03	1.21E-03
3	1.091	3.18	9.65E-03	6.92E-03	3.48E-03	2.64E-03	1.90E-03	1.81E-03
4	0.791	3.97	1.25E-02	8.94E-03	4.42E-03	3.33E-03	2.40E-03	2.29E-03
5	0.812	4.79	1.52E-02	1.09E-02	5.36E-03	4.02E-03	2.88E-03	2.74E-03
6	0.840	5.63	1.78E-02	1.28E-02	6.30E-03	4.72E-03	3.37E-03	3.21E-03
7	0.810	6.44	2.03E-02	1.46E-02	7.23E-03	5.41E-03	3.86E-03	3.66E-03
8	0.835	7.27	2.29E-02	1.65E-02	8.13E-03	6.08E-03	4.32E-03	4.10E-03
9	0.857	8.13	2.42E-02	1.74E-02	8.81E-03	6.68E-03	4.75E-03	4.51E-03
10	0.871	9.00	2.58E-02	1.87E-02	9.75E-03	7.46E-03	5.25E-03	4.96E-03
11	0.916	9.92	2.74E-02	2.00E-02	1.08E-02	8.32E-03	5.75E-03	5.43E-03
12	0.982	10.90	2.90E-02	2.13E-02	1.19E-02	9.26E-03	6.30E-03	5.92E-03
13	0.983	11.88	3.03E-02	2.25E-02	1.30E-02	1.02E-02	6.85E-03	6.42E-03
14	0.996	12.88	3.18E-02	2.38E-02	1.42E-02	1.12E-02	7.42E-03	6.93E-03
15	1.074	13.95	3.32E-02	2.51E-02	1.54E-02	1.22E-02	8.01E-03	7.46E-03
16	1.076	15.03	3.58E-02	2.70E-02	1.63E-02	1.29E-02	8.53E-03	7.96E-03
17	1.185	16.21	3.83E-02	2.88E-02	1.72E-02	1.35E-02	9.02E-03	8.44E-03
18	1.346	17.56	4.09E-02	3.07E-02	1.83E-02	1.43E-02	9.56E-03	8.95E-03
19	1.414	18.97	4.33E-02	3.25E-02	1.93E-02	1.51E-02	1.02E-02	9.56E-03
20	1.420	20.39	4.54E-02	3.42E-02	2.03E-02	1.58E-02	1.08E-02	1.02E-02
21	1.389	21.78	4.73E-02	3.56E-02	2.12E-02	1.66E-02	1.14E-02	1.08E-02

Note: At the end of Cycle 20, the maximum dpa at the pressure vessel wall occurs at an axial elevation about 10 cm above the midplane of the active fuel for the 0°, 10°, and 20° azimuths and at about 37 cm below the midplane of the active fuel for the 30°, 40° and 45° azimuths. However, the axial distribution is quite flat around axial midplane and the maximum dpa value is within ~1% of the midplane value.

Table 6-3

Relative Radial Distribution Of Neutron Fluence (E > 1.0 MeV)
Within The Reactor Vessel Wall

RADIUS	AZIMUTHAL ANGLE					
(cm)	0°	10°	20°	30°	40°	45°
198.039	1.000	1.000	1.000	1.000	1.000	1.000
203.943	0.516	0.520	0.528	0.524	0.531	0.520
209.846	0.234	0.238	0.244	0.241	0.246	0.236
215.750	0.101	0.104	0.108	0.106	0.109	0.104
221.653	0.039	0.042	0.046	0.045	0.047	0.044

Note:
Base Metal Inner Radius = 198.039
Base Metal 1/4T = 203.943
Base Metal 1/2T = 209.846
Base Metal 3/4T = 215.750
Base Metal Outer Radius = 221.653

Table 6-4

Relative Radial Distribution Of Iron Atom Displacements (dpa)
Within The Reactor Vessel Wall

RADIUS	AZIMUTHAL ANGLE					
(cm)	0°	10°	20°	30°	40°	45°
198.039	1.000	1.000	1.000	1.000	1.000	1.000
203.943	0.629	0.639	0.651	0.640	0.648	0.636
209.846	0.378	0.391	0.406	0.393	0.401	0.389
215.750	0.217	0.232	0.248	0.237	0.243	0.233
221.653	0.104	0.119	0.139	0.133	0.137	0.131

Note:
Base Metal Inner Radius = 198.039
Base Metal 1/4T = 203.943
Base Metal 1/2T = 209.846
Base Metal 3/4T = 215.750
Base Metal Outer Radius = 221.653

Table 6-5

Nuclear Parameters Used In The Evaluation Of Neutron Sensors

Monitor Material	Reaction of Interest	Target Atom Fraction	90% Response Range (MeV)	Product Half-life	Fission Yield (%)
Copper	^{63}Cu (n,α)	0.6917	4.8 – 11.7	5.271 y	
Iron	^{54}Fe (n,p)	0.0585	2.1 – 8.3	312.3 d	
Nickel	^{58}Ni (n,p)	0.6808	1.6 – 8.1	70.82 d	
Uranium-238	^{238}U (n,f)	0.9996	1.3 – 6.8	30.07 y	6.02
Neptunium-237	^{237}Np (n,f)	1.0000	0.4 – 4.3	30.07 y	6.17
Cobalt-Aluminum	^{59}Co (n,γ)	0.0015	non-threshold	5.271 y	

Note: The 90% response range is defined such that, in the neutron spectrum characteristic of the H. B. Robinson Unit 2 surveillance capsules, approximately 90% of the sensor response is due to neutrons in the energy range specified, with approximately 5% of the total response due to neutrons with energies below the lower limit and 5% of the total response due to neutrons with energies above the upper limit.

Table 6-6

Monthly Thermal Generation During The First 20 Fuel Cycles
Of The H. B. Robinson Unit 2 Reactor
(Reactor Power of 2300 MWt)

Year	Month	Thermal Generation (MWt-hr)	Year	Month	Thermal Generation (MWt-hr)	Year	Month	Thermal Generation (MWt-hr)
1970	10	17339	1973	5	325257	1975	12	848232
1970	11	17339	1973	6	1315814	1976	1	1356960
1970	12	17339	1973	7	1379687	1976	2	1519690
1971	1	315994	1973	8	1498106	1976	3	1593451
1971	2	315994	1973	9	1490895	1976	4	1513829
1971	3	315994	1973	10	1517185	1976	5	1425283
1971	4	0	1973	11	1144053	1976	6	1574338
1971	5	500000	1973	12	1457592	1976	7	1515096
1971	6	0	1974	1	1504428	1976	8	1570061
1971	7	0	1974	2	1504428	1976	9	1554326
1971	8	0	1974	3	1504428	1976	10	1470691
1971	9	1500000	1974	4	1539067	1976	11	0
1971	10	1634231	1974	5	237864	1976	12	772992
1971	11	1486726	1974	6	125088	1977	1	1586376
1971	12	1781736	1974	7	1547784	1977	2	775685
1972	1	1497683	1974	8	1499250	1977	3	1468421
1972	2	1536043	1974	9	1447142	1977	4	1247136
1972	3	1637212	1974	10	1462454	1977	5	1618214
1972	4	1565161	1974	11	1554379	1977	6	1514674
1972	5	294474	1974	12	1625232	1977	7	1492603
1972	6	962248	1975	1	1494979	1977	8	1214347
1972	7	1190975	1975	2	1467416	1977	9	764597
1972	8	1440808	1975	3	1562880	1977	10	819614
1972	9	1440195	1975	4	577104	1977	11	205392
1972	10	1537511	1975	5	220968	1977	12	1571170
1972	11	1348800	1975	6	1259069	1978	1	1314192
1972	12	1097499	1975	7	1476658	1978	2	0
1973	1	908362	1975	8	1616842	1978	3	0
1973	2	806836	1975	9	1493870	1978	4	157872
1973	3	611522	1975	10	1570219	1978	5	1528032
1973	4	0	1975	11	0	1978	6	1571645

Table 6-6 Cont'd

Monthly Thermal Generation During The First 20 Fuel Cycles
Of The H. B. Robinson Unit 2 Reactor
(Reactor Power of 2300 MWt)

Year	Month	Thermal Generation (MWt-hr)	Year	Month	Thermal Generation (MWt-hr)	Year	Month	Thermal Generation (MWt-hr)
1978	7	1280875	1981	2	1279260	1983	9	557630
1978	8	1607654	1981	3	1604554	1983	10	1342574
1978	9	1124904	1981	4	1545048	1983	11	89921
1978	10	1616050	1981	5	795101	1983	12	674378
1978	11	1559923	1981	6	877625	1984	1	783840
1978	12	1552214	1981	7	1523299	1984	2	0
1979	1	1503322	1981	8	0	1984	3	0
1979	2	1335576	1981	9	733663	1984	4	0
1979	3	1603906	1981	10	843842	1984	5	0
1979	4	490565	1981	11	182326	1984	6	0
1979	5	0	1981	12	1039692	1984	7	0
1979	6	0	1982	1	1361232	1984	8	0
1979	7	374532	1982	2	1140046	1984	9	0
1979	8	1635466	1982	3	0	1984	10	0
1979	9	1482838	1982	4	0	1984	11	0
1979	10	1556695	1982	5	0	1984	12	0
1979	11	1518386	1982	6	0	1985	1	139435
1979	12	1555205	1982	7	0	1985	2	779534
1980	1	1593955	1982	8	245143	1985	3	1537210
1980	2	1475827	1982	9	1029149	1985	4	1546428
1980	3	875306	1982	10	1331038	1985	5	1614490
1980	4	641866	1982	11	1265350	1985	6	1631878
1980	5	1070935	1982	12	1297145	1985	7	1613938
1980	6	1486150	1983	1	1227869	1985	8	1552003
1980	7	870228	1983	2	1141757	1985	9	1454410
1980	8	193421	1983	3	1309068	1985	10	1534891
1980	9	0	1983	4	943313	1985	11	1579162
1980	10	177910	1983	5	148543	1985	12	1633037
1980	11	1359907	1983	6	1271311	1986	1	952586
1980	12	916210	1983	7	1289251	1986	2	0
1981	1	1458329	1983	8	1330817	1986	3	235042

Table 6-6 Cont'd

Monthly Thermal Generation During The First 20 Fuel Cycles
Of The H. B. Robinson Unit 2 Reactor
(Reactor Power of 2300 MWt)

Year	Month	Thermal Generation (MWt-hr)	Year	Month	Thermal Generation (MWt-hr)	Year	Month	Thermal Generation (MWt-hr)
1986	4	1575463	1988	11	548743	1991	6	1648658
1986	5	1659478	1988	12	0	1991	7	1688126
1986	6	1537099	1989	1	0	1991	8	1514026
1986	7	1693481	1989	2	48962	1991	9	1209377
1986	8	1315582	1989	3	1523189	1991	10	1707888
1986	9	1344727	1989	4	921674	1991	11	1556198
1986	10	1695634	1989	5	1670738	1991	12	1687850
1986	11	1623266	1989	6	1640710	1992	1	1701650
1986	12	1557413	1989	7	1696130	1992	2	1596936
1987	1	1694474	1989	8	1153790	1992	3	1443259
1987	2	1508395	1989	9	0	1992	4	0
1987	3	1030087	1989	10	0	1992	5	0
1987	4	0	1989	11	0	1992	6	216605
1987	5	0	1989	12	406879	1992	7	1521367
1987	6	596657	1990	1	1635576	1992	8	1170295
1987	7	1378289	1990	2	1460758	1992	9	332138
1987	8	1268110	1990	3	1038809	1992	10	1664004
1987	9	1064311	1990	4	1289914	1992	11	1574194
1987	10	1676369	1990	5	782846	1992	12	1700767
1987	11	1559897	1990	6	1095941	1993	1	1703969
1987	12	1693757	1990	7	1518110	1993	2	1537817
1988	1	1426699	1990	8	1615483	1993	3	1699663
1988	2	0	1990	9	323914	1993	4	1644463
1988	3	675427	1990	10	0	1993	5	1562215
1988	4	947950	1990	11	0	1993	6	1634251
1988	5	796370	1990	12	0	1993	7	1429901
1988	6	1180342	1991	1	0	1993	8	1705349
1988	7	1698062	1991	2	0	1993	9	549792
1988	8	1634858	1991	3	1063373	1993	10	0
1988	9	402353	1991	4	1638281	1993	11	46478
1988	10	1245809	1991	5	1626468	1993	12	0

Table 6-6 Cont'd

Monthly Thermal Generation During The First 20 Fuel Cycles
Of The H. B. Robinson Unit 2 Reactor
(Reactor Power of 2300 MWt)

Year	Month	Thermal Generation (MWt-hr)	Year	Month	Thermal Generation (MWt-hr)	Year	Month	Thermal Generation (MWt-hr)
1994	1	0	1996	8	1676976	1999	3	1710206
1994	2	98532	1996	9	350686	1999	4	1648769
1994	3	422390	1996	10	444967	1999	5	1703362
1994	4	1516454	1996	11	1654896	1999	6	1651363
1994	5	1679846	1996	12	1709930	1999	7	1710317
1994	6	1651032	1997	1	1703858	1999	8	1694585
1994	7	1699111	1997	2	1544220	1999	9	1127681
1994	8	1435145	1997	3	1667978	1999	10	359518
1994	9	1652081	1997	4	1622494	1999	11	1654730
1994	10	1699663	1997	5	1710262	1999	12	1710648
1994	11	1633865	1997	6	1643304	2000	1	1701264
1994	12	1697400	1997	7	1700878	2000	2	1600138
1995	1	1697897	1997	8	1710262	2000	3	1690390
1995	2	1535057	1997	9	1642531	2000	4	1615594
1995	3	1696793	1997	10	1710648	2000	5	1710317
1995	4	1530641	1997	11	1391095	2000	6	1535002
1995	5	0	1997	12	1710372	2000	7	1710372
1995	6	371054	1998	1	1710372	2000	8	1710427
1995	7	1423056	1998	2	1544827	2000	9	1652798
1995	8	1705956	1998	3	318946	2000	10	1704852
1995	9	1618961	1998	4	718980	2000	11	1653350
1995	10	1708054	1998	5	1710482	2000	12	1710096
1995	11	1650259	1998	6	1624094	2001	1	1706508
1995	12	1700105	1998	7	1679902	2001	2	1533346
1996	1	1687133	1998	8	1696351	2001	3	1433875
1996	2	1596660	1998	9	1655172	2001	4	236808
1996	3	1698338	1998	10	1613330			
1996	4	1649431	1998	11	1655172			
1996	5	1705294	1998	12	1710538			
1996	6	1641703	1999	1	1642973			
1996	7	1696130	1999	2	1544827			

Table 6-7

Calculated $\phi(E > 1.0\ MeV)$ and C_j Factors at the Surveillance Capsule Center Core Midplane Elevation

Capsules S, V, and T

Fuel Cycle	$\phi(E > 1.0\ MeV)$ [n/cm^2-s]			C_j		
	Capsule S	Capsule V	Capsule T	S	V	T
1	1.19E+11	5.33E+10	1.71E+11	1.000	1.010	1.016
2		5.65E+10	1.70E+11		1.067	1.010
3		4.94E+10	1.45E+11		0.938	0.862
4			1.92E+11			1.137
5			1.77E+11			1.046
6			1.70E+11			1.007
7			1.64E+11			0.971
8			1.67E+11			0.993
Average	1.19E+11	5.28E+10	1.69E+11	1.000	1.000	1.000

Capsule X

Fuel Cycle	$\phi(E>1.0\ MeV)$ [n/cm^2-s]	Relative Reaction Rate (Cj)						
		Cu(n,α)	Fe(n,p)	Ni(n,p)	^{238}U(n,f)	^{237}Np(n,f)	Co(n,γ)(Cd)	Co(n,γ)
1	2.84E+10	0.445	0.369	0.361	0.324	0.290	0.245	0.252
2	2.94E+10	0.461	0.382	0.374	0.335	0.301	0.254	0.261
3	2.78E+10	0.437	0.361	0.354	0.317	0.284	0.240	0.246
4	3.05E+10	0.478	0.396	0.388	0.348	0.312	0.263	0.271
5	2.83E+10	0.445	0.367	0.360	0.322	0.289	0.244	0.251
6	2.77E+10	0.437	0.360	0.353	0.316	0.283	0.239	0.246
7	2.82E+10	0.443	0.367	0.359	0.322	0.288	0.244	0.251
8	2.69E+10	0.429	0.352	0.345	0.308	0.275	0.231	0.238
9	8.35E+10	0.921	0.913	0.911	0.904	0.893	0.876	0.882
10	1.05E+11	1.088	1.110	1.111	1.121	1.128	1.138	1.136
11	9.51E+10	1.013	1.020	1.020	1.023	1.026	1.029	1.029
12	8.93E+10	0.971	0.966	0.965	0.963	0.961	0.960	0.960
13	7.67E+10	0.851	0.836	0.835	0.829	0.825	0.821	0.821
14	7.60E+10	0.850	0.831	0.829	0.822	0.816	0.811	0.812
15	7.16E+10	0.810	0.786	0.784	0.775	0.769	0.762	0.763
16	1.28E+11	1.299	1.347	1.351	1.372	1.391	1.412	1.409
17	1.13E+11	1.179	1.201	1.203	1.212	1.220	1.230	1.228
18	1.02E+11	1.092	1.097	1.097	1.098	1.100	1.102	1.101
19	9.17E+10	1.002	0.994	0.994	0.990	0.987	0.983	0.983
20	8.00E+10	0.891	0.874	0.873	0.866	0.860	0.853	0.852

Table 6-8

Measured Sensor Activities And Reaction Rates

Surveillance Capsule S

Reaction	Axial Location	Radial Location	Measured Activity (dps/g)	Saturated Activity (dps/g)	Radially Adjusted Saturated Activity (dps/g)	Radially Adjusted Reaction Rate (rps/atom)
$^{63}Cu(n,\alpha)\,^{60}Co$	Top	190.923	1.66E+05	1.11E+06	Not used	
	Bottom	190.923	8.34E+04	5.57E+05	5.32E+05	8.11E-17
	Average					**8.11E-17**
$^{54}Fe\,(n,p)\,^{54}Mn$	Top	191.923	2.60E+06	4.79E+06	5.55E+06	8.87E-15
	Top-Mid	190.923	2.70E+06	4.97E+06	4.74E+06	7.57E-15
	Middle	191.923	2.62E+06	4.82E+06	5.59E+06	8.94E-15
	Bot-Mid	190.923	3.00E+06	5.52E+06	5.26E+06	8.41E-15
	Bottom	191.923	2.50E+06	4.60E+06	5.33E+06	8.53E-15
	Average					**8.47E-15**
$^{58}Ni\,(n,p)\,^{58}Co$	Middle	190.923	4.74E+07	7.18E+07	6.84E+07	9.77E-15
	Average					**9.77E-15**
$^{59}Co\,(n,\gamma)\,^{60}Co$ (Cd)	Top	191.923	5.84E+06	3.90E+07	4.49E+07	2.93E-12
	Middle	191.923	5.90E+06	3.94E+07	4.53E+07	2.96E-12
	Bottom	191.923	7.44E+06	4.97E+07	5.71E+07	3.73E-12
	Average					**3.20E-12**
$^{59}Co\,(n,\gamma)\,^{60}Co$	Top	191.923	1.83E+07	1.22E+08	1.19E+08	7.75E-12
	Bottom	191.923	2.06E+07	1.37E+08	1.33E+08	8.70E-12
	Average					**8.22E-12**

Note: Measured specific activities are corrected to the end of irradiation date of March 16, 1973.

Table 6-8 cont'd

Measured Sensor Activities And Reaction Rates

Surveillance Capsule V

Reaction	Axial Location	Radial Location	Measured Activity (dps/g)	Saturated Activity (dps/g)	Radially Adjusted Saturated Activity (dps/g)	Radially Adjusted Reaction Rate (rps/atom)
^{63}Cu (n,α) ^{60}Co	Top	190.923	1.18E+05	3.70E+05	3.54E+05	5.40E-17
	Bottom	190.923	1.12E+05	3.52E+05	3.36E+05	5.12E-17
	Average					**5.26E-17**
^{54}Fe (n,p) ^{54}Mn	Top	191.923	1.94E+06	2.72E+06	3.13E+06	5.01E-15
	Top-Mid	190.923	2.24E+06	3.14E+06	3.00E+06	4.79E-15
	Middle	191.923	2.12E+06	2.97E+06	3.43E+06	5.48E-15
	Bot-Mid	190.923	2.08E+06	2.91E+06	2.78E+06	4.44E-15
	Bottom	191.923	2.34E+06	3.28E+06	3.78E+06	6.04E-15
	Average					**5.15E-15**
^{58}Ni (n,p) ^{58}Co	Middle	190.923	4.19E+07	5.40E+07	5.15E+07	**7.36E-15**
^{238}U (n,f) ^{137}Cs (Cd)	Middle	191.155	2.75E+07	3.95E+08	Not Used	
^{237}Np (n,f) ^{137}Cs (Cd)	Middle	191.155	1.83E+07	2.63E+08	Not Used	
^{59}Co (n,γ) ^{60}Co (Cd)	Top	191.923	3.23E+06	1.01E+07	1.14E+07	7.43E-13
	Middle	191.923	4.83E+06	1.52E+07	1.71E+07	1.11E-12
	Bottom	191.923	6.90E+06	2.17E+07	2.44E+07	1.59E-12
	Average					**1.15E-12**
^{59}Co (n,γ) ^{60}Co	Top	191.923	1.68E+07	5.27E+07	5.01E+07	3.27E-12
	Middle	191.923	1.61E+07	5.04E+07	4.79E+07	3.12E-12
	Bottom	191.923	1.62E+07	5.08E+07	4.83E+07	3.15E-12
	Average					**3.18E-12**

Note: Measured specific activities are corrected to the end of irradiation date of October 31, 1975.

Table 6-8 cont'd

Measured Sensor Activities And Reaction Rates

Surveillance Capsule T

Reaction	Axial Location	Radial Location	Measured Activity (dps/g)	Saturated Activity (dps/g)	Radially Adjusted Saturated Activity (dps/g)	Radially Adjusted Reaction Rate (rps/atom)
^{63}Cu (n,α) ^{60}Co	Top	190.923	3.56E+05	7.76E+05	7.40E+05	1.13E-16
	Bottom	190.923	3.72E+05	8.10E+05	7.73E+05	1.18E-16
	Average					**1.15E-16**
^{54}Fe (n,p) ^{54}Mn	Top	190.923	3.10E+06	8.70E+06	8.29E+06	1.32E-14
	Top	191.923	2.58E+06	7.11E+06	8.26E+06	1.32E-14
	Middle	190.923	3.06E+06	8.58E+06	8.17E+06	1.31E-14
	Middle	191.923	2.56E+06	7.19E+06	8.34E+06	1.33E-14
	Bottom	190.923	3.35E+06	9.41E+06	8.96E+06	1.43E-14
	Bottom	191.923	2.58E+06	7.24E+06	8.41E+06	1.34E-14
	Average					**1.34E-14**
^{58}Ni (n,p) ^{58}Co	Middle	190.923	8.53E+06	1.28E+08	1.22E+08	**1.74E-14**
^{238}U (n,f) ^{137}Cs (Cd)	Middle	191.155	2.37E+06	1.63E+07	1.17E+07	**7.68E-14**
^{237}Np (n,f) ^{137}Cs (Cd)	Middle	191.155	1.25E+07	8.58E+07	8.45E+07	**5.30E-13**
^{59}Co (n,γ) ^{60}Co (Cd)	Top	191.923	2.54E+07	5.52E+07	6.35E+07	4.14E-12
	Middle	191.923	2.73E+07	5.94E+07	6.82E+07	4.45E-12
	Bottom	191.923	2.76E+07	6.00E+07	6.90E+07	4.50E-12
	Average					**4.36E-12**
^{59}Co (n,γ) ^{60}Co	Top	191.923	5.61E+07	1.22E+08	1.19E+08	7.76E-12
	Bottom	191.923	6.71E+07	1.46E+08	1.42E+08	9.29E-12
	Average					**8.53E-12**

Note: Measured specific activities are corrected to a counting date of October 8, 1982.

Table 6-8 cont'd

Measured Sensor Activities And Reaction Rates

Surveillance Capsule X [a]

Reaction	Axial Location	Radial Location	Measured Activity (dps/g)	Saturated Activity (dps/g)	Radially Adjusted Saturated Activity (dps/g)	Radially Adjusted Reaction Rate (rps/atom)
^{63}Cu (n,α) ^{60}Co	Top	190.923	3.31E+05	4.60E+05	4.39E+05	6.70E-17
	Bottom	190.923	3.15E+05	4.38E+05	4.18E+05	6.38E-17
	Average					**6.54E-17**
^{54}Fe (n,p) ^{54}Mn	Middle	190.923	2.67E+06	4.28E+06	4.08E+06	6.48E-15
	Middle	191.923	2.23E+06	3.58E+06	4.15E+06	6.58E-15
	Average					**6.53E-15**
^{58}Ni (n,p) ^{58}Co	Middle	190.923	1.45E+07	7.54E+07	7.18E+07	**1.03E-14**
^{238}U (n,f) ^{137}Cs (Cd)	Middle	191.155	2.01E+06	7.15E+06	4.97E+06	**3.27E-14**
^{237}Np (n,f) ^{137}Cs (Cd)	Middle	191.155	1.25E+07	4.50E+07	4.43E+07	**2.83E-13**
^{59}Co (n,γ) ^{60}Co (Cd)	Top	191.923	2.09E+07	2.94E+07	3.37E+07	2.20E-12
	Bottom	191.923	1.94E+07	2.73E+07	3.13E+07	2.04E-12
	Average					**2.12E-12**
^{59}Co (n,γ) ^{60}Co	Top	191.923	5.49E+07	7.73E+07	7.53E+07	4.91E-12
	Bottom	191.923	5.33E+07	7.50E+07	7.31E+07	4.77E-12
	Average					**4.84E-12**

Note: Measured specific activities are corrected to a counting date of September 1, 2001.

a. Saturated activities and reaction rates for capsule X are determined for the 0° location averaged over fuel cycles 9 through 20.

Table 6-9

Comparison of Measured, Calculated, and Best Estimate
Reaction Rates At The Surveillance Capsule Center

Capsule S

	Reaction Rate [rps/atom]				
Reaction	Measured	Calculated	Best Estimate	M/C	M/BE
$^{63}Cu(n,\alpha)^{60}Co$	8.11E-17	6.59E-17	7.81E-17	1.23	0.96
$^{54}Fe(n,p)^{54}Mn$	8.47E-15	7.92E-15	8.66E-15	1.07	1.02
$^{58}Ni(n,p)^{58}Co$	9.77E-15	1.10E-14	1.20E-14	0.89	1.22
$^{59}Co(n,\gamma)^{60}Co$	8.22E-12	6.19E-12	8.16E-12	1.33	0.99
$^{59}Co(n,\gamma)^{60}Co$ (Cd)	3.20E-12	2.88E-12	3.21E-12	1.11	1.00

Capsule V

	Reaction Rate [rps/atom]				
Reaction	Measured	Calculated	Best Estimate	M/C	M/BE
$^{63}Cu(n,\alpha)^{60}Co$	5.26E-17	4.05E-17	5.20E-17	1.30	0.99
$^{54}Fe(n,p)^{54}Mn$	5.15E-15	4.15E-15	5.25E-15	1.24	1.02
$^{58}Ni(n,p)^{58}Co$	7.36E-15	5.65E-15	7.22E-15	1.30	0.98
$^{59}Co(n,\gamma)^{60}Co$	3.18E-12	2.27E-12	3.16E-12	1.40	0.99
$^{59}Co(n,\gamma)^{60}Co$ (Cd)	1.15E-12	1.03E-12	1.15E-12	1.11	1.00

Table 6-9 cont'd

Comparison of Measured, Calculated, and Best Estimate
Reaction Rates At The Surveillance Capsule Center

Capsule T

	Reaction Rate [rps/atom]				
Reaction	Measured	Calculated	Best Estimate	M/C	M/BE
$^{63}Cu(n,\alpha)^{60}Co$	1.15E-16	9.13E-17	1.12E-16	1.26	0.97
$^{54}Fe(n,p)^{54}Mn$	1.34E-14	1.13E-14	1.34E-14	1.19	1.00
$^{58}Ni(n,p)^{58}Co$	1.74E-14	1.56E-14	1.82E-14	1.12	1.05
$^{238}U(n,f)^{137}Cs$ (Cd)	7.68E-14	5.80E-14	6.84E-14	1.32	0.89
$^{237}Np(n,f)^{137}Cs$ (Cd)	5.30E-13	4.61E-13	5.32E-13	1.15	1.00
$^{59}Co(n,\gamma)^{60}Co$	8.53E-12	8.52E-12	8.57E-12	1.00	1.00
$^{59}Co(n,\gamma)^{60}Co$ (Cd)	4.36E-12	3.97E-12	4.35E-12	1.10	1.00

Capsule X [a]

	Reaction Rate [rps/atom]				
Reaction	Measured	Calculated	Best Estimate	M/C	M/BE
$^{63}Cu(n,\alpha)^{60}Co$	6.54E-17	5.60E-17	6.36E-17	1.17	0.97
$^{54}Fe(n,p)^{54}Mn$	6.53E-15	6.48E-15	6.93E-15	1.01	1.06
$^{58}Ni(n,p)^{58}Co$	1.03E-14	8.93E-15	9.86E-15	1.15	0.96
$^{238}U(n,f)^{137}Cs$ (Cd)	3.26E-14	3.23E-14	3.45E-14	1.01	1.06
$^{237}Np(n,f)^{137}Cs$ (Cd)	2.82E-13	2.51E-13	2.74E-13	1.13	0.97
$^{59}Co(n,\gamma)^{60}Co$	4.84E-12	4.49E-12	4.83E-12	1.08	1.00
$^{59}Co(n,\gamma)^{60}Co$ (Cd)	2.12E-12	2.11E-12	2.13E-12	1.01	1.00

a. Reaction rates for capsule X are determined for the 0° location averaged over fuel cycles 9 through 20.

Table 6-10

Comparison of Calculated and Best Estimate Exposure Rates
At The Surveillance Capsule Center

Capsule ID	$\phi(E > 1.0\ MeV)$ [n/cm^2-s]			
	Calculated	Best Estimate (BE)	Uncertainty (1σ)	C/BE
S	1.19E+11	1.25E+11	8%	0.95
V	5.29E+10	6.56E+10	7%	0.81
T	1.69E+11	1.98E+11	6%	0.85
X [a]	9.31E+10	9.88E+10	6%	0.94

Capsule ID	Iron Atom Displacement Rate [dpa/s]			
	Calculated	Best Estimate (BE)	Uncertainty (1σ)	C/BE
S	2.01E-10	2.12E-10	9%	0.95
V	8.55E-11	1.05E-10	8%	0.82
T	2.83E-10	3.27E-10	7%	0.86
X [a]	1.55E-10	1.64E-10	7%	0.94

a. Exposure rates for capsule X are determined for the 0° location averaged over fuel cycles 9 through 20.

Table 6-11

Comparison of Calculated/Measured (C/M) Sensor Reaction Rate Ratios for Fast Neutron Threshold Reactions

Reaction	C/M Ratio			
	Capsule S	Capsule V	Capsule T	Capsule X
$^{63}Cu(n,\alpha)^{60}Co$	0.81	0.77	0.79	0.86
$^{54}Fe(n,p)^{54}Mn$	0.94	0.81	0.84	0.99
$^{58}Ni(n,p)^{58}Co$	1.13	0.77	0.90	0.87
$^{238}U(n,f)^{137}Cs$ (Cd)			0.76	0.99
$^{237}Np(n,f)^{137}Cs$ (Cd)			0.87	0.89
Average	0.96	0.78	0.83	0.92
% Standard Deviation	16.5	2.7	6.9	7.3

Note: The overall average C/M ratio for the set of sensor measurements is 0.87 with an associated standard deviation of 11.4%.

Table 6-12

Comparison of Calculated/ Best Estimate (C/BE) Exposure Rate Ratios

Capsule ID	C/BE Ratio	
	$\phi(E > 1.0$ MeV)	dpa/s
S	0.95	0.95
V	0.81	0.82
T	0.85	0.86
X	0.94	0.94
Average	0.89	0.89
% Standard Deviation	7.9	7.1

Table 6-13

Calculated Fast Neutron Exposure of Surveillance Capsules
Withdrawn from H. B. Robinson Unit 2

Capsule	Irradiation Time [EFPY]	Fluence (E > 1.0 MeV) [n/cm^2]	Iron Displacements [dpa]
S	1.28	4.79E+18	8.19E-03
V	3.18	5.30E+18	8.70E-03
T	7.27	3.87E+19	6.56E-02
X	20.39	4.49E+19	7.52E-02

Table 6-14

Calculated Maximum Fast Neutron Exposure of the H. B. Robinson Unit 2
Reactor Pressure Vessel at the Clad/Base Metal Interface at Selected Azimuthal Angles

Neutron Fluence [E > 1.0 MeV]

Cumulative Operating Time [EFPY]	Neutron Fluence [n/cm^2]					
	0.0 Degrees	10.0 Degrees	20.0 Degrees	30.0 Degrees	40.0 Degrees	45.0 Degrees
20.39 [a]	2.76E+19	2.05E+19	1.24E+19	9.69E+18	6.63E+18	6.19E+18
21.78 [b]	2.87E+19	2.14E+19	1.29E+19	1.02E+19	7.01E+18	6.56E+18
29.00	3.67E+19	2.73E+19	1.62E+19	1.27E+19	8.98E+18	8.45E+18
30.00	3.78E+19	2.81E+19	1.67E+19	1.30E+19	9.25E+18	8.71E+18
35.00	4.34E+19	3.22E+19	1.89E+19	1.48E+19	1.06E+19	1.00E+19
40.00	4.89E+19	3.63E+19	2.12E+19	1.65E+19	1.20E+19	1.13E+19
45.00	5.44E+19	4.04E+19	2.35E+19	1.82E+19	1.33E+19	1.26E+19
50.00	6.00E+19	4.45E+19	2.58E+19	2.00E+19	1.47E+19	1.40E+19

Iron Atom Displacements

Cumulative Operating Time [EFPY]	Iron Atom Displacements [dpa]					
	0.0 Degrees	10.0 Degrees	20.0 Degrees	30.0 Degrees	40.0 Degrees	45.0 Degrees
20.39 [a]	4.79E-02	3.42E-02	2.03E-02	1.58E-02	1.08E-02	1.02E-02
21.78 [b]	4.99E-02	3.56E-02	2.12E-02	1.66E-02	1.14E-02	1.08E-02
29.00	6.30E-02	4.54E-02	2.66E-02	2.07E-02	1.46E-02	1.39E-02
30.00	6.49E-02	4.68E-02	2.73E-02	2.13E-02	1.51E-02	1.43E-02
35.00	7.40E-02	5.35E-02	3.11E-02	2.41E-02	1.73E-02	1.65E-02
40.00	8.31E-02	6.03E-02	3.48E-02	2.70E-02	1.95E-02	1.86E-02
45.00	9.22E-02	6.71E-02	3.85E-02	2.98E-02	2.18E-02	2.08E-02
50.00	1.01E-01	7.39E-02	4.23E-02	3.26E-02	2.40E-02	2.29E-02

a. EFPY at end of cycle 20.
b. Estimated EFPY at end of cycle 21.

Note: Up to the end of cycle 21, EFPY is calculated based on a full operating power of 2300 MWt. For projections beyond cycle 21, the projections include a 1.5% plant uprating from 2300 MWt to 2335 MWt. Projections beyond cycle 21 are based on an average of cycles 16 to 21.

Table 6-15

Calculated Fast Neutron Exposure of the H. B. Robinson Unit 2 Upper Circumferential Vessel Weld at the Clad/Base Metal Interface at Selected Azimuthal Angles

Neutron Fluence [E > 1.0 MeV]

CumulativeOperating Time [EFPY]	Neutron Fluence [n/cm^2]					
	0.0 Degrees	10.0 Degrees	20.0 Degrees	30.0 Degrees	40.0 Degrees	45.0 Degrees
20.39 [a]	1.21E+19	8.93E+18	5.26E+18	4.11E+18	2.83E+18	2.65E+18
21.78 [b]	1.25E+19	9.29E+18	5.50E+18	4.30E+18	2.99E+18	2.80E+18
29.00	1.57E+19	1.16E+19	6.82E+18	5.32E+18	3.78E+18	3.56E+18
30.00	1.62E+19	1.20E+19	7.00E+18	5.46E+18	3.89E+18	3.67E+18
35.00	1.84E+19	1.36E+19	7.91E+18	6.16E+18	4.44E+18	4.20E+18
40.00	2.06E+19	1.52E+19	8.82E+18	6.87E+18	4.99E+18	4.73E+18
45.00	2.28E+19	1.69E+19	9.74E+18	7.57E+18	5.54E+18	5.26E+18
50.00	2.50E+19	1.85E+19	1.06E+19	8.27E+18	6.09E+18	5.79E+18

Iron Atom Displacements

Cumulative Operating Time [EFPY]	Iron Atom Displacements [dpa]					
	0.0 Degrees	10.0 Degrees	20.0 Degrees	30.0 Degrees	40.0 Degrees	45.0 Degrees
20.39 [a]	2.10E-02	1.49E-02	8.65E-03	6.73E-03	4.63E-03	4.36E-03
21.78 [b]	2.18E-02	1.55E-02	9.04E-03	7.05E-03	4.88E-03	4.61E-03
29.00	2.71E-02	1.94E-02	1.12E-02	8.71E-03	6.18E-03	5.87E-03
30.00	2.78E-02	1.99E-02	1.15E-02	8.94E-03	6.36E-03	6.04E-03
35.00	3.14E-02	2.26E-02	1.30E-02	1.01E-02	7.27E-03	6.92E-03
40.00	3.51E-02	2.54E-02	1.45E-02	1.13E-02	8.17E-03	7.79E-03
45.00	3.87E-02	2.81E-02	1.60E-02	1.24E-02	9.07E-03	8.66E-03
50.00	4.23E-02	3.08E-02	1.75E-02	1.36E-02	9.97E-03	9.53E-03

a. EFPY at end of cycle 20.

b. Estimated EFPY at end of cycle 21.

Note: Up to the end of cycle 21, EFPY is calculated based on a full operating power of 2300 MWt. For projections beyond cycle 21, the projections include a 1.5% plant uprating from 2300 MWt to 2335 MWt. Projections beyond cycle 21 are based on an average of cycles 16 to 21.

Table 6-16

Calculated Fast Neutron Exposure of the H. B. Robinson Unit 2 Lower Circumferential Vessel Weld at the Clad/Base Metal Interface at Selected Azimuthal Angles

Neutron Fluence [E > 1.0 MeV]

CumulativeOperating Time [EFPY]	Neutron Fluence [n/cm^2]					
	0.0 Degrees	10.0 Degrees	20.0 Degrees	30.0 Degrees	40.0 Degrees	45.0 Degrees
20.39 [a]	1.52E+19	1.20E+19	9.53E+18	8.23E+18	5.72E+18	5.35E+18
21.78 [b]	1.54E+19	1.22E+19	9.92E+18	8.62E+18	6.05E+18	5.67E+18
29.00	1.67E+19	1.36E+19	1.20E+19	1.07E+19	7.73E+18	7.29E+18
30.00	1.69E+19	1.38E+19	1.23E+19	1.10E+19	7.96E+18	7.51E+18
35.00	1.78E+19	1.48E+19	1.37E+19	1.24E+19	9.12E+18	8.63E+18
40.00	1.87E+19	1.58E+19	1.51E+19	1.38E+19	1.03E+19	9.75E+18
45.00	1.96E+19	1.67E+19	1.66E+19	1.52E+19	1.14E+19	1.09E+19
50.00	2.05E+19	1.77E+19	1.80E+19	1.66E+19	1.26E+19	1.20E+19

Iron Atom Displacements

Cumulative Operating Time [EFPY]	Iron Atom Displacements [dpa]					
	0.0 Degrees	10.0 Degrees	20.0 Degrees	30.0 Degrees	40.0 Degrees	45.0 Degrees
20.39 [a]	2.52E-02	2.01E-02	1.56E-02	1.34E-02	9.34E-03	8.80E-03
21.78 [b]	2.56E-02	2.05E-02	1.62E-02	1.41E-02	9.88E-03	9.32E-03
29.00	2.78E-02	2.29E-02	1.96E-02	1.74E-02	1.26E-02	1.20E-02
30.00	2.81E-02	2.32E-02	2.00E-02	1.79E-02	1.30E-02	1.23E-02
35.00	2.96E-02	2.48E-02	2.23E-02	2.02E-02	1.49E-02	1.42E-02
40.00	3.11E-02	2.65E-02	2.47E-02	2.25E-02	1.68E-02	1.60E-02
45.00	3.26E-02	2.81E-02	2.70E-02	2.48E-02	1.86E-02	1.78E-02
50.00	3.41E-02	2.97E-02	2.93E-02	2.71E-02	2.05E-02	1.97E-02

a. EFPY at end of cycle 20.
b. Estimated EFPY at end of cycle 21.

Note: Up to the end of cycle 21, EFPY is calculated based on a full operating power of 2300 MWt. For projections beyond cycle 21, the projections include a 1.5% plant uprating from 2300 MWt to 2335 MWt. Projections beyond cycle 21 are based on an average of cycles 16 to 21.

Table 6-17

Calculated Surveillance Capsule Lead Factors

Capsule	Location	Status	Present Exposure Lead Factor [a]	Future Exposure Lead Factor [b]
S	10°	Withdrawn EOC 1	1.90	-
V	20°	Withdrawn EOC 3	0.91	-
T	0°	Withdrawn EOC 8	2.80	-
X	40°, 0°	Withdrawn EOC 20	1.63	-
U	30°, 10°	In Reactor	1.41	2.02
Y	30°	In Reactor	0.92	1.04
W	40°	In Reactor	0.59	0.61
Z	40°	In Reactor	0.59	0.61

a. Present exposure lead factors are the ratio of capsule fluence (E > 1.0 MeV) to the maximum vessel fluence (E > 1.0 MeV) at the time of withdrawal or at the end of cycle 20.

b. Future exposure lead factors are the ratio of capsule fluence rate (E > 1.0 MeV) to the maximum vessel fluence rate (E > 1.0 MeV) for exposure after the end of cycle 20, projected using the average of cycles 16 through 21.

Table 6-18

Calculated Fast Neutron Exposure of the H. B. Robinson Unit 2 Nozzle Components

Cumulative Operating Time [efpy]	Neutron Fluence [E > 1.0 MeV] (n/cm^2)			
	Inlet Nozzle Weld	Inlet Nozzle Shell	Outlet Nozzle Weld	Outlet Nozzle Shell
29	2.47E+17	2.19E+17	1.59E+17	1.21E+17
30	2.54E+17	2.25E+17	1.64E+17	1.25E+17
35	2.88E+17	2.56E+17	1.86E+17	1.42E+17
40	3.23E+17	2.86E+17	2.08E+17	1.58E+17
45	3.57E+17	3.17E+17	2.30E+17	1.75E+17
50	3.92E+17	3.48E+17	2.53E+17	1.92E+17

7 SURVEILLANCE CAPSULE REMOVAL SCHEDULE

The following surveillance capsule removal schedule meets the intent of ASTM E185-82 and is recommended for future capsules to be removed from the H.B. Robinson Unit 2 reactor vessel. This recommended removal schedule is applicable to 29 EFPY of operation.

TABLE 7-1

H.B. Robinson Unit 2 Reactor Vessel Surveillance Capsule Withdrawal Schedule

Capsule	Location	Lead Factor[a]	Removal Time (EFPY)[b]	Fluence (n/cm^2, $E > 1.0$ MeV)[a]
S	280°	1.90	1.28	4.79×10^{18} (c)
V	290°	0.91	3.18	5.30×10^{18} (c)
T	270°	2.80	7.27	3.87×10^{19} (c)
X	50°	1.63	20.39	4.49×10^{19} (c)
U[f]	30°	1.41 (2.02)	29.8	6.00×10^{19} (d)
Y	150°	0.92 (1.04)	Standby	(e)
W	40°	0.59 (0.61)	Standby	(e)
Z[g]	230°	0.59 (0.61)	Standby	(e)

Notes:

(a) Updated in Capsule X dosimetry analysis. Lead Factor in Parentheses are for Future Cycles.

(b) Effective Full Power Years (EFPY) from plant startup.

(c) Plant specific evaluation.

(d) Capsule U will reach a fluence of approximately 6.00×10^{19} (50 EFPY Peak Fluence) at approximately 29.8 EFPY. Thus, it should be pulled at the closest outage to 29.8 EFPY.

(e) If further material data is desired, then it is recommended that these capsules be moved to a higher lead factor location and then removed once their accumulated neutron fluence equals the license renewal (50 EFPY) fluence on the vessel inner surface.

(f) Moved to Capsule "S" Location (280°) at Cycle 8.

(g) Capsule Z was inadvertently removed from the H.B. Robinson 2 Reactor Vessel. At this time it is unconfirmed that Capsule Z was re-installed into the vessel or placed in the spent fuel pool.